DESIGN OF EXPERIMENT BASED OPTIMIZATION OF A DIRECT CONTACT BLOOD BRAIN BARRIER IN VITRO MODEL FOR NEUROACTIVITY SCREENING

by

Kelsey E. Lubin

A Dissertation

Submitted to the Faculty of Purdue University

In Partial Fulfillment of the Requirements for the degree of

Doctor of Philosophy

Department of Industrial & Physical Pharmacy

West Lafayette, Indiana

August 2019

THE PURDUE UNIVERSITY GRADUATE SCHOOL
STATEMENT OF COMMITTEE APPROVAL

Dr. Gregory T. Knipp, Chair
Department of Industrial and Physical Pharmacy
Dr. Stephen R. Byrn
Department of Industrial and Physical Pharmacy
Dr. Rodolfo Pinal
Department of Industrial and Physical Pharmacy
Dr. Jean-Christophe Rochet
Department of Medicinal Chemistry and Molecular Pharmacology
Dr. Yoon Yeo
Department of Industrial and Physical Pharmacy

Approved by:

Dr. Rodolfo Pinal
Head of the Graduate Program

I dedicate this dissertation to my mother and father, Barbara and Frank Lubin, and my sister Courtney Lubin. The support they have given me throughout this journey has been invaluable and I cannot express my gratitude enough.

ACKNOWLEDGMENTS

I would firstly like to acknowledge my advisor Dr. Gregory Knipp who has provided me with a supportive environment to improve as a scientist. The growth I have made in his laboratory both scientifically and professionally is immeasurable, and I am thankful for his continued guidance throughout.

I would like to thank my committee members: Dr. Stephen Byrn, Dr. Rodolfo Pinal, Dr. Jean-Christophe Rochet, Dr. Elizabeth Topp, and Dr. Yoon Yeo. They have all contributed to this project and pushed me to make novel improvements on this work to ultimately become a better researcher.

I also express my greatest appreciation to my fellow lab members and colleagues: Dr. Christopher Kulczar, Dr. Monika Lavan, Dr. Aimable Ngendahimana, and Mr. Matthew Behymer. They have each contributed to fostering a collaborative lab space and making my time a Purdue enjoyable. Additionally, I would like to thank the staff and faculty of the Department of Industrial and Physical Pharmacy. The environment of the department has been inviting and encouraging to say the least.

Lastly, I would like to acknowledge my thanks to my family and friends, both near and far, who have believed in me and supported me unconditionally. My time at Purdue has been enjoyable because of all of you.

TABLE OF CONTENTS

LIST OF TABLES

LIST OF FIGURES

ABSTRACT

Author: Lubin, Kelsey, E. PhD
Institution: Purdue University
Degree Received: August 2019
Title: Design of Experiment Based Optimization of a Direct Contact Blood Brain Barrier In Vitro Model for Neuroactivity Screening
Committee Chair: Gregory T. Knipp

Neurotherapeutics are an essential drug class that is often forgotten or neglected due to the difficulties associated with pharmaceutical development and approval. These compounds face high rates of attrition in clinical trials and late stage development predominantly due to the restrictiveness of the blood brain barrier (BBB). The inherent role of the BBB is to protect and maintain the homeostatic environment around the neuronal cells in the brain parenchyma. This is accomplished by the BBB posing not only as a physical barrier through its restrictive tight junctions that prevent paracellular permeation, but also through the high expression levels of efflux transporters and drug metabolizing enzymes that prevent transcellular permeation of potential drug compounds. In attempting to deliver compounds to the brain the intended outcome is often over-shot to the point of causing neurotoxic implications. One way to mitigate the difficulties associated with drug delivery to the brain and early evaluation of potential toxic compounds is to develop *in vitro* cell-based models that mimic the *in vivo* BBB and neurovascular unit (NVU). The mainstays of the BBB phenotype are presented in the brain microvessel endothelial cells (BMECs) and are regulated and influenced by the close contacts of supporting cells of the NVU such as astrocytes, pericytes, and neurons. An *in vitro* model that can mimic the close contacts between these four cell types and is capable of being implemented in pharmaceutical development for BBB permeability and neuroactivity screening could lead to better selection of hit and lead candidates, and ultimately reduce the attrition rates of neurotherapeutics.

Direct contact coculture and triculture models have been developed in our laboratory that mimic the *in vivo* cell-cell contacts between the different cell types of the NVU and provide increased barrier properties in comparison to other models utilizing indirect contact between cell types. Early development and optimization of these models was accomplished using the human cerebral endothelial cell line hCMEC/D3. Although this cell line proved useful in early validation stages, it was decided that a different endothelial cell source would be sought out. Work was done using iPSC derived endothelial cells (iCell® endothelial cells) and an alternative immortalized human brain endothelial cell line (HBEC-5i). Both cell lines proved to be amenable to the direct contact coculture and triculture models, with the iCell® models showing greater barrier properties in comparison to those using the HBEC-5i cell line. However, drawbacks of the iCell® model were observed in extending culturing of the cells causing the cells to "roll" to the middle of the filter and proving to be cost prohibitive for extensive optimization. Ultimately, the HBEC-5i cell line was chosen for continued development and optimization due to its immortalized origin and potential for replacing the hCMEC/D3 cell line in the direct contact models.

Optimization of the direct contact triculture using the HBEC-5i cell line was required as all of the previous development was performed using the hCMEC/D3 cells. Typically, optimization of *in vitro* systems is performed in a one factor at a time manner or not at all. Given the large number of factors that can influence the outcome of this model, a design of experiments (DOE) based optimization approach was taken. DOEs are traditionally used in process optimization of non-biologically based systems; however, the production of the direct contact triculture is a process that could greatly benefit from extensive optimization. The seeding densities of all three cell types used in the triculture (astrocytes, pericytes, and HBEC-5i), the extracellular matrix used, and the length of culture time post endothelial cell plating were the factors chosen for

the optimization process given the observations made during early development of the model. The conditions were optimized for barrier tightness by measuring the permeability of a 4 kD dextran as a paracellular marker because the model would have limited utility without adequate tight junction formation. Based on the results of this work, optimized conditions were determined in a significantly reduced amount of time as compared to traditionally used cell model optimization methods and an *in vitro* BBB screening tool that mimics the physiology of the NVU was developed. Given the outcomes of these studies it can be seen that a DOE optimization approach should be considered for development of biologically based systems to understand interactions between key system factors and to reduce the time to develop these necessary systems.

BBB permeability is not the only factor that slows development of neurotherapeutics. The intent of many of these compounds is to elicit an effect on the neuronal environment; however, permeability and neuroactivity are often evaluated separately even though they are inherently linked *in vivo*. Further enhancement of the optimized direct contact triculture was done to develop a screening tool that could assess neuroactivity of a compound as it is related to its brain permeability. The *in vitro* NVU model was developed by adding human neurons to the basolateral chamber of the direct contact triculture so permeating compounds would accumulate in the receiver chamber and their neuronal effects could be measured. During development of this model it was seen that the addition of neurons both increases tightness of the apical BBB model, but also increases viability of the neurons themselves. This is likely due to the facilitation of cross-talk between the four cell types of the NVU due to the proximity of the cells in the model system. The BBB permeability linked neuroactivity of marker compounds was measured by neuronal viability and neurite outgrowth in response to compound accumulation over the neurons during the course of BBB permeation. The results of this assay showed that the model is capable of being used to

assess both BBB permeability and the subsequent neuroactivity of a given compound, and that the inclusion of additional cell types from the NVU further increases the physiological relevancy of the model. This work shows that the NVU model is an enhancement of the direct contact triculture model and can be easily implemented in the early development stages of neurotherapeutic compounds. Ultimately, this model has the potential to increase the number of brain targeting compounds by facilitating early, predictive assessment and rank ordering of large compound libraries for continued development.

CHAPTER 1. IN VITRO MODELS OF THE BLOOD BRAIN BARRIER: STRUCTURE BASED APPROACHES FOR PERMEABILITY AND NEUROACTIVITY SCREENING

1.1 Abstract

High attrition rates in later stages of development and clinical trial testing with currently selected lead neuroactive candidates have been determined to often be due to a lack of efficacy or potential associated neurotoxicity, which most *in vitro* screening models fail to detect. Currently, *in vitro* screening models of the blood brain barrier (BBB) provide an essential tool for the hit to lead selection and optimization of neurotherapeutics, yet are lacking in their ability to demonstrate properties required to succeed *in vivo*. Therefore, the development of a physiologically relevant *in vitro* model of the BBB that demonstrates good *in vivo* relationship of both brain permeability and neuroactivity screening might provide enhanced predictability and lead to superior lead selection of neurotherapeutics with improved potential for translation. In order for the BBB *in vitro* model to meet the desired *in vivo* performance metrics, the presence of more restrictive barrier properties, inclusion of critical cells that comprise the physiological neurovascular unit, and the expression of influx and efflux transporters and drug metabolizing enzymes are requisite. In addition, the coupling of permeability to neuronal response in an efficient screening tool would provide a better metric for prioritization. The goal of this introduction and the subsequent chapters is to demonstrate the importance of incorporating the physiology of the BBB in *in vitro* screening tools followed by a recommendation for an ideal *in vitro* model to fill the current lack of a single neurotherapeutic screening tool in pharmaceutical industry.

1.2 The Blood Brain Barrier

The blood-brain barrier (BBB) is found in the brain capillaries and is one of three central nervous system (CNS) barriers. Unlike the other CNS barriers, the BBB is a highly restrictive barrier predominantly made up of the single endothelium layer that lines the microvessels of the brain and is responsible for maintaining homeostasis.[1–3] This is accomplished by controlling the movement of ions and nutrients between the peripheral blood and the brain through passive, facilitative, and active transport.[4] It is important to note that this regulation is critical as neurons rely on highly controlled ion levels to function. In addition, the BBB functions to protect the brain from harmful xenobiotics through active efflux and restrictive tight junctions. The disruption of the BBB has been shown to be a contributing factor or direct result of many neurological diseases or injuries such as Alzheimer's, Parkinson's, dementia, mental illness, brain tumors, and traumatic brain injury (TBI).[3,5,6] These neurological disorders are still under served in terms of the availability of new drugs targeting the brain due to the difficulties associated with developing compounds and formulations that cross the BBB.[7–9] This is despite considerable debate over the implied effects of these disorders on the BBB integrity.

The BBB is a restrictive barrier due to its tight junctions, high expression of luminal and abluminal influx and efflux transporters, and a higher metabolic capacity in comparison to peripheral endothelium.[10] Routes of permeation across the BBB include paracellular permeation of hydrophilic molecules through highly restrictive tight junctional complex pores, transcellular permeation of lipophilic molecules, facilitative and active transport, metabolism, and transcytosis, which the latter appears to be a minimal pathway of drug delivery.[10] However, the ability to exploit these pathways through drug development is difficult due to the restrictiveness of the BBB as a whole and its high functional expression of efflux transporters and largely under investigated drug

metabolizing enzymes.[9] In conjunction with the brain microvessel endothelial cells (BMECs), astrocytes, pericytes, neurons, microglia, and extracellular matrix proteins interact to form the neurovascular unit (NVU).[1,11] The multiple cell types and matrix proteins all contribute to the unique *in vivo* phenotype of the NVU, and in many ways it should be defined as the BBB instead of the conventional emphasis on the BMECs.

1.3 The Neurovascular Unit – Interactions with the Endothelium

The BBB is made up of endothelial cells that line the microvessels of the brain, with supporting cells of the neurovascular unit contributing to its phenotype (Fig. 1.1).[1,10,12] The supporting cells, specifically astrocytes and pericytes, along with matrix proteins are thought to contribute to the phenotype of the BBB expressed in BMECs though direct contact and multiple signaling pathways.[11,10,13] The pericytes cover approximately one third of the abluminal surface of the BBB endothelium and participate in regulation of the BMECs.[14,15] The abluminal surface of the BMECs and attached pericytes are nearly fully covered by astrocytic endfeet that play a role in the formation and maintenance of the NVU.[10,14] Neurons are also considered to be part of the NVU because these are the cells that are directly affected by the maintenance or disruption of the BMECs and supporting cells.[16] Additionally, it is suspected that neurons can influence the function of the BMECs through various interactions and as a result of injury or disease state.[5] The extracellular matrix (ECM) is considered a non-cellular component of the NVU as it acts as a mainstay for the endothelium and proteins (e.g., collagen IV, laminin, vitronectin, etc.) can differentially influence the expression and integrity of tight junction associated proteins in the BMECs.[16] Normal function and coordination of all cellular and non-cellular components of the NVU is imperative for maintaining homeostasis and phenotypic expression of the physiological *in*

vivo BBB. Disruption of any of the NVU components could lead to the improper function of the BBB and a loss of neuronal protection. Therefore, *in vitro* models utilized in early preclinical screening should better mimic the *in vivo* NVU to provide proper rigor and compound selection based on the real barriers to function in pharmaceutical development. To do so, one must understand some of the critical properties of the different cell types and ECM found in the NVU.

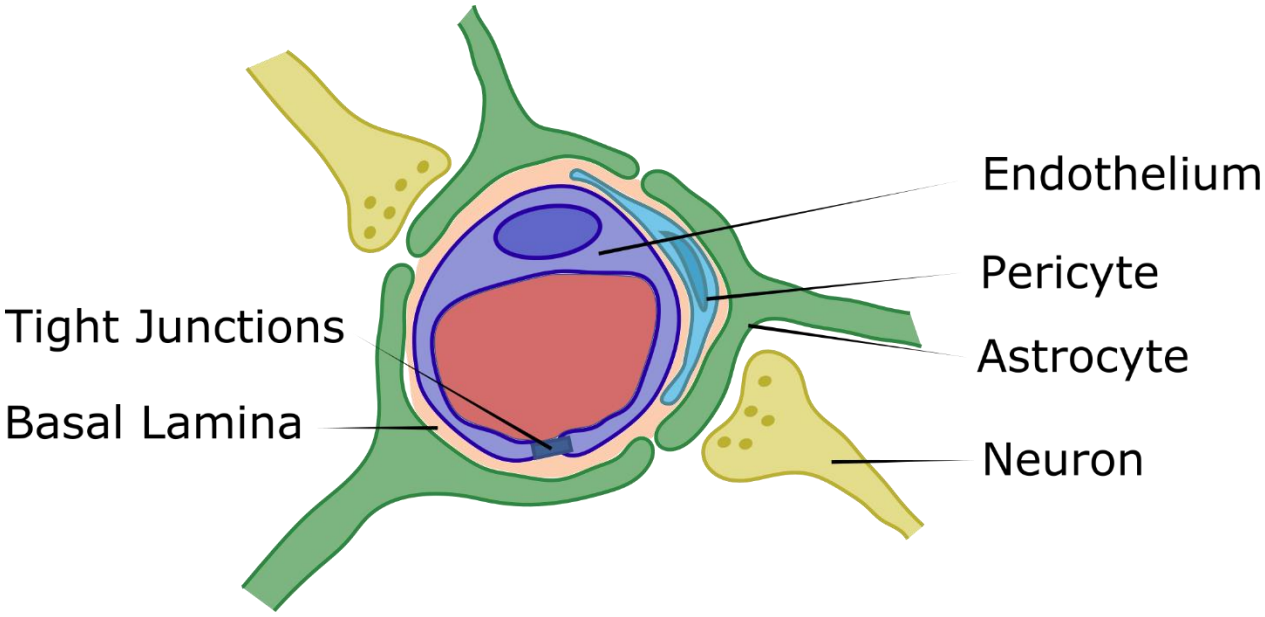

Figure 1.1. Anatomy of the blood brain barrier and neurovascular unit in cross sectional view. BMECs (purple) line the microvessel forming tight junctions between adjacent cells. Pericytes (blue) are ensheathed in the basal lamina and fully surrounded by astrocytic endfeet (green). Astrocytes make contact with nearby neurons (yellow) and respond to fluctuations in neuronal health.

1.3.1 *Astrocytes*

Astrocytes are part of the glial cell family, and are non-neuronal cells responsible for maintaining homeostasis in the brain and neural protection.[17] The glial cells also include oligodendroglia (primarily function to produce myelin that sheaths the axons and regulates ion fluxes) and microglia (appear to have a role in the neuroimmune response). It should be noted that the brain does not have a lymphatic system in the traditional sense and the glial cells are largely

attributed with the control of the neuronal extracellular fluid (interstitial fluid; ISF) composition that is critical for normal brain function. Currently, there is considerable attention being paid to the ISF and the role it plays in governing local response and clearance through the glymphatic space and into the CSF for parenchymal waste excretion that goes beyond our discussions here.[18–24] However, in future studies the ability to bridge *in vitro* screening models that incorporate the glymphatic characteristics could prove to be highly valuable to better assess *in vivo* exposure and delineate factors contributing to disease pathogenesis. It is mentioned here based on the fact that the astrocytes are thought to play an essential role in controlling the ISF through the function of aquaporin 4 and in regulating ion homeostasis, as well as contributing to solute clearance.[17,25–27]

In the NVU, astrocytes surround the endothelium and are linked to each other through gap junctions and outward projecting endfeet that can interact with neurons and in rare cases other glial cells. Traditionally, the morphology of astrocytes has been dubbed "star-like" for Latin translation of astro (star) and cyte (cell), however, with advanced imaging techniques, astrocytes have been shown to be morphologically complex as spongiform cells with nanoscale projections to adequately correspond with synapses.[28–30] These astrocytic endfeet are found in close contact with the BMECs, with the two cell types separated by an extracellular matrix only 15-20 nm thick.[14,31] The astrocytic endfeet cover up to 99% of the capillaries, where each astrocyte contacts around four neurons and interacts with five blood vessels without overlap, making them the cellular link between the capillary and neuron.[14,32–34] Their numerous interactions with the BBB and neuronal soma reinforce the idea that astrocytes are a key contributor to the BBB phenotype rather than just serving as a supporting cell.[35]

Astrocytes are characterized and identified by the expression of the intermediate filament (IF) glial fibrillary acidic protein (GFAP) as part of their cytoskeleton. Astrocytes express 10

distinct isoforms of GFAP in addition to other IF proteins.[36–38] GFAP and other IF proteins have been demonstrated to be necessary for maintaining the integrity of the BBB, where their absence can lead to disruption of myelination resulting in CNS disorders.[39] Conversely, the upregulation or overexpression of IFs, specifically GFAP, has been linked to astrogliosis that results from CNS damage or injury.[40] Studies suggest that astrocytes react to BBB injury by overexpressing GFAP, in conjunction with cellular proliferation and hypertrophy, in an effort to protect the brain parenchyma from penetration of pathogens, making GFAP expression levels a marker for BBB injury.[41]

The roles of astrocytes are important in BMEC induction and regulation, as first suggested by their close proximity to the endothelium. Astrocytic endfeet are involved in ion and water volume regulation due to the localization of K^+ ion channels and water channel aquaporin 4 (AQP4); where the localization and density of the AQP4 forms orthogonal arrays of particles (OAPs) that are highly structured square assembly of particles within the membrane.[42,43] These OAPs define the polarization of the astroglial membranes, where OAPs are present in high density at the endfeet in contact with the BBB basal lamina compared to much lower densities at the endfeet closest to the neuron.[44,45] The differential OAP membrane localization is also proposed to be associated with the expression of the basal lamina protein agrin, thus suggesting that the basal lamina is closely associated with the polarization of astrocytes and is involved in astrocyte-endothelial interactions and induction.[10,44]

In addition to induction of the endothelium through polarization of the endfeet, astrocytes secrete factors that play a role in BBB development and maintenance of normal barrier function. These astrocytic factors include vascular endothelial growth factor (VEGF), basic fibroblast growth factor (bFGF), glial cell line-derived neurotrophic factor (GDNF), and angeopoetin-1

(ANG-1).[10,46,47] These factors all participate in some aspect of endothelial growth, modulation, or maintenance and are essential to up keeping the BBB phenotype. The induction of BBB properties can be seen in the localization of transporters expressed in the endothelium, increases in barrier tightness through tight junction protein modulation, and maintenance of overall NVU homeostasis. This is supported by numerous *in vitro* and *in vivo* studies that observed changes in the BBB integrity in response to a deficiency in certain astrocytic factors.[46,48,49] Additionally, astrocytes will up- or downregulate the secretion of these factors in response to disease, trauma, or disruption of the BBB making the expression levels of each possible indicators of disease states. For example, astrocytes secrete the cytokine transforming growth factor β (TGF-β) after a pro-inflammatory insult. Models are needed to develop a better understanding of the signaling pathways and astrocyte-BMEC interactions which may further elucidate pathways for therapeutic development and could lead to early detection of CNS disorders. However, there are other cells comprising the NVU which function synergistically to maintain the integrity of the BBB.

1.3.2 *Pericytes*

Pericytes, another cell type found in the NVU, are found enveloped in the basal lamina between the endothelium and fully engulfed by the astrocytic endfeet. Pericyte distribution is not continuous along the endothelium and covers approximately one-third of the abluminal surface of the endothelial cell.[14] These cells are oval shaped with processes that wrap around the endothelium in various arrays. Pericytes have been shown to influence the regulation of the endothelium, through tight junction maintenance, as well as astrocytes via the influence on AQP4 localization.[15] Similarly to astrocytes, the influence of pericytes on the BBB phenotype is highly dependent on soluble factors and the polarization of membranes.

Although the early development of the BBB has yet to be fully understood, it is suggested that pericytes play an integral role in the induction of barrier properties during embryogenesis.[50] Pericytes arise earlier in development compared to astrocytes during which time a functional BBB is present before astrocyte appearance.[13,50] This strongly suggests that pericytes are essential for BBB development, angiogenesis, and continued maintenance. Pericytes also play a role in BBB regulation, proliferation of the endothelium, and the diameter of the capillary.[51] Both *in vitro* and *in vivo* studies have shown the importance of pericytes in the polarization of astrocytes and barrier properties of endothelial tight junctions, and that loss of pericyte function is linked to aging and age-dependent neurodegeneration.[50,52] For example, lack of pericytes or loss of pericyte function has been shown to have implications in Alzheimer's disease pathology making it an essential part of the NVU for maintaining the BBB.[53] Additionally, pericytes act on capillary blood flow through vasoconstriction or dilation in response to electrical neuronal signaling.[54] The interaction between pericytes and endothelial cells is supported by the close contacts between the two cell types through the formation of peg-socket junctions, adhesion plaques, and a shared basement membrane.[13,51]

Pericyte-endothelial intracellular signaling is essential for the NVU by influencing pericyte recruitment, attachment, maintenance, and endothelial evolution.[13] The recruitment and survival of pericytes in the NVU is attributed to the secretion of platelet-derived growth factor B (PDGF-B) by the endothelium and binding to pericytes expressing PDGF receptor-β (PDGFRβ).[55,56] Pericytes and BBB endothelial cells both express TGF-β receptors (TGFβR) that bind TGF-β secreted by the endothelium, pericytes, and glial cells result in a signaling cascade between all cell types that is required for development of BBB capillaries.[57,58] Additionally, Notch signaling, which plays a role in vascular development, has been shown to occur between pericytes and the BBB

endothelium.[59,60] All of the pericyte-endothelium cross-talk occurs within the shared basement membrane, potentially suggesting that the composition of the basal lamina and extracellular matrix plays an important role in BBB development and maintenance.

1.3.3 *Extracellular Matrix and Basement Membrane Proteins*

The extracellular matrix (ECM), also referred to as the basement membrane (BM) or basal lamina, is comprised of many different proteins and proteoglycans that are primarily secreted by the endothelium, astrocytes, and/or pericytes. Each cell type within the NVU express ECM receptors (e.g., integrins) and secrete ECM proteins (e.g. collagens) or ligands to enable synergistic contributions that both enable attachment and provide the integrity of the NVU.[61] ECM receptors integrin and dystroglycan are responsible for anchoring the cytoskeleton of NVU cells to the ECM and respond to variations in the BM environment by regulating signal transduction pathways between cell types.[62] ECM proteins and ligands include fibronectin, collagen IV, laminins, nidogen, and perlecan (heparin sulfate proteoglycan 2) which all interact to keep the cells of the NVU in close contact by anchoring them to the ~20 nm thick basal lamina.[4,16,61]

ECM receptor interactions with ECM ligands has been demonstrated to influence tight junctional protein expression in BBB endothelium, as suggested by observed increases in permeability when ligand binding is inhibited.[63] Additionally, *in vitro* studies have shown that all cells of the NVU are required for adequate ECM expression levels, as observed when endothelial cells are cultured with astrocytes and pericytes.[64] The ECM secreted by astrocytes also has an effect on pericyte differentiation, in addition to endothelial influences, as seen when culturing pericytes on a basement of astrocytic laminins.[65] As mentioned above, the exchange of growth factors and astrocyte-pericyte-endothelial cross-talk occurs within the ECM making the

composition of the ECM and its response to disruption imperative for adequate barrier maintenance of the BBB.

1.3.4 *Neurons*

The role of the NVU is to protect and maintain the brain parenchymal ISF composition. Hence, the structural and molecular integrity of the BBB and its components is essential to neuronal health and function. Neurovascular coupling, signaling, provides a synergistic response relationship between neural activity and cerebral blood flow, and as such, the NVU works as a functional barrier that responds to neuronal energy demands.[66] Neurons predominantly signal the BBB by astrocytic interactions due to the astrocyte contact with both neuronal soma and capillaries.[33] These cell-cell interactions then in turn influence the state of the BBB.[67] In addition, the release of glutamate can affect neuron activity and has been shown to influence cerebral blood flow that occurs though signal transduction and relaxation of pericytes surrounding the endothelium.[68] Continuing research has revealed that neurovascular coupling is a multidimensional and coordinated response between multiple cell types having influence across all cerebral vasculature rather than only signaling between the neuron and local blood vessels.[69] The synchronization of the NVU with neural activity makes the integrity of the barrier's function essential for maintaining a healthy brain environment.

1.4 BBB Endothelium

The brain microvessel endothelial cells that line the capillaries help comprise the BBB. The endothelium is not inherently unique to the BBB, despite significant functional differences, however the properties are largely induced by the other cells and soluble factors found in the NVU.

This coordination of signaling makes the BBB endothelium unique compared to peripheral vasculature.[2] Key phenotypic factors of the BBB endothelium include the restrictive tight junctions, a lack of fenestrations, and high expression of efflux proteins and drug metabolizing enzymes that, combined, function to maintain the ISF homeostasis and limit xenobiotics from traversing the BBB into the parenchymal environment.

1.4.1 *Tight Junctions*

The structure of BMEC tight junctions is depicted in Figure 1.2. Tight junctions are a complex of multiple transmembrane and cytosolic proteins that span the space between endothelial cells, where they function to limit the passive diffusion of polar solutes through the paracellular gap to maintain polarity between the extracellular spaces.[1,44,70] The complexes are found in other endothelial and epithelial barriers throughout the body. However, the tight junctional complexes between the BMECs in the NVU are considered to be the tightest and most restrictive in comparison to the periphery.[71,72]

The tight junctional proteins that contribute most to the restrictive barrier are those that connect across the intercellular cleft to anchor neighboring cells to one another. Occludin was the first spanning protein shown to localize tight junctions; however multiple studies of occludin deficient models suggest that it does not play an integral role in the formation of tight junction strands, but is important for physiology and regulation of tight junction formation.[44,71,73–75] Claudins were next identified as another gap spanning protein shown to have similar folding properties to occludin, but are not homologous in sequence.[76] Claudins are thought to be the gap spanning proteins that contribute most predominantly to the restrictiveness of the barrier to hydrophilic small molecules, where claudins and occludins synergistically function to maintain the barrier phenotype.[77,78] There are over 25 proteins in the *claudin* family have been identified in

man and mouse, however only claudin-1, -3, -5, and -12 have been identified in the human brain endothelium with claudin-5 being most abundant.[79–81] Junctional adhesion molecules (JAMS) are also found in the intercellular cleft and contribute to the paracellular barrier via cell-cell adhesion as well as involvement in leukocyte migration.[82] The tight junction proteins spanning the intercellular cleft anchor into the cell via cytosolic scaffolding proteins, zonula occluden proteins

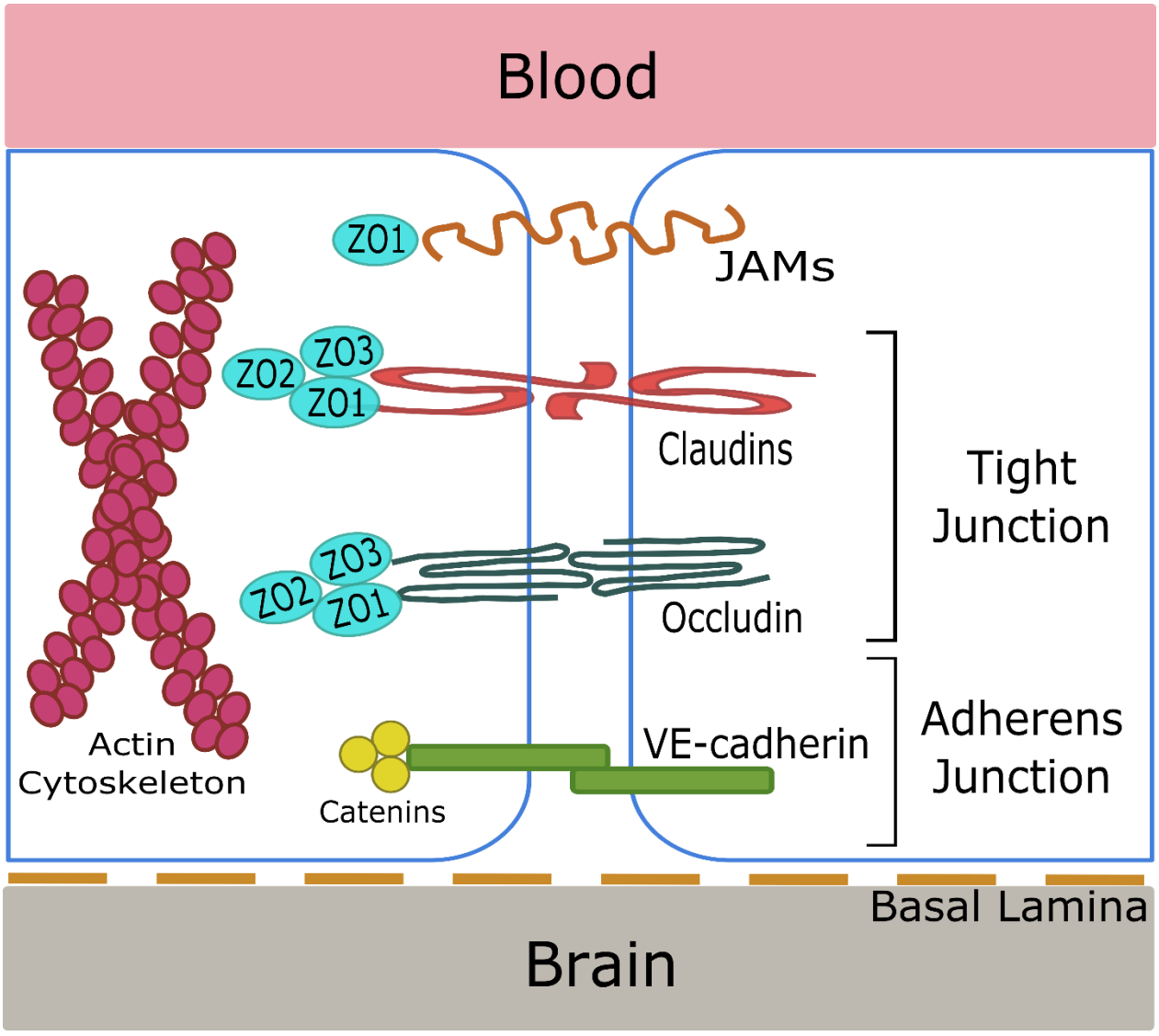

Figure 1.2. Structure of tight junctions formed by the BBB endothelium. Tight junction cleft spanning proteins between adjacent endothelial cells include claudin-3 and -5, occludin, and JAMs which anchor to ZO-1,-2, and -3. Adherens junctions provide structure to cell adhesion and the formation of tight junctions via catenin interactions with actin cytoskeleton. Figure is drawn without supporting cells for simplification. (Modified from Abbott, N.J. *et al.* 2010 and Begley, D.J. 2006)[1,2]

-1, -2, and -3 (ZO-1, -2, -3). Zonula occludens are important for localizing and anchoring of tight junction complexes.[71,83,84]

In addition to tight junctions, adherens junctions span the intercellular cleft, but do not contribute to the prevention of paracellular permeation. Instead, adherens junctions are basally located and provide support and structural integrity to the BBB.[1,70] These complexes are made up of intercellular VE-cadherin attached to catenin scaffolds, which provide initial structure for the formation of tight junctions.[84] Disruption of the adherens junction proteins can result in loss of barrier properties, which also suggests that crosstalk between tight junction and adherens junction proteins is essential for barrier maintenance.[44,84]

1.4.2 *Efflux Transporters*

In addition to the restriction of paracellular permeation of hydrophilic solutes between extracellular spaces, many lipophilic molecules are limited in their ability to traverse the BBB due to their substrate affinity and capacity for relatively highly expressed ATP-binding cassette (ABC) multidrug resistance conferring transporters. ABC transporters that possess broad substrate specificities, function unidirectionally to limit vectorial permeation, and participate the concerted metabolism of xenobiotics in a manner to protect the brain parenchym.[86] ABC transporters that are most prevalent in the BBB include P-glycoprotein (P-gp, MDR-1, *ABCB1*), Multidrug Resistance Proteins (MRPs), and Breast Cancer Resistance Protein (BCRP).[86] Efflux is predominantly an active mechanism involving ABC and potentially SLC transporter isoforms. Collectively, efflux transporters prevent penetration of potential endogenous and exogenous neurotoxicants, but also present a significant challenge for the permeation of neurotherapeutics.

P-gp expression in brain endothelial cells was first discovered in 1989.[87] P-gp, along with many other ABC transporters, localize at the luminal membrane.[88] However, it should be noted

that some MRPs have been found to be expressed on the basal or brain parenchymal side of the membrane, with abluminal function believed to limit several neurotrophic factors from diffusing out of the brain ISF.[89] ABC transporters have also been suggested to work in concert to modulate the permeation of solutes, which is hypothesized to be due to significant substrate specificity overlap between related isoforms.[90] When combined, ABC and Solute Carrier (SLC) efflux transporter isoforms function to protect the brain environment consequentially results in reduced *in vivo* neurotherapeutic efficacy in the brain neuronal parenchyma that is not currently accounted for in current *in vitro* screening methods.

1.4.3 *Drug Metabolizing Enzymes and Drug Transporters*

In addition to tight junction and efflux transporter expression, the BBB expresses a number of drug metabolizing enzymes (DMEs) and drug transporters that maintain a homeostatic environment (as introduced above), transport neurotrophic factors essential for neurological function into and out of the brain parenchyma, and breakdown xenobiotics and toxins into manageable metabolites.[91] Drug transporters and DMEs interact in other organ systems, often in a concerted manner. However, investigations into the interplay between transporter and metabolism mediated permeation across the NVU are limited, and thus represent a significant unmet need in order to properly evaluate their impact on neurotherapeutic exposure in *in vitro* models that mimic the *in vivo* physiology.[91]

Drug metabolizing enzymes primarily act on xenobiotics and endogenous compounds by metabolizing parent compounds into potentially inactive water soluble metabolites that can more readily excreted from the BBB. However, many metabolites have been demonstrated to either have a therapeutic or toxic effect, thus making this interplay more pressing to understand. DMEs within the BBB metabolize molecules by both Phase I and Phase II pathways. Phase I metabolism,

breakdown into polar solutes that can readily be cleared, is done through oxidation, reduction, or hydrolysis by cytochrome P450 (CYP) enzymes and other oxidases.[92] Phase II metabolism, conjugation of metabolites with other substrates to achieve molecules that are sufficiently polar for clearance, occurs at the BBB by transferase enzymes such as methyltransferases, sulfotransferases, and glutathione *S*-transferases (GST), with GSTs being most abundant.[92,93] Metabolizing enzymes have a great impact on drug disposition in healthy patients, and have been shown to be of greater importance in disease states. DMEs, as well as MRPs, are often over expressed in neurological disease states and should be taken into account since this could be causing metabolic breakdown of therapeutic agents at the BBB that is not seen in healthy models.[94,95]

Drug transporters in the brain that are responsible for carrier mediated transport (CMT) by facilitative or active processes that facilitate the permeation of specific exogenous and endogenous molecules including neurotrophic factors such as amino acids, ions, fatty acids, and sugars across the BBB fall into the class of solute carriers (SLCs). The SLCs most prevalent in the BBB are GLUT1 (glucose), MCT1 (monocarboxylic acid), LAT1 (neutral amino acid), CAT1 (basic amino acid), and CNT2 (purine nucleoside).[93,96,97] All of these transporters function to maintain a healthy brain environment and provide the brain parenchyma with essential nutrients and factors that are unable to cross by way of passive diffusion due to physicochemical properties or concentration gradients.

Another type of transport system in the brain is the receptor mediated transcytosis (RMT) pathway. RMT is made up of protein receptors that function to move ligands from the blood to the brain, the brain to the blood, or into the capillary endothelium via transcytosis.[96] For example, insulin is not produced in the brain; therefore, it is transported into the brain parenchyma via the

insulin receptor.[98] Peptides and large molecules are necessary for brain health, but an overwhelming majority of large biological molecules do not appreciably passively traverse the BBB. Therefore, the data suggests that specialized RMT pathways are required for the transport of BBB of oligopeptides and proteins such as insulin, transferrin, and immunoglobulin G (IgG) molecules.[96,99]

Transcriptomic and proteomic analysis of isolated human brain capillaries has been performed to reveal the most abundant DMEs and influx and efflux drug transporters in order to understand which transporters have the biggest impact on drug disposition.[93] Knowledge of transporter and enzyme expression and function, in healthy and diseased states, can be used in the development of new BBB drug delivery methods.

1.5 Challenges in BBB Drug Delivery

Therapeutic agents targeting neurological disorders are often thwarted by the significant barrier properties and endogenous defense mechanisms of the BBB. The expression of continuous tight junctions, influx and efflux drug transporters, and drug metabolizing enzymes prevents the majority of drugs from crossing the BBB into the brain parenchyma. The vast majority of both large and small molecules do not cross the BBB.[9] Given the complexity of the BBB and NVU, there are a number of different approaches to develop drugs that can cross or interact to reach the site of action. However, despite the alternative routes, there has been minimal success for clinical translation of these agents.

1.5.1 *Delivery Methods for Crossing the BBB*

There are a number of drug delivery methods that have been developed in an attempt to get molecules to cross into the brain parenchyma (Fig. 1.3).[100] This includes, but is not limited to: medicinal chemistry screening to select small molecules with the right balance of lipid/water solubility required to achieve effective brain permeation; drug delivery systems aimed at bypassing the BBB by route of administration (*i.e.* intranasal delivery across the arachnoid membrane into the olfactory CSF); targeting CMT pathways through pro-drugs; inhibition of efflux transport by administration of co-drug efflux inhibitors; and delivery of large molecules via RMT through the use of a molecular Trojan horse.[9,99,101]

There is a limited number of traditional therapeutics that are known to traverse the NVU that in general have a molecular weight less than around 400 Da, are capable of forming < 8-10 hydrogen bonds, and possess relatively high lipid solubility. However, these agents largely act on a few CNS disorders including epilepsy, mood disorders, and chronic pain.[9,99] These compounds are proposed to permeate the NVU by way of passive lipid based diffusion predicated on their increased hydrophobicity. In contrast, current novel therapeutic high throughput screening tends to yield molecules with higher molecular weight and hydrogen bonding because of the trend to generate compounds that fit receptor binding sites. The drawback of this is that BBB drug transporters (i.e. GLUT1, LAT1, and CAT1) are highly specific for neurotrophic factors (generally oligopeptides and proteins that stimulate neuronal growth, protection, or maintenance). Since high throughput screening is often unsuccessful in finding new molecules that will passively permeate the BBB, an enhanced transporterphoric approach should be evaluated based on the neurotrophic transporter binding and capacity properties to enhance the ability to improve active delivery.[9,102–104]

A number of carrier mediated transporters are present throughout the BBB endothelium and function to move essential neurotrophic factors between the blood and brain. Designing drug molecules to mimic the structure of the specific substrates of these transporters is one method to enhance drug delivery across the BBB.[9,96,99] One such example is administration of L-DOPA for the treatment of Parkinson's Disease, which crosses the BBB by way of LAT1, a neutral amino acid transporter.[105] There are several family members of the Na^+- and Cl^--dependent neurotransporters (SCDNTs) including the γ-aminobutyric acid transporter members GAT-1,

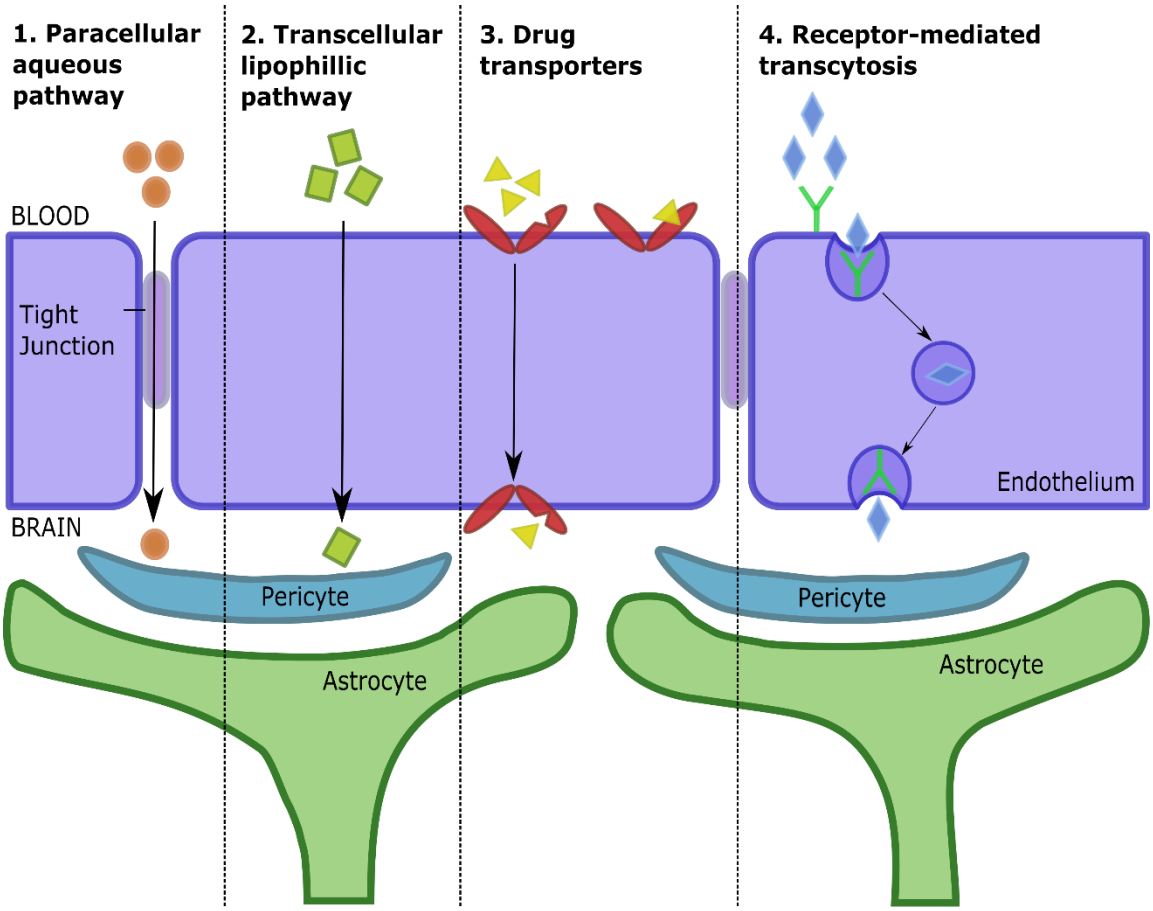

Figure 1.3. Routes of permeation across the BBB that can be targeted for brain drug delivery. Paracellular routes are limited to small water-soluble molecules while agents permeating transcellularly are a small group of lipid-soluble small molecules. Carrier mediated transport (CMT), efflux transport inhibition, and receptor mediated transcytosis (RMT) are the routes that can be best exploited for drug delivery methods across the BBB. (Modified from Abbott, N.J, *et al.* 2006 and Abbott, N.J. and Romero, I.A., 1996)[10,100]

GAT-2, and GAT-3 that can modulate brain permeation and neuronal function.[106] Several other drug transporters including Organic Transporting Polypeptide 2 (OATP2; SLCO1B1) and the Organic Anion Transporter 3 (OAT3; SLC22a8) can play a role in SLC mediated efflux out of the brain parenchyma.[107–110]

Efflux is an essential component of the BBB to maintain homeostasis and prevent the permeation of xenobiotics and toxins into the brain, however they also oppose the permeation of many different drug classes based on their broad substrate specificities. The presence of efflux transporters can thus limit neurotherapeutic effectiveness. There are cases where a strategy for minimizing efflux transporter effects can be achieved with co-administration of a competitive transporter inhibitor with a higher affinity. This approach can ultimately increase the brain permeation of the therapeutic agent, but may also be detrimental.[9,111] Inhibition of efflux transporters (*i.e.* P-gp) can also increase the potential neurotoxicity through either leading to accumulation of the neurotherapeutic or inhibiting the removal of other neurotoxic agents from the parenchyma. Thus, deleterious side effects may result from limited endogenous efflux protection of the brain parenchyma.[101]

Ligand specific receptor mediated transcytosis pathways are essential for the movement of large molecules in a bidirectional manner between the brain and blood. In order to utilize this pathway, small molecules, peptides, and proteins can be conjugated with monoclonal antibodies (mAbs) specific for the RMT pathway to act as a molecular Trojan horse.[112] This method of engineering mAb-conjugated large molecules that can be disease specific to become brain-penetrating neurotherapeutics has been given significant attention do the potential promise for the treatment of brain and CNS disorders that do not respond to the small class of molecules that freely diffuse across the brain.[113,114] However, despite the attention that has been paid to the area since

the 1980's, minimal clinical applications arising from the RMT strategy have been realized.[115,116] We posit that better models are needed to more adequately mimic the *in vivo* NVU barrier to efficiently advance promising RMT vehicles where there is belief that this is still an emerging area of research.[117–119] Supporting the premise that antibodies are capable of traversing the BBB/NVU is some significant data generated by companies that demonstrate brain interstitial fluid levels of mAbs as reviewed by Wang and colleagues.[18] The main philosophical question that needs to be raised is whether or not targeting brain microvessel endothelial cell receptors will provide the capacity needed to treat targeted therapeutic disorders.

In summary, the major drawback of exploiting endogenous BBB transport pathways for drug delivery is the potential for chronic treatment to result in neurotoxic side effects. It is essential to keep in mind the possibility of transporter mediated delivery approaches are also laborious and associated with higher production costs and there is a need to re-evaluate whether or not clinic success will be realized for the mitigation of neurological disorders that often require chronic treatment. We hypothesize that the utilization of more rigorous *in vitro* screening methodologies during development may potentially help to mitigate unforeseen clinical outcome issues that have been observed in later stages of the pipeline.

1.5.2 *Effects on Drug Development*

Many have postulated that the cellular complexity of the NVU is a significant contributing factor behind the observed high clinical attrition rates of neurotherapeutics. The ability to identify moderate to high lipophilic compounds from lead candidates that more selectively permeate the BBB in efficacious concentrations, without appreciable accumulation or off target neurotoxicity arising from excess brain parenchymal exposure, is quite difficult using current early preclinical *in vitro* and *in vivo* models.[120,121] As stated above, the relatively small class of drugs that can cross

the BBB that are generally lipid-soluble small molecules (<400 kD) that have a potential to treat some neurological disorders. Some smaller, more hydrophilic molecules can traverse the barrier as well, but they normally mimic the characteristics of important signaling molecules like GABA or DOPA. Sometimes overlooked is the significant need for complex biologics that can also aid the mitigation of neurological disorders. The development of brain permeating disease-specific small and large molecules has demonstrated some potential promise via RMT permeation utilizing a molecular Trojan horse, but there has been a long history of this promise going unrealized.[113,122] Moreover, there are also regulatory challenges associated with the approval of brain targeting drugs that have further increased the pressure on the pharmaceutical industry to begin significantly divesting from research in the area.[123,124] It is clear that therapeutics for brain and CNS disorders require the longest development and approval time, have the lowest success rate, and are the most costly of all drug classes.[124] Thus, despite the increasing presence of neurodevelopmental and neurodegenerative disorders across populations, the risk to reward ratio for a company is quite high. This is despite an increase in BBB drug delivery strategies that have become available over the last few decades. However, innovation in the development of more rigorous, physiologically relevant screening tools that can be used to effectively test these methods in a streamlined and cost-effective manner has not paralleled the research efforts in drug delivery and are postulated to be correlative with the failure rates.[125,126] Therefore, the full potential of these novel delivery methods cannot be utilized until there is equal effort put into the development of predictive permeability and toxicity screening methods to adequately test new compounds for potential therapeutic use.

1.6 Screening Tools for BBB Permeability

Tools for screening BBB permeability of hit and lead compounds during discovery and development stages are essential for selecting molecules and delivery methods to continue with in later stages of drug product development. Development of predictive screening tools can help to mitigate the high attrition rates of drugs needing to cross the BBB to target neurological diseases. The most useful tool for *in vitro* screening would have the following attributes: reproducible and validated permeation measurements, potential to evaluate early toxicological markers, and evaluate the drug-BBB interactions in the context of signaling; amenability to moderate to high throughput use; ease of implementation; and a significantly greater semblance to the *in vivo* environment. Moreover, the need to utilize human cell sources is also important as species differences are a confounder and do lead to preclinical advancement prior to clinical failure. Currently, a combination of screening tools meeting one or more of these criterion are used in industry, although there is opportunity for the implementation of a ubiquitous system that is predictive of *in vivo* outcomes and can increase the efficiency of the development of neurotherapeutics by reducing attrition rates in later stages.[126–128]

1.7 Assessing In Vitro Models

The two main methods for analyzing the "tightness" and/or restrictive integrity for *in vitro* models of the BBB are transendothelial electrical resistance (TEER) and analysis of the permeation of markers that traverse cellular barriers via paracellular, transcellular, and active transport. These methods offer an inferred validation aimed at assessing the barrier formation, expression, and function of the BBB endothelium. However, they have been traditionally utilized for monolayer integrity, and do not offer the ability to extend data interpretation to more complex models where

cell layering and permeation linked activity can also be determined. Although the latter is of considerably higher *in vivo* relevance, markers for these types of analysis have not been identified to our knowledge and we rely on the traditional permeants for optimization and validation. A long term goal of the laboratory will be to identify alternative marker compounds that offer better assessment of more complex models, where in the thesis we do evaluate some candidates that may fit under this category.

Tight junction formation is a hallmark of the endothelial and epithelial barriers, but is of particular importance in BBB *in vitro* models due to the high *in vivo* paracellular restriction observed in comparison to other barriers. The least invasive way to monitor indirect "tight junction formation" is by way of TEER, which is more rapid and can be continuously evaluated in contrast to assessing the permeation of solutes or dyes that may alter the barrier properties and often prevent repeated studies. TEER measures the electrical resistance of a barrier by monitoring the current between two electrodes in response to a voltage of a given frequency.[129] Resistance of the cell layer, R_{CELL}, is inversely proportional to the surface area of the permeable support, M_{AREA}, the cells are plated on, so values are reported as Ohm·cm^2.[130]

$$TEER = R_{CELL}(\Omega) \times M_{AREA}\,(cm^2) \qquad \text{(eq. 1)}$$

In vivo TEER values have been reported from 1500 to 6000 Ω·cm^2, whereas *in vitro* models can range from 50 to 2500 Ω·cm^2 depending on the cell source and medium additives used.[131,132] Although TEER is a noninvasive method for barrier integrity during the time of culture for *in vitro* models, it is highly variable to several factors including temperature, electrode placement, and medium conditions; therefore, the use of permeable solutes is often a more reliable and reproducible measure of barrier "tightness".[130] Note, tightness is relative as we generally assume

that the cells are in a monolayer configuration with tight junctions restricting ion and hydrophilic substrate flux, however cells can overgrow and form multilayers which will still restrict flux.

The apparent permeability, P_{app}, of a solute across a cellular barrier is based on the amount of the solute that moves to the receiver chamber in a given time as calculated by the following equation (eq. 2)

$$P_{app}(^{cm}/_{sec}) = \frac{^{dM}/_{dt}}{C_0 * SA * 60}$$

(eq. 2)

where $^{dM}/_{dt}$ represents the rate of compound movement across the cell layer, C_0 is the initial concentration of compound in the donor chamber, SA is the surface area of the filter support, and 60 is a correction factor that converts from minutes to seconds. This equation only holds true when sink conditions are maintained, otherwise additional information like appreciable cell accumulation and loss of sink in the receiver need to be mathematically incorporated. The apparent permeability measures the permeation across the entire system including the filter support. The effective permeability, P_{eff}, represents the permeation of the solute across the cell layer alone, and can be calculated by subtraction of the permeability across the filter support alone, P_{filter} (eq. 3).

$$\frac{1}{P_{app}} = \frac{1}{P_{eff}} + \frac{1}{P_{filter}}$$

(eq. 3)

Permeability of paracellular markers of ranging sizes can be used to interpret the tightness of the barrier and estimate an average pore size using the Renkin molecular sieving function as the size of the marker approaches the pore radii.[97,133–135] Transcellular markers and actively transported substrates can be used in similar permeability screening assays to assess the integrity of the lipid

membrane and function of SLC and ABC transporters. In each of these cases, mass balance must be accounted for and sink conditions must be maintained.

Efflux transporter function can be assessed using either bidirectional permeability assays or a cellular uptake assay in the presence or absence of an efflux inhibitor. Bidirectional permeability involves measuring the movement of a solute in both the apical to basolateral (A-B) and the basolateral to apical (B-A) directions.[136–138] Bidirectional assays are used to calculate the efflux ratio (eq. 4), where an efflux marker resulting in a ratio greater than or equal to 2.5 implies good transporter expression and function on the apical surface.

$$Efflux\ Ratio, 2.5\ \geq\ \frac{P_{app}\ B \rightarrow A}{P_{app}\ A \rightarrow B}$$

(eq. 4)

Bidirectional screening can be challenging due to the requirement for apical membrane localization of transporters. Cellular accumulation or uptake studies can be performed to assess efflux transporter function in place of bidirectional permeability, however cellular uptake studies cannot be used to interpret membrane localization of transporters. There are several efflux transporters expressed on the basolateral membrane as well, where the efflux ratio of 0.4 or lower can be indicative of the function of these isoforms. However, these are often overlooked and underappreciated. Interestingly, there have been studies that have suggested P-gp may be expressed on both the apical and basolateral surfaces of the brain microvessel endothelial cells, which may present confounding data when using *in vitro* models.

Additional molecular biology based techniques can be used for in depth evaluation of a given model. These assessments could include antibody staining for the evaluation of protein expression and localization, proteomic screening for protein expression levels, and morphological visualization of cell types. Although these methods provide a deep understanding of the barrier

properties and cellular phenotypes with the model, they do not lend themselves for robust screening. These advanced techniques should be used in early development and validation of *in vitro* models to gain understanding of attributes that cannot be elucidated using traditional permeability assessment methods.

1.8 Non-cell Based Models

In vivo and *in situ* models are typically cost and time prohibitive for screening a large number of compounds or delivery methods.[127,128] Due to the lower costs and higher throughput capabilities *in silico* and *in vitro* screening models offer a more rapid option for screening larger compound libraries that may traverse the NVU and reach the brain parenchyma. Though *in silico* models may be the highest throughput, the intricacies of the NVU, as well as formulations, are difficult to mimic computationally in part due to the fact that most screens rely heavily on physicochemical properties/structure-activity relationships that limit their predictive efficiency. Hence, *in vitro* permeability models that are not cell based have been the mainstay of early preclinical screening as they tend to have some physiological semblance and are considered more predictive of *in vivo* permeation via the lipid bilayer passive transcellular pathway.[126] One of the primary non-cell based *in vitro* models, parallel artificial membrane permeability assays (PAMPA), was first developed to measure gastrointestinal absorption of compounds using an artificial lipid membrane and have been subsequently modified to provide better predictions of BBB permeability[139,140] Although it offers high throughput, PAMPA-BBB lacks the presence of all proteins, transporters, and cell types of the NVU as well as the ability to predict permeation of compounds that do not passively diffuse across physiologically resembling cell based methods.[141] Thus, *in silico* and non-cell based *in vitro* assays are most useful in early discovery stages to

support hit compound identification due to the larger capacity for chemical libraries, however lead candidate selection requires a more in depth consideration of drug interactions with the BBB-like cell based models that can help in the prioritization process by revealing potential confounding issues including transporter and metabolism effects.[128]

1.9 Cell Sources for In Vitro Models

The chosen cell sources for *in vitro* BBB models has evolved with the field as isolation, immortalization, and stem cell reprogramming techniques have improved.[142–152] The cells of choice have only continued to expand, however selection should be predicated on the phenotypic objectives being sought with the screen as some sources are more appropriate than others. Although the ideal cell model for neurotherapeutic screening would be derivative of the human brain, there is utility for animal and modified non-brain cell models.

1.9.1 *Animal Cell Sources*

Early cell based models were achieved by isolation of whole animal brain capillaries, primarily from murine, bovine, and porcine sources, which were later purified to primary endothelial cells.[143,145,153,154] Isolation and purification techniques require intricate and lengthy protocols that are not conducive for extended culturing even though they often show promise in key BBB characteristics.[155,156] Primary animal BBB endothelial cells are limited to larger animal sources (bovine, porcine, etc.) due to low purification yields of smaller species. Since rat and mouse species are often used for early *in vivo* studies, these species can be preferred for animal based *in vitro* BBB screening because of the ease of translation. Due to the low yield of rodent

primary cells, immortalized cell lines from mouse (cEND and cerebEND) and rat (RBE4) sources have been developed and well characterized for permeability screening.[157,158]

Bovine endothelial cells were frequently used in primary cultures due to the ability to isolate a large number of cells from a single brain. These cultures showed high endothelial resistance, differentiated tight junctions, and adequate P-gp expression.[143,144,159,160] It has been shown that there is a high degree of variability in primary bovine model performance in inter- and intra-laboratory culture of the same model, which has led to the development of ready-to-use screening tools for bovine based systems.[159–161] Primary porcine endothelial cells have also been established for *in vitro* screening showing high electrical resistance in comparison to other primary cell sources, along with transporter and efflux expression.[145,154] Immortalized cell lines of bovine and porcine brain endothelium were established for permeability screening; however, due to the availability and superior barrier properties of primary cells they were not as readily studied despite the advantages of reproducibility and ease of culture.[162,163]

Animal cell sources were most useful in the early establishment of cell based *in vitro* models because of their availability and the lack of readily accessible human based sources. These systems helped to establish the foundation of *in vitro* BBB permeability screening, but with the shift to human cell sources, the early animal based models are not relied on as heavily as they once were.

1.9.2 *Human Cell Sources*

Unlike the accessibility of primary animal brain endothelium, primary human brain cells are harder to obtain due to ethical issues and the high variability in human sources. Some have gone on to establish protocols for human brain endothelial cell isolation; however, the study of and availability of these sources are limited.[152,164] With continued interest in neurodegenerative

disorders and the knowledge of phenotypic differences of diseased versus healthy states, primary brain cells from Parkinson's or Alzheimer's patients were commercially available (Lonza Scientific, discontinued) and postulated for utility in later stage screening of entities attempting to treat these conditions. For general screening studies, interest should remain in immortalized, transfected, and stem cell derived sources for reproducible *in vitro* permeability assays. After early screens, the ability to utilize phenotypic sources of cells should then be used on a small scale for confirmatory purposes.

One of the key characteristics of the BBB is the high expression of efflux transporters, specifically P-gp. Because of this, many non-brain human cell sources are used to predict efflux ratios of potential neurotherapeutics. Mandin-Darby Canine Kidney (MDCK) cells have lower expressions of P-gp but, a derivation of this cell line transfected with the P-gp *MDR1* gene (MDR1-MDCK) has been used to model efflux of the BBB.[141,165] Although the MDR1-MDCK cell line is useful for predicting P-gp efflux, the results of such studies are difficult to correlate to *in vivo* BBB efflux due to the differences in expression levels and tight junction formation of BBB endothelium compared to peripheral or alternative epithelial barriers.[166]

Immortalized human BBB endothelial cell lines have been established to have a reliable source for *in vitro* studies where results can be reproducible between laboratories. There are many immortalized cell lines available including hCMEC/D3, BB19, TY10, hBMEC, HBEC-5i, and others. Comparisons and independent studies of these cell lines have frequently been performed showing that hBMEC and hCMEC/D3 cells show the best barrier properties based on electrical resistance, permeability of various markers, and expression of tight junction proteins.[146,167,168] The hCMEC/D3 cell line is the most studied of all available immortalized sources since its establishment in 2005.[168] Studies of this cell line have shown expression of tight junction proteins,

reproducibility of *in vitro* permeation results, and expression and function of various transporters which all aid in its frequent use in the field.[97,146,167,169,170] Since the hCMEC/D3 cell line is doubly transfected with SV40 and hTERT oncogen and has been so frequently used, it is not as stable in the phenotypic expression of BBB proteins as it was originally. For example, recent studies have revealed a loss of P-gp expression at higher passage numbers, which we have also observed (unpublished results), and relatively "leaky" tight junctions in comparison with other human brain endothelial cell sources.[131,170] The use of HBEC-5i cells for *in vitro* permeability screening has started to increase since they were first developed for the study of cerebral malaria.[171] Studies, including our laboratory's in-house model development with HBEC-5i cells detailed in this thesis, have supported the contention that they show promise comparative to the hCMEC/D3 cells and potentially other immortalized sources—based on critical BBB functional characteristics.[172,173]

In an effort to move away from the reliance on immortalized cell lines and improve the *in vivo* relevance of BBB screening tools, there has been a shift in the field of *in vitro* cell models to BMEC endothelial cultures derived from stem cell sources. These cell lines are a derivative of human induced pluripotent stem cells (hiPSCs) and reprogrammed to differentiate into endothelium with expression of BBB traits.[151,174] Studies have shown higher electrical resistance, lower paracellular permeability, functional transporters, and localization of tight junction proteins at cell-cell contacts for iPSC derived enothelium.[151,174] Models utilizing these sources are not well characterized as there is cell source heterogeneity and the pluripotency concerns that need further investigation to advance the field from its infancy. However, early screening and optimization has been successful with additives and conditioned medium and demonstrates the considerable promise that may be realized for stem cell derived BBB/NVU as the future *in vitro* screens are developed to advance the field.[175] The establishment of hiPSC brain endothelial cells fills the gap

between primary and immortalized cell sources. Stem cell derived endothelium offers a renewable and robust source for *in vitro* screening similar to immortalized cells, while also mimicking *in vivo* BBB endothelium at levels equivalent to those seen in primary cells.[150,176] Some work has been done to streamline the process; however, the methods are still intricate and culture method dependent (*i.e.* matrigel source) for hiPSC brain endothelium differentiation, suggesting that there is still method refinement required before the use of these cell sources can be widespread.[131,177–179]

1.10 Cell Based In Vitro Models

In vitro cell based BBB screening models have been predominantly developed as Transwell® assays as the filter support system readily lends itself to the measurement of permeation markers and drugs of interest across the cell barrier. These models also enable the easy assessment of TEER and marker permeability in a streamlined fashion without the need for an elaborate screening set-up. One flaw with the Transwell® configuration for BBB screening is that they do not mimic the tubule formation of *in vivo* capillaries or incorporate shear stress of fluid flow over the endothelium.[126,180] Shear stress due to fluid flow over the endothelium has been shown to increase barrier properties, particularly paracellular tightness, making *in vitro* models that mimic capillary flow a way in enhance *in vivo* relevancy.[181–185] The evolution of flow enabled microfluidic and related models, alternatively identified as BBB-on-a-chip where cells are either plated on a membrane or ECM surface, is that they can allow for capillary like configurations.[119,182,186–188] While there have been some very compelling results demonstrated using these microfluidic approaches, issues including the lack of capillary like “tubule” formation of the endothelium, cellular overgrowth, experimental variability in approaches, and differences in marker compound

permeation requires that standardization of the methods is warranted.[188] Models that incorporate tubule formation involve seeding cells in a perfused gelatinized ECM and benefit from a three dimensional representation of the BBB as opposed to other models that mimic the BBB in a two dimensional manner.[177,180,189,190] Although these systems mimic capillary formation, the tubules formed are significantly larger than *in vivo* due to the need for high seeding densities and subsequent potential for clumping or stacking of the cells which can clog the perfused ECM. Ultimately, there are drawbacks to all *in vitro* models with each having their place in the development pipeline. An *in vitro* model should be reproducible, easy to use, and amenable to larger scale screening studies. For these reasons, the Transwell® system is the simplest to use and can most easily be scaled to accommodate large libraries in comparison to microfluidic or 3D models which require more intricate plating methods.

1.10.1 *Incorporating the NVU*

In vitro assays on permeable supports were originally established as monolayers of solely the endothelium. Monoculture models are easy to implement, but are entirely dependent on the inherent characteristics of the endothelial cell line. Early research included modifications to culturing and media conditions to establish protocols for these assays, which demonstrated that certain BBB characteristics of endothelial cell lines could be enhanced via culturing methods.[144,191–193] With the continued efforts to understand the milieu of the BBB and NVU, researchers realized the importance of the supporting cells to the phenotypic expression of the endothelium.[10,15,31,32,194] Multicellular co- and triculture systems were developed and showed an increased complexity and increased barrier properties in comparison monolayer models.

The other cells of the NVU, astrocytes, pericytes, neurons, and microglia, have been well established as key factors in the induction of endothelial barrier properties. Given this, the *in vitro*

models incorporating aspects of the NVU in culture methods should result in the best screening tools with the most *in vivo* relevancy. Astrocytes are the NVU cell type that is most prevalent in coculture systems. This is likely due the extensive research on the interactions between the endothelium and the astrocytes as well as the knowledge of their estimated 99% coverage of the microvessel, suggesting that they would play a more important role than pericytes or neurons in the induction of barrier properties.[10,14] Coculture models were established by plating astrocytes in the basolateral well plate or on the reverse side of the permeable filter support.[195–198] Although the addition of astrocytes to the *in vitro* system showed increased barrier properties compared to monolayers, it was later observed that the surface the astrocytes are plated on, as well as filter specifications, plays a large role in the tightness of the model.[197] The use of pericytes in coculture systems was not as prevalent; however, pericytes have been shown to play a major role in angiogenesis and vascular development.[50,58,199–201]

All cells of the NVU are critical in the induction of barrier properties; therefore, BBB *in vitro* models continued to increase in complexity by moving to the next logical step—triculture, inclusion of both astrocytes and pericytes with endothelial cells.[202] Triculture models include variations in the seeding surface of astrocytes and pericytes (one on the basolateral well plate and the other on the reverse side of the filter support) with endothelial cells seeded on the apical side of the filter.[131,203–205] Neurons have also been shown to influence barrier properties which led to the inclusion of neurons in some multicellular *in vitro* systems.[149,206] Triculture models increase the complexity of the screening tools making them less manageable for larger assays, but the inclusion of multiple cell types increases the *in vivo* relevancy of the model which is ultimately the goal of an *in vitro* BBB screening tool.[207]

The way in which the different cells of co- and triculture models are arranged can vary based on which surface the cells types are seeded on. Typically, each cell type is seeded on a different surface to make up the system; however, this is not relevant comparative to the *in vivo* cell-cell contacts. *In vivo*, the endothelium, pericytes, and astrocytes are separated by the basal lamina which is approximately 20 nm thick.[4] In multicellular models the different cell types are separated by at least 10 µm when they are plated on opposite sides of the filter support, making the distance ~500 times greater compared to *in vivo*. *In vitro* models that seed cells on both sides of the filter support are often deemed "contact" models, while those which seed on the apical filter surface and basolateral well plate are referred to as "non-contact" models in the field. These terms are misleading as both systems involve indirect contact between different cell types due to the inclusion of a filter support or seeding on different surfaces (Fig. 1.4). The cell-cell signaling

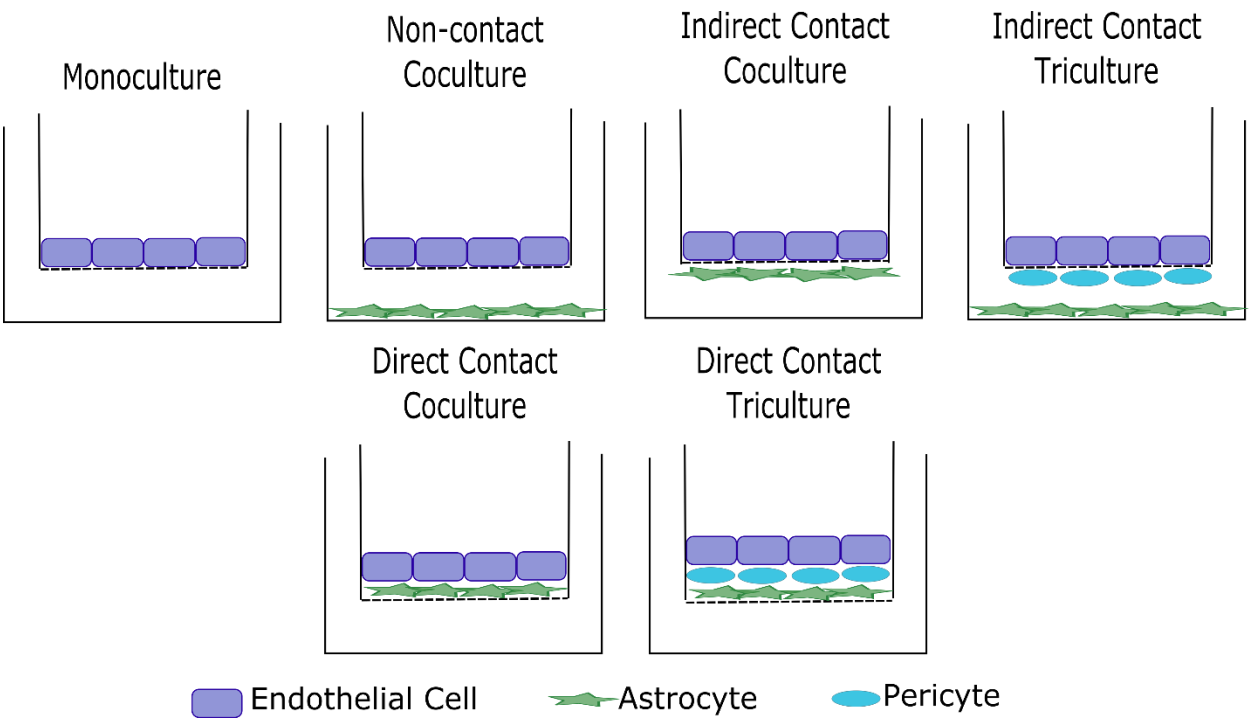

Figure 1.4. Commonly used *in vitro* models of the BBB incorporating multiple cells of the neurovascular unit. In this review the "indirect contact" models are commonly referred to as "contact models" in the field but in fact lack direct contact between the different cell types of the NVU due to the separation of plating surfaces.

between the NVU is essential for the induction of barrier properties as shown in direct contact co- and triculture models.[31,208,209] These direct contact *in vitro* models involve the sequential seeding of cell types on top of one another to establish a fully apical model (Fig. 1.4). Direct contact plating methodologies increase the *in vivo* relevancy of the screening tool and eliminate the need to manipulate the orientation of the filter support during cell seeding which complicates the implementation of the model for large screening assays.

1.10.2 *Combining Neuroactivity Screening*

Although neurons do contribute to endothelial induction, the greatest utility of neurons in screening tools is to assess the implications compounds have on neuroactivity.[206,210,211] As compounds cross the BBB they may have potentially positive, negligible, or negative effects on neurons and the associated neuronal environment encountered in the brain parenchyma. The incorporation of neurons into an *in vitro* system adds another aspect of screening during pharmaceutical development where one can fundamentally assess how permeability is linked to neuronal effects. BBB permeability and neurotoxicity have traditionally been assessed separately by comparing neuronal health after incubation with a compound at the concentration derived post *in vitro* BBB assay.[210] Separation of the two screens is time consuming, but it is a start for the assessment of the full impact of BBB permeability linked neuroactivity. The current neurotoxicity testing requirements are based on behavioral and pathological outcomes from *in vivo* screening; however, the implementation of established *in vitro* models can aid in understanding biological and molecular implications of neurotherapy or neurotoxicity, and possibly mitigate later stage failures due to the inability to predict beneficial or adverse responses early in the preclinical screening and development stages.[212] BBB-linked neuroactivity should be evaluated by first understanding if a compound crosses the BBB, followed by an in depth look at its implications on

barrier integrity and responses in the brain neuronal parenchyma.[213] It is also important to establish the endpoint measurements of these models as neurotherapeutic or neurotoxic compounds can have effects on cells of the NVU or specifically neuronal health.[214]

1.11 The Physiologically Relevant, Enhanced In Vitro Model

In vitro models for BBB screening are meant for use as tools during pharmaceutical development to help mitigate the high attrition rates in *in vivo* testing and clinical trials. The implementation of a universal physiologically relevant *in vitro* model enabling permeability and neuronal response assessment would provide investigators with a tool to more relevantly down select and rank hit and lead candidate compounds, formulations, and delivery approaches before moving on to higher cost testing. Such an *in vitro* BBB screening tool would need to meet the following criteria: (1) ease of implementation for users; (2) cost effective for large screening assays; (3) *in vivo* correlation and physiological relevancy; (4) provide utility in both BBB permeability and neuroactivity screening. Based on the current technologies available and the needs of the field, the best *in vitro* model would consist of fully human cell lines derived from either primary or stabilized phenotypic iPSC sources, incorporate all cells of the NVU in direct cell-cell contact, and combine permeability and neurotherapeutic/neurotoxic testing in a single streamlined system (Fig. 1.5).

Ultimately, the goal of developing new *in vitro* models of the BBB is to effectively replace the current tools that are being used in order to increase the chances for success in the development of neurotherapeutics. The current models being used by investigators including the pharmaceutical industry are predominantly of non-human and non-brain origins making it difficult to predict outcomes of *in vivo* testing. Additionally, the ideal *in vitro* model should aim to be a standard tool

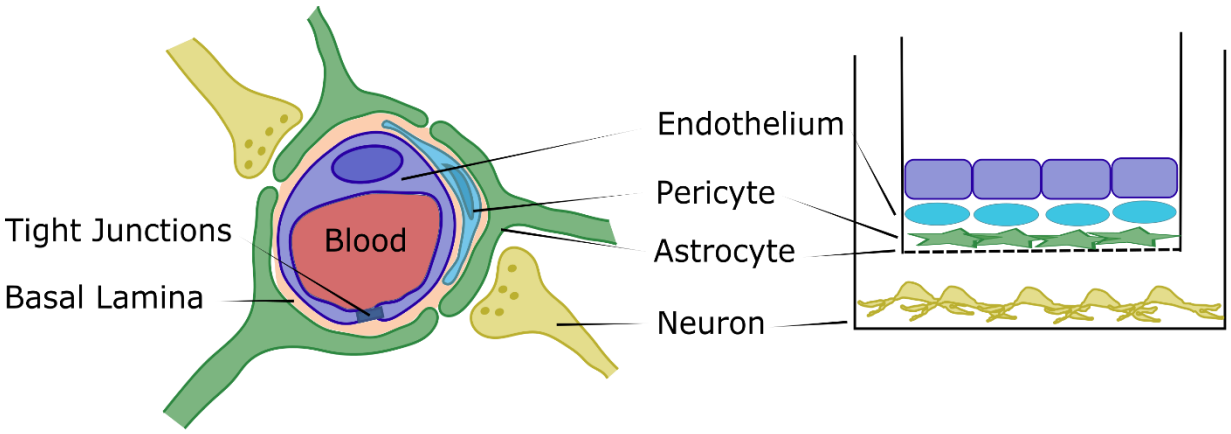

Figure 1.5. The physiologically relevant, enhanced *in vitro* BBB screening model will incorporate all cell types of the NVU in direct cell-cell contact. This model is relevant to the *in vivo* physiology and incorporates BBB permeability and neurotoxicity screening in one system.

that can be implemented across CNS therapeutic programs. The establishment of a standard *in vitro* BBB screening tool has the potential to have a lasting impact on the market of neurotherapeutics by increasing the chances of selecting successful compounds for further development.

The work detailed in this thesis aims to improve on the previously established direct contact co- and triculture models using design of experiments (DOE) based optimization and alternative cell sources. Detailed herein is the establishment of a physiologically relevant, enhanced model of the NVU (Fig. 1.5) to assess BBB-permeability linked neuroactivity of marker compounds. The early development work detailed in the following chapters establishes this model as a promising screening tool that can be incorporated in hit and lead candidate screening to ultimately reduce the number of *in vitro* models required for preliminary evaluation and potentially reduce attrition rates of neurotherapeutics in later stages of development.

1.12 References

1. Abbott, N. J., Patabendige, A. A. K., Dolman, D. E. M., Yusof, S. R. & Begley, D. J. Structure and function of the blood-brain barrier. *Neurobiol. Dis.* **37**, 13–25 (2010).
2. Begley, D. J. Structure and Function of the Blood-Brain Barrier. in *Enhancement in Drug Delivery* (eds. Touitou, E. & Barry, B. W.) 575–592 (CRC Press, 2006).
3. Weiss, N., Miller, F., Cazaubon, S. & Couraud, P.-O. The blood-brain barrier in brain homeostasis and neurological diseases. *Biochim. Biophys. Acta BBA - Biomembr.* **1788**, 842–857 (2009).
4. Serlin, Y., Shelef, I., Knyazer, B. & Friedman, A. Anatomy and Physiology of the Blood-Brain Barrier. *Semin. Cell Dev. Biol.* **38**, 2–6 (2015).
5. Persidsky, Y., Ramirez, S. H., Haorah, J. & Kanmogne, G. D. Blood–brain Barrier: Structural Components and Function Under Physiologic and Pathologic Conditions. *J. Neuroimmune Pharmacol.* **1**, 223–236 (2006).
6. Abbott, N. J. & Friedman, A. Overview and introduction: The blood–brain barrier in health and disease. *Epilepsia* **53**, 1–6 (2012).
7. Abbott, N. J. Blood-brain barrier structure and function and the challenges for CNS drug delivery. *J. Inherit. Metab. Dis.* **36**, 437–449 (2013).
8. Berger, J. R. *et al.* Importance and hurdles to drug discovery for neurological disease. *Ann. Neurol.* **74**, 441–446 (2013).
9. Pardridge, W. M. The Blood-Brain Barrier: Bottleneck in Brain Drug Development. *NeuroRx* **2**, 3–14 (2005).
10. Abbott, N. J., Rönnbäck, L. & Hansson, E. Astrocyte-endothelial interactions at the blood-brain barrier. *Nat. Rev. Neurosci.* **7**, 41–53 (2006).

11. Mäe, M., Armulik, A. & Betsholtz, C. Getting to know the cast - cellular interactions and signaling at the neurovascular unit. *Curr. Pharm. Des.* **17**, 2750–2754 (2011).

12. Iadecola, C. & Nedergaard, M. Glial regulation of the cerebral microvasculature. *Nat. Neurosci.* **10**, 1369–1376 (2007).

13. Winkler, E. A., Bell, R. D. & Zlokovic, B. V. Central nervous system pericytes in health and disease. *Nat. Neurosci.* **14**, 1398–1405 (2011).

14. Mathiisen, T. M., Lehre, K. P., Danbolt, N. C. & Ottersen, O. P. The perivascular astroglial sheath provides a complete covering of the brain microvessels: An electron microscopic 3D reconstruction. *Glia* **58**, 1094–1103 (2010).

15. Armulik, A. *et al.* Pericytes regulate the blood-brain barrier. *Nature* **468**, 557–561 (2010).

16. Hawkins, B. T. & Davis, T. P. The Blood-Brain Barrier/Neurovascular Unit in Health and Disease. *Pharmacol. Rev.* **57**, 173–185 (2005).

17. Dombrowski, S., Najm, I. & Janigro, D. Central Nervous System Microenvironment and Neuronal Excitability. in *The Neuronal Environment: Brain Homeostasis in Health and Disease* (ed. Walz, W.) 3–24 (Humana Press, 2002). doi:10.1007/978-1-59259-108-4_1

18. Wang, Q. *et al.* Monoclonal antibody exposure in rat and cynomolgus monkey cerebrospinal fluid following systemic administration. *Fluids Barriers CNS* **15**, 10 (2018).

19. Keep, R. F., Jones, H. C. & Drewes, L. R. The year in review: progress in brain barriers and brain fluid research in 2018. *Fluids Barriers CNS* **16**, 4 (2019).

20. Benveniste, H., Lee, H. & Volkow, N. D. The Glymphatic Pathway: Waste Removal from the CNS via Cerebrospinal Fluid Transport. *Neurosci. Rev. J. Bringing Neurobiol. Neurol. Psychiatry* **23**, 454–465 (2017).

21. Ratner, V. *et al.* Cerebrospinal and interstitial fluid transport via the glymphatic pathway modeled by optimal mass transport. *NeuroImage* **152**, 530–537 (2017).

22. Abbott, N. J., Pizzo, M. E., Preston, J. E., Janigro, D. & Thorne, R. G. The role of brain barriers in fluid movement in the CNS: is there a 'glymphatic' system? *Acta Neuropathol. (Berl.)* **135**, 387–407 (2018).

23. Nedergaard, M. Neuroscience. Garbage truck of the brain. *Science* **340**, 1529–1530 (2013).

24. Plog, B. A. & Nedergaard, M. The Glymphatic System in Central Nervous System Health and Disease: Past, Present, and Future. *Annu. Rev. Pathol.* **13**, 379–394 (2018).

25. Mestre, H. *et al.* Aquaporin-4-dependent glymphatic solute transport in the rodent brain. *eLife* **7**, (2018).

26. Yin, M. *et al.* Astroglial water channel aquaporin 4-mediated glymphatic clearance function: A determined factor for time-sensitive treatment of aerobic exercise in patients with Alzheimer's disease. *Med. Hypotheses* **119**, 18–21 (2018).

27. Verheggen, I. C. M., Van Boxtel, M. P. J., Verhey, F. R. J., Jansen, J. F. A. & Backes, W. H. Interaction between blood-brain barrier and glymphatic system in solute clearance. *Neurosci. Biobehav. Rev.* **90**, 26–33 (2018).

28. Bushong, E. A., Martone, M. E. & Ellisman, M. H. Maturation of astrocyte morphology and the establishment of astrocyte domains during postnatal hippocampal development. *Int. J. Dev. Neurosci. Off. J. Int. Soc. Dev. Neurosci.* **22**, 73–86 (2004).

29. Medvedev, N. *et al.* Glia selectively approach synapses on thin dendritic spines. *Philos. Trans. R. Soc. Lond. B. Biol. Sci.* **369**, 20140047 (2014).

30. Schiweck, J., Eickholt, B. J. & Murk, K. Important Shapeshifter: Mechanisms Allowing Astrocytes to Respond to the Changing Nervous System During Development, Injury and Disease. *Front. Cell. Neurosci.* **12**, (2018).

31. Bouchaud, C., Le Bert, M. & Dupouey, P. Are close contacts between astrocytes and endothelial cells a prerequisite condition of a blood-brain barrier? The rat subfornical organ as an example. *Biol. Cell* **67**, 159–165 (1989).

32. Oberheim, N. A., Wang, X., Goldman, S. & Nedergaard, M. Astrocytic complexity distinguishes the human brain. *Trends Neurosci.* **29**, 547–553 (2006).

33. Halassa, M. M., Fellin, T., Takano, H., Dong, J.-H. & Haydon, P. G. Synaptic islands defined by the territory of a single astrocyte. *J. Neurosci. Off. J. Soc. Neurosci.* **27**, 6473–6477 (2007).

34. Bushong, E. A., Martone, M. E., Jones, Y. Z. & Ellisman, M. H. Protoplasmic astrocytes in CA1 stratum radiatum occupy separate anatomical domains. *J. Neurosci. Off. J. Soc. Neurosci.* **22**, 183–192 (2002).

35. Nag, S. Morphology and properties of astrocytes. *Methods Mol. Biol. Clifton NJ* **686**, 69–100 (2011).

36. Hol, E. M. & Pekny, M. Glial fibrillary acidic protein (GFAP) and the astrocyte intermediate filament system in diseases of the central nervous system. *Curr. Opin. Cell Biol.* **32**, 121–130 (2015).

37. Pekny, M. & Pekna, M. Astrocyte intermediate filaments in CNS pathologies and regeneration. *J. Pathol.* **204**, 428–437 (2004).

38. Pekny, M. & Wilhelmsson, U. GFAP and Astrocyte Intermediate Filaments. in *Handbook of Neurochemistry and Molecular Neurobiology* 289–314 (Springer, Boston, MA, 2006). doi:10.1007/978-0-387-30381-9_14

39. Liedtke, W. *et al.* GFAP Is Necessary for the Integrity of CNS White Matter Architecture and Long-Term Maintenance of Myelination. *Neuron* **17**, 607–615 (1996).

40. Yang, Z. & Wang, K. K. W. Glial fibrillary acidic protein: from intermediate filament assembly and gliosis to neurobiomarker. *Trends Neurosci.* **38**, 364–374 (2015).

41. Liao, C.-W. *et al.* Blood–brain barrier impairment with enhanced SP, NK-1R, GFAP and Claudin-5 expressions in experimental cerebral toxocariasis. *Parasite Immunol.* **30**, 525–534 (2008).

42. Rash, J. E., Yasumura, T., Hudson, C. S., Agre, P. & Nielsen, S. Direct immunogold labeling of aquaporin-4 in square arrays of astrocyte and ependymocyte plasma membranes in rat brain and spinal cord. *Proc. Natl. Acad. Sci. U. S. A.* **95**, 11981–11986 (1998).

43. Moroni, R. F., Inverardi, F., Regondi, M. C., Pennacchio, P. & Frassoni, C. Developmental expression of Kir4.1 in astrocytes and oligodendrocytes of rat somatosensory cortex and hippocampus. *Int. J. Dev. Neurosci.* **47**, 198–205 (2015).

44. Wolburg, H. & Lippoldt, A. Tight junctions of the blood-brain barrier: development, composition and regulation. *Vascul. Pharmacol.* **38**, 323–337 (2002).

45. Wolburg, H., Wolburg-Buchholz, K., Fallier-Becker, P., Noell, S. & Mack, A. F. Chapter one - Structure and Functions of Aquaporin-4-Based Orthogonal Arrays of Particles. in *International Review of Cell and Molecular Biology* (ed. Jeon, K. W.) **287**, 1–41 (Academic Press, 2011).

46. Alvarez, J. I., Katayama, T. & Prat, A. Glial influence on the Blood Brain Barrier. *Glia* **61**, 1939–1958 (2013).

47. Cabezas, R. *et al.* Astrocytic modulation of blood brain barrier: perspectives on Parkinson's disease. *Front. Cell. Neurosci.* **8**, (2014).

48. Lee, S.-W. *et al.* SSeCKS regulates angiogenesis and tight junction formation in blood-brain barrier. *Nat. Med.* **9**, 900–906 (2003).

49. Argaw, A. T., Gurfein, B. T., Zhang, Y., Zameer, A. & John, G. R. VEGF-mediated disruption of endothelial CLN-5 promotes blood-brain barrier breakdown. *Proc. Natl. Acad. Sci. U. S. A.* **106**, 1977–1982 (2009).

50. Daneman, R., Zhou, L., Kebede, A. A. & Barres, B. A. Pericytes are required for blood-brain barrier integrity during embryogenesis. *Nature* **468**, 562–566 (2010).

51. Armulik, A., Genové, G. & Betsholtz, C. Pericytes: Developmental, Physiological, and Pathological Perspectives, Problems, and Promises. *Dev. Cell* **21**, 193–215 (2011).

52. Bell, R. D. *et al.* Pericytes control key neurovascular functions and neuronal phenotype in the adult brain and during brain aging. *Neuron* **68**, 409–427 (2010).

53. Winkler, E. A., Sagare, A. P. & Zlokovic, B. V. The pericyte: A Forgotten Cell Type with Important Implications for Alzheimer's disease? *Brain Pathol. Zurich Switz.* **24**, 371–386 (2014).

54. Hamilton, N. B., Attwell, D. & Hall, C. N. Pericyte-mediated regulation of capillary diameter: a component of neurovascular coupling in health and disease. *Front. Neuroenergetics* **2**, (2010).

55. Hellström, M., Kalén, M., Lindahl, P., Abramsson, A. & Betsholtz, C. Role of PDGF-B and PDGFR-beta in recruitment of vascular smooth muscle cells and pericytes during embryonic blood vessel formation in the mouse. *Dev. Camb. Engl.* **126**, 3047–3055 (1999).

56. Abramsson, A., Lindblom, P. & Betsholtz, C. Endothelial and nonendothelial sources of PDGF-B regulate pericyte recruitment and influence vascular pattern formation in tumors. *J. Clin. Invest.* **112**, 1142–1151 (2003).

57. Lebrin, F., Deckers, M., Bertolino, P. & Ten Dijke, P. TGF-beta receptor function in the endothelium. *Cardiovasc. Res.* **65**, 599–608 (2005).

58. Dohgu, S. *et al.* Brain pericytes contribute to the induction and up-regulation of blood-brain barrier functions through transforming growth factor-beta production. *Brain Res.* **1038**, 208–215 (2005).

59. Hofmann, J. J. & Iruela-Arispe, M. L. Notch signaling in blood vessels: who is talking to whom about what? *Circ. Res.* **100**, 1556–1568 (2007).

60. Wang, Y., Pan, L., Moens, C. B. & Appel, B. Notch3 establishes brain vascular integrity by regulating pericyte number. *Dev. Camb. Engl.* **141**, 307–317 (2014).

61. Baeten, K. M. & Akassoglou, K. Extracellular Matrix and Matrix Receptors in Blood-Brain Barrier Formation and Stroke. *Dev. Neurobiol.* **71**, 1018–1039 (2011).

62. Hannocks, M.-J., Huppert, J., Zhang, X., Korpos, E. & Sorokin, L. The Contribution of the Extracellular Matrix to the BBB in Steady State and Inflammatory Conditions. in *The Blood Brain Barrier and Inflammation* 49–60 (Springer, Cham, 2017). doi:10.1007/978-3-319-45514-3_3

63. Osada, T. *et al.* Interendothelial claudin-5 expression depends on cerebral endothelial cell-matrix adhesion by B 1-integrins. *J. Cereb. Blood Flow Metab.* **31**, 1972–1985 (2011).

64. Thomsen, M. S., Birkelund, S., Burkhart, A., Stensballe, A. & Moos, T. Synthesis and deposition of basement membrane proteins by primary brain capillary endothelial cells in a murine model of the blood–brain barrier. *J. Neurochem.* **140**, 741–754 (2017).

65. Yao, Y., Chen, Z.-L., Norris, E. H. & Strickland, S. Astrocytic laminin regulates pericyte differentiation and maintains blood brain barrier integrity. *Nat. Commun.* **5**, 3413 (2014).

66. Schurr, A. Neuronal Energy Requirements. in *The Neuronal Environment: Brain Homeostasis in Health and Disease* (ed. Walz, W.) 25–54 (Humana Press, 2002). doi:10.1007/978-1-59259-108-4_2

67. Banerjee, S. & Bhat, M. A. Neuron-Glial Interactions in Blood-Brain Barrier Formation. *Annu. Rev. Neurosci.* **30**, 235–258 (2007).

68. Hall, C. N. *et al.* Capillary pericytes regulate cerebral blood flow in health and disease. *Nature* **508**, 55–60 (2014).

69. Iadecola, C. The Neurovascular Unit Coming of Age: A Journey through Neurovascular Coupling in Health and Disease. *Neuron* **96**, 17–42 (2017).

70. Haseloff, R. F., Dithmer, S., Winkler, L., Wolburg, H. & Blasig, I. E. Transmembrane proteins of the tight junctions at the blood-brain barrier: structural and functional aspects. *Semin. Cell Dev. Biol.* **38**, 16–25 (2015).

71. Bauer, H.-C., Krizbai, I. A., Bauer, H. & Traweger, A. 'You Shall Not Pass'-tight junctions of the blood brain barrier. *Front. Neurosci.* **8**, 392 (2014).

72. Kniesel, U. & Wolburg, H. Tight Junctions of the Blood–Brain Barrier. *Cell. Mol. Neurobiol.* **20**, 57–76 (2000).

73. Furuse, M. *et al.* Occludin: a novel integral membrane protein localizing at tight junctions. *J. Cell Biol.* **123**, 1777–1788 (1993).

74. Saitou, M. *et al.* Complex phenotype of mice lacking occludin, a component of tight junction strands. *Mol. Biol. Cell* **11**, 4131–4142 (2000).

75. Buschmann, M. M. *et al.* Occludin OCEL-domain interactions are required for maintenance and regulation of the tight junction barrier to macromolecular flux. *Mol. Biol. Cell* **24**, 3056–3068 (2013).

76. Furuse, M., Fujita, K., Hiiragi, T., Fujimoto, K. & Tsukita, S. Claudin-1 and -2: novel integral membrane proteins localizing at tight junctions with no sequence similarity to occludin. *J. Cell Biol.* **141**, 1539–1550 (1998).

77. Tsukita, S. & Furuse, M. Occludin and claudins in tight-junction strands: leading or supporting players? *Trends Cell Biol.* **9**, 268–273 (1999).

78. Cording, J. *et al.* In tight junctions, claudins regulate the interactions between occludin, tricellulin and marvelD3, which, inversely, modulate claudin oligomerization. *J. Cell Sci.* **126**, 554–564 (2013).

79. Mineta, K. *et al.* Predicted expansion of the claudin multigene family. *FEBS Lett.* **585**, 606–612 (2011).

80. Schrade, A. *et al.* Expression and localization of claudins-3 and -12 in transformed human brain endothelium. *Fluids Barriers CNS* **9**, 6 (2012).

81. Nitta, T. *et al.* Size-selective loosening of the blood-brain barrier in claudin-5-deficient mice. *J. Cell Biol.* **161**, 653–660 (2003).

82. Martìn-Padura, I. *et al.* Junctional Adhesion Molecule, a Novel Member of the Immunoglobulin Superfamily That Distributes at Intercellular Junctions and Modulates Monocyte Transmigration. *J. Cell Biol.* **142**, 117–127 (1998).

83. Katsuno, T. *et al.* Deficiency of zonula occludens-1 causes embryonic lethal phenotype associated with defected yolk sac angiogenesis and apoptosis of embryonic cells. *Mol. Biol. Cell* **19**, 2465–2475 (2008).

84. Stamatovic, S. M., Johnson, A. M., Keep, R. F. & Andjelkovic, A. V. Junctional proteins of the blood-brain barrier: New insights into function and dysfunction. *Tissue Barriers* **4**, e1154641 (2016).

85. Tietz, S. & Engelhardt, B. Brain barriers: Crosstalk between complex tight junctions and adherens junctions. *J. Cell Biol.* **209**, 493–506 (2015).

86. Löscher, W. & Potschka, H. Blood-brain barrier active efflux transporters: ATP-binding cassette gene family. *NeuroRx J. Am. Soc. Exp. Neurother.* **2**, 86–98 (2005).

87. Cordon-Cardo, C. *et al.* Multidrug-resistance gene (P-glycoprotein) is expressed by endothelial cells at blood-brain barrier sites. *Proc. Natl. Acad. Sci.* **86**, 695–698 (1989).

88. Demeule, M., Jodoin, J., Gingras, D. & Béliveau, R. P-glycoprotein is localized in caveolae in resistant cells and in brain capillaries. *FEBS Lett.* **466**, 219–224 (2000).

89. Roberts, L. M. *et al.* Subcellular localization of transporters along the rat blood-brain barrier and blood-cerebral-spinal fluid barrier by in vivo biotinylation. *Neuroscience* **155**, 423–438 (2008).

90. Polli, J. W. *et al.* An Unexpected Synergist Role of P-Glycoprotein and Breast Cancer Resistance Protein on the Central Nervous System Penetration of the Tyrosine Kinase Inhibitor Lapatinib (N-{3-Chloro-4-[(3-fluorobenzyl)oxy]phenyl}-6-[5-({[2-(methylsulfonyl)ethyl]amino}methyl)-2-furyl]-4-quinazolinamine; GW572016). *Drug Metab. Dispos.* **37**, 439–442 (2009).

91. Kapitulnik, J. Drug Transport and Metabolism in the Blood–Brain Barrier. *Front. Pharmacol.* **2**, (2011).

92. Shawahna, R., Decleves, X. & Scherrmann, J.-M. Hurdles with using in vitro models to predict human blood-brain barrier drug permeability: a special focus on transporters and metabolizing enzymes. *Curr. Drug Metab.* **14**, 120–136 (2013).

93. Shawahna, R. *et al.* Transcriptomic and Quantitative Proteomic Analysis of Transporters and Drug Metabolizing Enzymes in Freshly Isolated Human Brain Microvessels. *Mol. Pharm.* **8**, 1332–1341 (2011).

94. Ghosh, C., Puvenna, V., Gonzalez-Martinez, J., Janigro, D. & Marchi, N. Blood-Brain Barrier P450 Enzymes and Multidrug Transporters in Drug Resistance: A Synergistic Role in Neurological Diseases. *Curr. Drug Metab.* **12**, 742–749 (2011).

95. Ghosh, C. *et al.* Pathophysiological implications of neurovascular P450 in brain disorders. *Drug Discov. Today* **21**, 1609–1619 (2016).

96. Pardridge, W. M. Drug transport across the blood–brain barrier. *J. Cereb. Blood Flow Metab.* **32**, 1959–1972 (2012).

97. Carl, S. M. *et al.* ABC and SLC transporter expression and proton oligopeptide transporter (POT) mediated permeation across the human blood--brain barrier cell line, hCMEC/D3 [corrected]. *Mol. Pharm.* **7**, 1057–1068 (2010).

98. Pardridge, W. M., Eisenberg, J. & Yang, J. Human blood-brain barrier insulin receptor. *J. Neurochem.* **44**, 1771–1778 (1985).

99. Pardridge, W. M. BLOOD-BRAIN BARRIER DRUG TARGETING: THE FUTURE OF BRAIN DRUG DEVELOPMENT. *Mol. Interv.* **3**, 90 (2003).

100. Abbott, N. J. & Romero, I. A. Transporting therapeutics across the blood-brain barrier. *Mol. Med. Today* **2**, 106–113 (1996).

101. Banks, W. A. From blood-brain barrier to blood-brain interface: new opportunities for CNS drug delivery. *Nat. Rev. Drug Discov.* **15**, 275–292 (2016).

102. Kazim, S. F. & Iqbal, K. Neurotrophic factor small-molecule mimetics mediated neuroregeneration and synaptic repair: emerging therapeutic modality for Alzheimer's disease. *Mol. Neurodegener.* **11**, 50 (2016).

103. Zhu, J., Jiang, Y., Xu, G. & Liu, X. Intranasal administration: a potential solution for cross-BBB delivering neurotrophic factors. *Histol. Histopathol.* **27**, 537–548 (2012).

104. Cai, J. *et al.* Potential therapeutic effects of neurotrophins for acute and chronic neurological diseases. *BioMed Res. Int.* **2014**, 601084 (2014).

105. Kageyama, T. *et al.* The 4F2hc/LAT1 complex transports l-DOPA across the blood–brain barrier. *Brain Res.* **879**, 115–121 (2000).

106. Takanaga, H., Ohtsuki, S., Hosoya Ki, null & Terasaki, T. GAT2/BGT-1 as a system responsible for the transport of gamma-aminobutyric acid at the mouse blood-brain barrier. *J. Cereb. Blood Flow Metab. Off. J. Int. Soc. Cereb. Blood Flow Metab.* **21**, 1232–1239 (2001).

107. Hladky, S. B. & Barrand, M. A. Elimination of substances from the brain parenchyma: efflux via perivascular pathways and via the blood-brain barrier. *Fluids Barriers CNS* **15**, 30 (2018).

108. Asaba, H. *et al.* Blood-brain barrier is involved in the efflux transport of a neuroactive steroid, dehydroepiandrosterone sulfate, via organic anion transporting polypeptide 2. *J. Neurochem.* **75**, 1907–1916 (2000).

109. Ohtsuki, S. *et al.* Role of blood-brain barrier organic anion transporter 3 (OAT3) in the efflux of indoxyl sulfate, a uremic toxin: its involvement in neurotransmitter metabolite clearance from the brain. *J. Neurochem.* **83**, 57–66 (2002).

110. Miyajima, M., Kusuhara, H., Fujishima, M., Adachi, Y. & Sugiyama, Y. Organic anion transporter 3 mediates the efflux transport of an amphipathic organic anion, dehydroepiandrosterone sulfate, across the blood-brain barrier in mice. *Drug Metab. Dispos. Biol. Fate Chem.* **39**, 814–819 (2011).

111. Nicita, F. *et al.* Efficacy of verapamil as an adjunctive treatment in children with drug-resistant epilepsy: A pilot study. *Seizure* **23**, 36–40 (2014).

112. Pardridge, W. M. Drug and gene targeting to the brain with molecular trojan horses. *Nat. Rev. Drug Discov.* **1**, 131–139 (2002).

113. Pardridge, W. M. Targeted delivery of protein and gene medicines through the blood–brain barrier. *Clin. Pharmacol. Ther.* **97**, 347–361 (2015).

114. Zeiadeh, I., Najjar, A. & Karaman, R. Strategies for Enhancing the Permeation of CNS-Active Drugs through the Blood-Brain Barrier: A Review. *Mol. J. Synth. Chem. Nat. Prod. Chem.* **23**, (2018).

115. Fishman, J. B., Rubin, J. B., Handrahan, J. V., Connor, J. R. & Fine, R. E. Receptor-mediated transcytosis of transferrin across the blood-brain barrier. *J. Neurosci. Res.* **18**, 299–304 (1987).

116. Triguero, D., Buciak, J. & Pardridge, W. M. Capillary depletion method for quantification of blood-brain barrier transport of circulating peptides and plasma proteins. *J. Neurochem.* **54**, 1882–1888 (1990).

117. Stanimirovic, D. B., Sandhu, J. K. & Costain, W. J. Emerging Technologies for Delivery of Biotherapeutics and Gene Therapy Across the Blood-Brain Barrier. *BioDrugs Clin. Immunother. Biopharm. Gene Ther.* **32**, 547–559 (2018).

118. Pardridge, W. M. Delivery of Biologics Across the Blood-Brain Barrier with Molecular Trojan Horse Technology. *BioDrugs Clin. Immunother. Biopharm. Gene Ther.* **31**, 503–519 (2017).

119. Wevers, N. R. *et al.* A perfused human blood-brain barrier on-a-chip for high-throughput assessment of barrier function and antibody transport. *Fluids Barriers CNS* **15**, 23 (2018).

120. Kesselheim, A. S., Hwang, T. J. & Franklin, J. M. Two decades of new drug development for central nervous system disorders. *Nat. Rev. Drug Discov.* **14**, 815–816 (2015).

121. Gribkoff, V. K. & Kaczmarek, L. K. The Need for New Approaches in CNS Drug Discovery: Why Drugs Have Failed, and What Can Be Done to Improve Outcomes. *Neuropharmacology* **120**, 11–19 (2017).

122. Pardridge, W. M. Why is the global CNS pharmaceutical market so under-penetrated? *Drug Discov. Today* **7**, 5–7 (2002).

123. Choi, D. W. *et al.* Medicines for the mind: policy-based 'pull' incentives for creating breakthrough CNS drugs. *Neuron* **84**, 554–563 (2014).

124. Miller, G. Is pharma running out of brainy ideas? *Science* **329**, 502–504 (2010).

125. Hersh, D. S. *et al.* Evolving Drug Delivery Strategies to Overcome the Blood Brain Barrier. *Curr. Pharm. Des.* **22**, 1177–1193 (2016).

126. Bicker, J., Alves, G., Fortuna, A. & Falcão, A. Blood–brain barrier models and their relevance for a successful development of CNS drug delivery systems: A review. *Eur. J. Pharm. Biopharm.* **87**, 409–432 (2014).

127. Abbott, N. J. Prediction of blood–brain barrier permeation in drug discovery from in vivo, in vitro and in silico models. *Drug Discov. Today Technol.* **1**, 407–416 (2004).

128. Nielsen, P. A., Andersson, O., Hansen, S. H., Simonsen, K. B. & Andersson, G. Models for predicting blood–brain barrier permeation. *Drug Discov. Today* **16**, 472–475 (2011).

129. Benson, K., Cramer, S. & Galla, H.-J. Impedance-based cell monitoring: barrier properties and beyond. *Fluids Barriers CNS* **10**, 5 (2013).

130. Srinivasan, B. *et al.* TEER measurement techniques for in vitro barrier model systems. *J. Lab. Autom.* **20**, 107–126 (2015).

131. Helms, H. C. *et al.* In vitro models of the blood-brain barrier: An overview of commonly used brain endothelial cell culture models and guidelines for their use. *J. Cereb. Blood Flow Metab. Off. J. Int. Soc. Cereb. Blood Flow Metab.* **36**, 862–890 (2016).

132. Butt, A. M., Jones, H. C. & Abbott, N. J. Electrical resistance across the blood-brain barrier in anaesthetized rats: a developmental study. *J. Physiol.* **429**, 47–62 (1990).

133. Ghandehari, H., Smith, P. L., Ellens, H., Yeh, P. Y. & Kopecek, J. Size-dependent permeability of hydrophilic probes across rabbit colonic epithelium. *J. Pharmacol. Exp. Ther.* **280**, 747–753 (1997).

134. Knipp, G. T., Ho, N. F., Barsuhn, C. L. & Borchardt, R. T. Paracellular diffusion in Caco-2 cell monolayers: effect of perturbation on the transport of hydrophilic compounds that vary in charge and size. *J. Pharm. Sci.* **86**, 1105–1110 (1997).

135. Sorensen, M. *et al.* The effect of beta-turn structure on the permeation of peptides across monolayers of bovine brain microvessel endothelial cells. *Pharm. Res.* **14**, 1341–1348 (1997).

136. Nicolazzo, J. A., Charman, S. A. & Charman, W. N. Methods to assess drug permeability across the blood-brain barrier. *J. Pharm. Pharmacol.* **58**, 281–293 (2006).

137. Mahar Doan, K. M. *et al.* Passive permeability and P-glycoprotein-mediated efflux differentiate central nervous system (CNS) and non-CNS marketed drugs. *J. Pharmacol. Exp. Ther*. **303**, 1029–1037 (2002).

138. Polli, J. W. *et al.* Rational use of in vitro P-glycoprotein assays in drug discovery. *J. Pharmacol. Exp. Ther.* **299**, 620–628 (2001).

139. Di, L., Kerns, E. H., Fan, K., McConnell, O. J. & Carter, G. T. High throughput artificial membrane permeability assay for blood–brain barrier. *Eur. J. Med. Chem.* **38**, 223–232 (2003).

140. Mensch, J. *et al.* Application of PAMPA-models to predict BBB permeability including efflux ratio, plasma protein binding and physicochemical parameters. *Int. J. Pharm.* **395**, 182–197 (2010).

141. Di, L., Kerns, E. H., Bezar, I. F., Petusky, S. L. & Huang, Y. Comparison of blood–brain barrier permeability assays: in situ brain perfusion, MDR1-MDCKII and PAMPA-BBB. *J. Pharm. Sci*. **98**, 1980–1991 (2009).

142. Takakura, Y. *et al.* Hexose uptake in primary cultures of bovine brain microvessel endothelial cells. II. Effects of conditioned media from astroglial and glioma cells. *Biochim. Biophys. Acta* **1070**, 11–19 (1991).

143. Audus, K. L. & Borchardt, R. T. Characterization of an in vitro blood-brain barrier model system for studying drug transport and metabolism. *Pharm. Res.* **3**, 81–87 (1986).

144. Audus, K. L. & Borchardt, R. T. Bovine brain microvessel endothelial cell monolayers as a model system for the blood-brain barrier. *Ann. N. Y. Acad. Sci.* **507**, 9–18 (1987).

145. Fischer, S., Wobben, M., Kleinstück, J., Renz, D. & Schaper, W. Effect of astroglial cells on hypoxia-induced permeability in PBMEC cells. *Am. J. Physiol. Cell Physiol.* **279**, C935-944 (2000).

146. Weksler, B., Romero, I. A. & Couraud, P.-O. The hCMEC/D3 cell line as a model of the human blood brain barrier. *Fluids Barriers CNS* **10**, 16 (2013).

147. Canfield, S. G. *et al.* An isogenic blood-brain barrier model comprising brain endothelial cells, astrocytes, and neurons derived from human induced pluripotent stem cells. *J. Neurochem.* **140**, 874–888 (2017).

148. Agarwal, N., Lippmann, E. S. & Shusta, E. V. Identification and expression profiling of blood-brain barrier membrane proteins. *J. Neurochem.* **112**, 625–635 (2010).

149. Lippmann, E. S., Weidenfeller, C., Svendsen, C. N. & Shusta, E. V. Blood-brain barrier modeling with co-cultured neural progenitor cell-derived astrocytes and neurons. *J. Neurochem.* **119**, 507–520 (2011).

150. Lippmann, E. S., Al-Ahmad, A., Palecek, S. P. & Shusta, E. V. Modeling the blood–brain barrier using stem cell sources. *Fluids Barriers CNS* **10**, 2 (2013).

151. Lippmann, E. S. *et al.* Derivation of blood-brain barrier endothelial cells from human pluripotent stem cells. *Nat. Biotechnol.* **30**, 783–791 (2012).

152. Mitchell, R. W., Edmundson, C. L., Miller, D. W. & Hatch, G. M. On the mechanism of oleate transport across human brain microvessel endothelial cells. *J. Neurochem.* **110**, 1049–1057 (2009).

153. Bowman, P. D. *et al.* Primary culture of capillary endothelium from rat brain. *In Vitro* **17**, 353–362 (1981).

154. Patabendige, A., Skinner, R. A., Morgan, L. & Abbott, N. J. A detailed method for preparation of a functional and flexible blood-brain barrier model using porcine brain endothelial cells. *Brain Res.* **1521**, 16–30 (2013).

155. Joó, F. & Karnushina, I. A procedure for the isolation of capillaries from rat brain. *Cytobios* **8**, 41–48 (1973).

156. DeBault, L. E., Kahn, L. E., Frommes, S. P. & Cancilla, P. A. Cerebral microvessels and derived cells in tissue culture: isolation and preliminary characterization. *In Vitro* **15**, 473–487 (1979).

157. Burek, M., Salvador, E. & Förster, C. Y. Generation of an immortalized murine brain microvascular endothelial cell line as an in vitro blood brain barrier model. *J. Vis. Exp. JoVE* e4022 (2012). doi:10.3791/4022

158. Roux, F. & Couraud, P.-O. Rat brain endothelial cell lines for the study of blood-brain barrier permeability and transport functions. *Cell. Mol. Neurobiol.* **25**, 41–58 (2005).

159. Culot, M. *et al.* An in vitro blood-brain barrier model for high throughput (HTS) toxicological screening. *Toxicol. In Vitro* **22**, 799–811 (2008).

160. Vandenhaute, E., Sevin, E., Hallier-Vanuxeem, D., Dehouck, M.-P. & Cecchelli, R. Case study: adapting in vitro blood–brain barrier models for use in early-stage drug discovery. *Drug Discov. Today* **17**, 285–290 (2012).

161. Helms, H. C. *et al.* An Electrically Tight In Vitro Blood–Brain Barrier Model Displays Net Brain-to-Blood Efflux of Substrates for the ABC Transporters, P-gp, Bcrp and Mrp-1. *AAPS J.* **16**, 1046–1055 (2014).

162. Sobue, K. *et al.* Induction of blood–brain barrier properties in immortalized bovine brain endothelial cells by astrocytic factors. *Neurosci. Res.* **35**, 155–164 (1999).

163. Teifel, M. & Friedl, P. Establishment of the Permanent Microvascular Endothelial Cell Line PBMEC/C1-2 from Porcine Brains. *Exp. Cell Res.* **228**, 50–57 (1996).

164. Bernas, M. J. *et al.* Establishment of primary cultures of human brain microvascular endothelial cells to provide an in vitro cellular model of the blood-brain barrier. *Nat. Protoc.* **5**, 1265–1272 (2010).

165. Wang, Q. *et al.* Evaluation of the MDR-MDCK cell line as a permeability screen for the blood-brain barrier. *Int. J. Pharm.* **288**, 349–359 (2005).

166. Cecchelli, R. *et al.* Modelling of the blood-brain barrier in drug discovery and development. *Nat. Rev. Drug Discov.* **6**, 650–661 (2007).

167. Eigenmann, D. E. *et al.* Comparative study of four immortalized human brain capillary endothelial cell lines, hCMEC/D3, hBMEC, TY10, and BB19, and optimization of culture conditions, for an in vitro blood–brain barrier model for drug permeability studies. *Fluids Barriers CNS* **10**, 33 (2013).

168. Weksler, B. B. *et al.* Blood-brain barrier-specific properties of a human adult brain endothelial cell line. *FASEB J. Off. Publ. Fed. Am. Soc. Exp. Biol.* **19**, 1872–1874 (2005).

169. Ohtsuki, S. *et al.* Quantitative Targeted Absolute Proteomic Analysis of Transporters, Receptors and Junction Proteins for Validation of Human Cerebral Microvascular Endothelial Cell Line hCMEC/D3 as a Human Blood–Brain Barrier Model. *Mol. Pharm.* **10**, 289–296 (2013).

170. Tai, L. M. *et al.* Polarized P-glycoprotein expression by the immortalised human brain endothelial cell line, hCMEC/D3, restricts apical-to-basolateral permeability to rhodamine 123. *Brain Res.* **1292**, 14–24 (2009).

171. Wassmer, S. C., Combes, V., Candal, F. J., Juhan-Vague, I. & Grau, G. E. Platelets Potentiate Brain Endothelial Alterations Induced by Plasmodium falciparum. *Infect. Immun.* **74**, 645–653 (2006).

172. Puech, C. *et al.* Assessment of HBEC-5i endothelial cell line cultivated in astrocyte conditioned medium as a human blood-brain barrier model for ABC drug transport studies. *Int. J. Pharm.* **551**, 281–289 (2018).

173. Jiang, W. *et al.* HIV-1 Transactivator Protein Induces ZO-1 and Neprilysin Dysfunction in Brain Endothelial Cells via the Ras Signaling Pathway. *Oxidative Medicine and Cellular Longevity* (2017). doi:10.1155/2017/3160360

174. Stebbins, M. J. *et al.* Differentiation and characterization of human pluripotent stem cell-derived brain microvascular endothelial cells. *Methods San Diego Calif* **101**, 93–102 (2016).

175. Lippmann, E. S., Al-Ahmad, A., Azarin, S. M., Palecek, S. P. & Shusta, E. V. A retinoic acid-enhanced, multicellular human blood-brain barrier model derived from stem cell sources. *Sci. Rep.* **4**, 4160 (2014).

176. Aday, S., Cecchelli, R., Hallier-Vanuxeem, D., Dehouck, M. P. & Ferreira, L. Stem Cell-Based Human Blood–Brain Barrier Models for Drug Discovery and Delivery. *Trends Biotechnol.* **34**, 382–393 (2016).

177. Palmiotti, C. A. *et al.* In vitro cerebrovascular modeling in the 21st century: current and prospective technologies. *Pharm. Res.* **31**, 3229–3250 (2014).

178. Patel, R. & Alahmad, A. J. Growth-factor reduced Matrigel source influences stem cell derived brain microvascular endothelial cell barrier properties. *Fluids Barriers CNS* **13**, (2016).

179. Hollmann, E. K. *et al.* Accelerated differentiation of human induced pluripotent stem cells to blood-brain barrier endothelial cells. *Fluids Barriers CNS* **14**, 9 (2017).

180. Jamieson, J. J., Searson, P. C. & Gerecht, S. Engineering the human blood-brain barrier in vitro. *J. Biol. Eng.* **11**, (2017).

181. van der Helm, M. W., van der Meer, A. D., Eijkel, J. C. T., van den Berg, A. & Segerink, L. I. Microfluidic organ-on-chip technology for blood-brain barrier research. *Tissue Barriers* **4**, (2016).

182. Rusanov, A. L., Luzgina, N. G., Barreto, G. E. & Aliev, G. Role of Microfluidics in Blood-Brain Barrier Permeability Cell Culture Modeling: Relevance to CNS Disorders. *CNS Neurol. Disord. Drug Targets* **15**, 301–309 (2016).

183. Wang, Y. I., Abaci, H. E. & Shuler, M. L. Microfluidic blood-brain barrier model provides in vivo-like barrier properties for drug permeability screening. *Biotechnol. Bioeng.* **114**, 184–194 (2017).

184. Griep, L. M. *et al.* BBB ON CHIP: microfluidic platform to mechanically and biochemically modulate blood-brain barrier function. *Biomed. Microdevices* **15**, 145–150 (2013).

185. Cucullo, L., Hossain, M., Puvenna, V., Marchi, N. & Janigro, D. The role of shear stress in Blood-Brain Barrier endothelial physiology. *BMC Neurosci.* **12**, 40 (2011).

186. Modarres, H. P. *et al.* In vitro models and systems for evaluating the dynamics of drug delivery to the healthy and diseased brain. *J. Control. Release Off. J. Control. Release Soc.* **273**, 108–130 (2018).

187. Bang, S. *et al.* A Low Permeability Microfluidic Blood-Brain Barrier Platform with Direct Contact between Perfusable Vascular Network and Astrocytes. *Sci. Rep.* **7**, 8083 (2017).

188. Wolff, A., Antfolk, M., Brodin, B. & Tenje, M. In Vitro Blood-Brain Barrier Models-An Overview of Established Models and New Microfluidic Approaches. *J. Pharm. Sci.* **104**, 2727–2746 (2015).

189. Cho, H. *et al.* Three-Dimensional Blood-Brain Barrier Model for in vitro Studies of Neurovascular Pathology. *Sci. Rep.* **5**, 15222 (2015).

190. Chrobak, K. M., Potter, D. R. & Tien, J. Formation of perfused, functional microvascular tubes in vitro. *Microvasc. Res.* **71**, 185–196 (2006).

191. Deli, M. A., Dehouck, M. P., Abrahám, C. S., Cecchelli, R. & Joó, F. Penetration of small molecular weight substances through cultured bovine brain capillary endothelial cell monolayers: the early effects of cyclic adenosine 3',5'-monophosphate. *Exp. Physiol.* **80**, 675–678 (1995).

192. Eigenmann, D. E., Jähne, E. A., Smieško, M., Hamburger, M. & Oufir, M. Validation of an immortalized human (hBMEC) in vitro blood-brain barrier model. *Anal. Bioanal. Chem.* **408**, 2095–2107 (2016).

193. Furie, M. B., Cramer, E. B., Naprstek, B. L. & Silverstein, S. C. Cultured endothelial cell monolayers that restrict the transendothelial passage of macromolecules and electrical current. *J. Cell Biol.* **98**, 1033–1041 (1984).

194. Al Ahmad, A., Taboada, C. B., Gassmann, M. & Ogunshola, O. O. Astrocytes and pericytes differentially modulate blood-brain barrier characteristics during development and hypoxic insult. *J. Cereb. Blood Flow Metab. Off. J. Int. Soc. Cereb. Blood Flow Metab.* **31**, 693–705 (2011).

195. Malina, K. C.-K., Cooper, I. & Teichberg, V. I. Closing the gap between the in-vivo and in-vitro blood–brain barrier tightness. *Brain Res.* **1284**, 12–21 (2009).

196. Demeuse, P. *et al.* Compartmentalized coculture of rat brain endothelial cells and astrocytes: a syngenic model to study the blood–brain barrier. *J. Neurosci. Methods* **121**, 21–31 (2002).

197. Wuest, D. M., Wing, A. M. & Lee, K. H. Membrane configuration optimization for a murine in vitro blood–brain barrier model. *J. Neurosci. Methods* **212**, 211–221 (2013).

198. Li, G. *et al.* Permeability of endothelial and astrocyte cocultures: in vitro blood-brain barrier models for drug delivery studies. *Ann. Biomed. Eng.* **38**, 2499–2511 (2010).

199. Zozulya, A., Weidenfeller, C. & Galla, H.-J. Pericyte-endothelial cell interaction increases MMP-9 secretion at the blood-brain barrier in vitro. *Brain Res.* **1189**, 1–11 (2008).

200. Lai, C.-H. & Kuo, K.-H. The critical component to establish in vitro BBB model: Pericyte. *Brain Res. Brain Res. Rev.* **50**, 258–265 (2005).

201. Thanabalasundaram, G., El-Gindi, J., Lischper, M. & Galla, H.-J. Methods to assess pericyte-endothelial cell interactions in a coculture model. *Methods Mol. Biol. Clifton NJ* **686**, 379–399 (2011).

202. McConnell, H. L., Kersch, C. N., Woltjer, R. L. & Neuwelt, E. A. The Translational Significance of the Neurovascular Unit. *J. Biol. Chem.* **292**, 762–770 (2017).

203. Thomsen, L. B., Burkhart, A. & Moos, T. A Triple Culture Model of the Blood-Brain Barrier Using Porcine Brain Endothelial cells, Astrocytes and Pericytes. *PloS One* **10**, e0134765 (2015).

204. Hatherell, K., Couraud, P.-O., Romero, I. A., Weksler, B. & Pilkington, G. J. Development of a three-dimensional, all-human in vitro model of the blood–brain barrier using mono-, co-, and tri-cultivation Transwell models. *J. Neurosci. Methods* **199**, 223–229 (2011).

205. Maherally, Z. *et al.* Real-time acquisition of transendothelial electrical resistance in an all-human, in vitro, 3-dimensional, blood–brain barrier model exemplifies tight-junction integrity. *FASEB J.* **32**, 168–182 (2017).

206. Xue, Q. *et al.* A Novel Brain Neurovascular Unit Model with Neurons, Astrocytes and Microvascular Endothelial Cells of Rat. *Int. J. Biol. Sci.* **9**, 174–189 (2013).

207. O. Ogunshola, O. In Vitro Modeling of the Blood-Brain Barrier: Simplicity Versus Complexity. *Curr. Pharm. Des.* **17**, 2755–2761 (2011).

208. Kulczar, C., Lubin, K. E., Lefebvre, S., Miller, D. W. & Knipp, G. T. Development of a direct contact astrocyte-human cerebral microvessel endothelial cells blood-brain barrier coculture model. *J. Pharm. Pharmacol.* **69**, 1684–1696 (2017).

209. Knipp, G. T., Ngendahimana, A., Kulczar, C., Lubin, K. E. & Lavan, M. Blood Brain Barrier Models and Methods to Generate and Use the Same.

210. Hallier-Vanuxeem, D. *et al.* New strategy for alerting central nervous system toxicity: Integration of blood–brain barrier toxicity and permeability in neurotoxicity assessment. *Toxicol. In Vitro* **23**, 447–453 (2009).

211. Sherman, S. P. & Bang, A. G. High-throughput screen for compounds that modulate neurite growth of human induced pluripotent stem cell-derived neurons. *Dis. Model. Mech.* **11**, (2018).

212. Bal-Price, A. K., Hogberg, H. T., Buzanska, L. & Coecke, S. Relevance of in vitro neurotoxicity testing for regulatory requirements: Challenges to be considered. *Neurotoxicol. Teratol.* **32**, 36–41 (2010).

213. Schultz, L. *et al.* Evaluation of drug-induced neurotoxicity based on metabolomics, proteomics and electrical activity measurements in complementary CNS in vitro models. *Toxicol. In Vitro* **30**, 138–165 (2015).

214. Schmidt, B. Z. *et al.* In vitro acute and developmental neurotoxicity screening: an overview of cellular platforms and high-throughput technical possibilities. *Arch. Toxicol.* **91**, 1–33 (2017).

CHAPTER 2. DEVELOPMENT OF AN INNOVATIVE DIRECT CONTACT IN VITRO BLOOD BRAIN BARRIER PERMEABILITY MODEL: BRAIN MICROVESSEL ENDOTHELIAL CELL LINE SCREENING

2.1 Abstract

The development of cell based *in vitro* screening tools for assessing blood brain barrier (BBB) permeation of hit and lead compounds is one way to mitigate attrition rates observed in later stages of clinical trials for neurotherapeutic agents. We have previously developed physiologically relevant models of the BBB that mimic the direct cell-cell contacts between the multiple cells types of the neurovascular unit (NVU) by seeding primary astrocytes and pericytes in a direct layered configuration with the brain microvessel endothelial cells (BMECs). These models were developed using the immortalized human cerebral microvessel endothelial cell line (hCMEC/D3), but with recent advances in the field and further characterization of this cell line its limitations have become apparent. In an effort to further enhance the model we have investigated alternative endothelial cell sources which include the human induced pluripotent stem cell (hiPSC) derived iCell® Endothelial Cell (Cellular Dynamics Inc, Madison, WI, USA) and the immortalized human brain endothelial cell line (HBEC-5i). Both cell sources demonstrated amenability to the direct contact multi-cellular models, but present an apparent need for extensive optimization. The work presented here provides the basis for the subsequent optimization and enhancement of the direct contact models presented in Chapters 3 and 4.

2.2 Introduction

The discovery and development of neurotherapeutic agents that can traverse the blood brain barrier (BBB) has long been a considerable area of interest for drug delivery based on the

poor translation rates associated with the approval of these agents. Amongst the greatest challenge leading to the high clinical attrition rates is often hypothesized to be due to the restrictiveness of the BBB, where highly lipophilic compounds may lead to neurotoxicity or alternatively many compounds cannot traverse the barrier and lower parenchymal exposure results in a lack of efficacy.[1] We posit that there is room for improvement upon *in vitro* BBB cell screening models for early lead candidate selection and development stages, which if more rigor is incorporated agents would have an increased likeliness of success. The *in vivo* the BBB is different from the peripheral endothelium due its continuous barrier and formation of restrictive tight junctions, high expression of drug transporter and metabolizing isoforms, and the inclusion of supporting cells (astrocytes, pericytes, and the endothelial cells) of the neurovascular unit (NVU), this making these attributes requisite considerations for the early *in vitro* BBB cell screening models.[2–5] Towards this goal, evolution of *in vitro* BBB cell screening models reveals a trend where incorporating these multiple cell types in various culturing configurations within a Transwell® have been demonstrated to enhance many key barrier properties within the model.[2,6–10] However, these culturing methods are laborious and involve plating multiple cell lines separately where the brain microvessel endothelial cells are seeded as a monolayer on the apical surface and the astrocytes and pericytes are cultured on basolateral side of the Transwell® filter support or the bottom of the culture dish. These indirect culturing models lack *in vivo* relevant contact between the multiple cell types of the neurovascular unit, which is thought to be essential for enhancing the BBB phenotype through cell-cell signaling.[11,12]

We have developed a novel *in vitro* BBB cell screening model that involves plating three cell types of the neurovascular unit (astrocytes, pericytes, and endothelial cells) in direct contact on the apical side of a Transwell® filter support. This is an enhancement of the previously

developed direct contact coculture model where we layered astrocytes and then BMECs to form a confluent lawn to further the *in vivo* relevancy and improve the barrier properties of the model (Fig. 2.1).[13] The triculture cell layer configuration has been shown to provide a physiologically relevant contact between the different cell layers that is necessary to improve the expression of the BBB phenotype in comparison to endothelial monolayers or indirect contact models. Early development and optimization of the direct contact coculture and triculture models in our laboratory was done so with the human cerebral microvessel endothelial cell line (hCMEC/D3).[13–15] This cell line had been well established in the field of BBB and NVU *in vitro* research and is a mainstay when choosing a human immortalized cell line for cell-based model development.[10,16,17] However, many have noticed the limitations of this cell line due to its extensive use, higher passages, and reduced *in vivo* relevant tight junction and drug transporter expression.[15,17–20] Although the hCMEC/D3 cell proved to be useful for the early development of the direct contact models, we have since considered alternative cell lines that may better reflect the expression of the *in vivo* BMECs and can be utilized for further optimization and validation of the models that may have more *in vivo* relevant attributes.

Recent advancements in the field have focused on using endothelial cells that are derived from human induced pluripotent stem cell (hiPSCs) sources as a surrogate for difficult to obtain primary cells. There are some challenges with hiPSCs since they are source dependent, not as robust as immortalized cells that are relatively easier to culture, and they lack the expression of some key validation characteristics of the BBB endothelium.[10] Alternatively, endothelial cells derived from hiPSCs offer a more robust alternative to primary cells and may offer some of the benefits of phenotypic expression that immortalized cell lines tend to lack, especially with increasing passage.[21–24] Through the utilization of hiPSC derived endothelial cells in the novel

direct contact triculture model, it is possible to elucidate and enhance the key validation characteristics of an *in vitro* NVU cell screening model that are not found in other commonly used indirect contact models. In this work we have explored the use of the iCell® Endothelial Cell from Cellular Dynamics Inc. (Madison, WI) as the hiPSCs they offer are preprogrammed to possess an endothelial phenotype and have been observed to be more restrictive than primary cells. Cellular Dynamics also offers other hiPSC supporting cells including preprogrammed astrocytes and phenotypically diverse neurons semblant of normal and pathological conditions (e.g. Parkinson's Disease). Herein, we have shown that the iCell® hiPSC endothelial cells are amenable to the direct contact models. The main issues we encountered were that the cells proved to be passage limited and cost prohibitive for the extensive optimization that was required for the multi-cellular systems.

Immortalized cell lines are highly amenable to the extensive culturing demands required for optimization of an *in vitro* model. As an alternative to the hCMEC/D3 cell line we explored using the human brain endothelial cell line HBEC-5i. These cells were developed from a pooled patient sample of cerebral cortex fragments that were absent of brain pathological diseases and were subsequently transfected with simian virus 40 (SV40). Whereas, the hCMEC/D3 cell line was derived from a single epilepsy patient and doubly transfected with SV40 and human telomerase reverse transcriptase (hTERT), where the oncogenic transformation can yield more plasticity to the cells.[14,25,26] The HBEC-5i cell line has typically been used in the study of cerebral malaria, but has seen recent interest in the field of BBB and NVU research.[26–31] These cells have been found to express a large number of tight junction proteins, high transendothelial electrical resistance (TEER) that is comparable to other brain endothelial cell lines, and have good expression of efflux transporters.[27,30,31] Recently, the HBEC-5i cell line has been used for *in vitro* modeling of the BBB showing functional expression of ABC transporters and stable barrier

properties over multiple days of culture suggesting that is a viable alternative to the hCMEC/D3 cell line and other immortalized BMEC sources.[30,31] From the early optimization work that we have done using the HBEC-5i cell line we have seen that it will be more amenable to meet the demands required for the continued optimization of the direct contact triculture model and all further improvements.

Herein, the work done in exploring alternative cell lines for the direct contact BBB models we have developed is presented. Although the trend of the field has been moving towards using iPSC derived cell sources, we have chosen to prioritize the continued development of the *in vitro* models over the exploration of more *in vivo* representative cell lines. We believe that, upon validation of the model (Chapters 3 and 4), development of an in-house iPSC cell source for the cells of the NVU can be explored in the future. Based on the results found here we have demonstrated that the HBEC-5i cell line is a good alternative for the often used hCMEC/D3 cell line when looking for an immortalized cell that can respond to the robust culturing methods of high throughput *in vitro* model optimization.

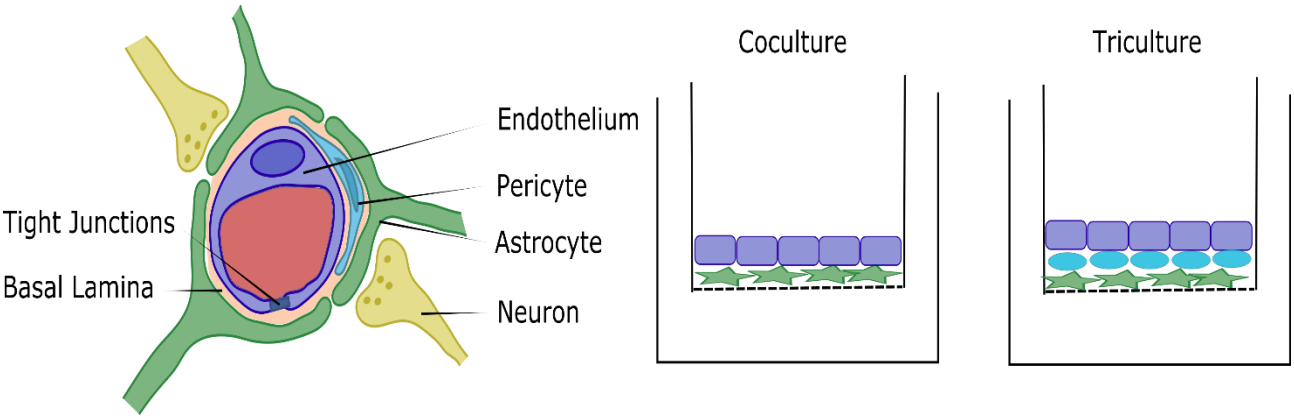

Figure 2.1. Cross section depiction of the neurovascular unit *in vivo* (left) and how it relates to the direct contact coculture (middle) and triculture (right) models. The coculture contains brain endothelial cells (purple) seeded directly atop a layer of human astrocytes (green). The triculture improves on the coculture by adding a layer of pericytes (blue) to mimic the *in vivo* configuration of the endothelium and two supporting cell types.

2.3 Materials and Methods

2.3.1 *Materials*

Transwell® filters of 12 mm 0.4 µm pore size, T-75 culture flasks, Matrigel®, mouse laminin, and type I rat tail collagen were purchased from Corning (Corning, NY, USA). Hank's balanced salt solution (HBSS), lipid concentrate, and Dulbecco's Modified Eagle Medium/Nutrient Mixture F-12 (DMEM/F-12) were obtained from Gibco (Carlsbad, CA, USA). Fetal bovine serum (FBS), penicillin/streptomycin, ascorbic acid, hydrocortisone, and fibronectin were purchased from MilliporeSigma (St. Louis, MO, USA). HEPES (2-[4-(2-hydroxyethyl)piperazin-1-yl]ethanesulfonic acid) was obtained from J.T. Baker (Phillipsburg, NJ, USA). EBM-2 growth medium was purchased from Lonza Group (Walkersville, MD, USA). Endothelial cell growth supplement (ECGS) was purchased from Alfa Aesar (Haverhill, MA, USA). Poly-L-lysine (PLL) was purchased from Trevigen (Gaithersburg, MD, USA). Radiolabeled compounds were purchased from Moravek Biochemicals Inc. (Brea, CA, USA). The iCell® endothelial cells and iCell® endothelial cell media and supplements were purchased from Cellular Dynamics Inc. (Madison, WI, USA). VascuLife® VEGF Endothelial Medium Complete Kit was purchased from Lifeline Cell Technology (Frederick, MD, USA). Basic human growth factor (bFGF), human brain primary astrocytes, human brain primary vascular pericytes, astrocyte medium, pericyte medium, and astrocyte and pericyte growth factors were all obtained from ScienCell Research Laboratories (Carlsbad CA, USA). HBEC-5i cells were purchased from ATCC (Manassas, VA, USA).

2.3.2 *Cell Culture*

The iCell® endothelial cells were cultured in T-75 flasks pre-coated with fibronectin and subcultured at 80-90% confluency. Culture medium was prepared according to CDI recommendation using VascuLife® VEGF basal medium supplemented with rhVEG LifeFactor®, rh EGF LifeFactor®, rh FGF basic LifeFactor®, rh IGF-1 LifeFactor®, ascorbic acid LifeFactor®, hydrocortisone hemisuccinate LifeFactor®, heparin sulfate LifeFactor®, L-glutamine LifeFactor®, and iCell® Endothelial Cells Medium Supplement. Human Brain Endothelial Cells (HBEC-5i) were maintained in T-75 culture flasks pre-coated with Type I rat tail collagen with medium changes every 3 days and subcultured at 80-90% confluency—cells were utilized between passage 22 and 30. HBEC-5i culture medium was made up of Dulbecco's Modified Eagle Medium/Nutrient Mixture F-12 (DMEM/F-12) supplemented with 10% FBS, 15 mM HEPES, and 40 ug/mL endothelial cell growth supplement (ECGS). In some assays both endothelial cell lines were maintained in culture medium optimized for the hCMEC/D3 cell line. This consisted of EBM-2 basal medium supplemented with 5% FBS, 1% penicillin/streptomycin, bFGF, hydrocortisone, ascorbic acid, lipid concentrate, and HEPES. Human astrocytes and human brain vascular pericytes are maintained in T-75 culture flasks pre-coated with poly-L-lysine with medium changes every 3 days and subcultured at 80-90% confluency—cells were utilized between passage 4 and 10. Astrocyte culture medium was made up of Astrocyte Medium supplemented with 5% FBS, astrocyte growth supplement, and penicillin/streptomycin. Pericyte culture medium was made up of Pericyte Medium supplemented with 5% FBS, pericyte growth supplement, and penicillin/streptomycin. All cells were kept in humidified environment at 37 °C with 5% CO_2.

2.3.3 *BBB In Vitro Models*

For monoculture studies, the iCell® endothelial cells are plated on 0.4 µm Corning Costar 12-well polyester Transwell® filters which were pretreated 3 µg/cm^2 of fibronectin. Cells were seeded at a density of 1 x 10^5 cells/cm^2, 3 x 10^5 cells/cm^2, or 6 x 10^5 cells/cm^2 and allowed to grow for 8 days in endothelial medium, with medium changes every other day, before performing a study. HBEC-5i monoculture studies were performed at seeding densities of 50,000 to 125,000 cells/cm^2 with cells plated on filter supports pre-coated with 60 µg/cm^2 type I rat tail collagen and cultured for 3 to 7 days with assessment on days 3, 4, 5, 6, and 7.

For the direct contact coculture studies of the iCell® endothelial cells, primary human astrocytes were seeded on filter supports pre-treated with 5 µg/cm^2 poly-L-lysine (PLL) at 40,000 cells/cm^2 and cultured for 48 hours prior to endothelial cell seeding atop the astrocyte layer at a density of 30,000 or 60,000 cells/cm^2 and cultured for an additional 8 days in endothelial medium. HBEC-5i direct contact cocultures were plated in a similar fashion with pericyte-endothelial and astrocyte-endothelial coculture both being evaluated. Additionally, HBEC-5i cells were seeded at a single density of 75,000 cells/cm^2. HBEC-5i cocultures were maintained in either supplemented DMEM/F-12 or EBM-2.

Direct contact tricultures of the iCell® endothelial cells were prepared by first by plating human astrocytes at 40,000 cells/ cm^2 on Transwell® filter supports pre-treated with 5 µg/cm^2 PLL and allowed to grow in astrocyte medium for 48 hours. Prior to plating pericytes, apical medium was replaced with astrocyte medium containing 6 µg/mL PLL and allowed to incubate for 4 hours. Human brain vascular pericytes were plated at 40,000 cells/cm^2 and grown for 48 hours in pericyte medium. After 48 hours, apical medium was changed with pericyte medium containing 6 µg/mL of fibronectin and incubated for 4 hours. The iCell® Endothelial Cells were plated in endothelial

medium at 30,000 cells/cm^2 or 60,000 cells/cm^2 with medium changes every other day. Cultures were maintained for 8 days post endothelial cell plating in the recommended VascuLife® medium supplemented as directed or by the in-house optimized complete EBM-2 medium. HBEC-5i direct contact tricultures were prepared by seeding astrocytes on a PLL coated filter support at 40,000 cells/cm^2, followed by pericyte plating at 40,000 cells/cm^2 48 hours post astrocyte seeding. HBEC-5i cells were seeded 48 following pericyte plating at a density of 75,000 cells/cm^2 and maintained for an additional 5 or 7 days in complete DMEM/F-12 or EBM-2 medium.

2.3.4 *Permeability Assays*

The optimal day for permeability studies, for iCell® endothelial cultures was determined via transendothelial electrical resistance (TEER) by using an EVOM2 Epithelial Volt/Ohm Meter and STX2 Chopstick Electrode. Optimal barrier tightness was achieved when TEER ($\Omega \cdot cm^2$) trends peaked and leveled off. TEER results were normalized by subtracting background resistance from the filter and matrix proteins.

Paracellular permeability studies were conducted on all models in triplicate on a rocking platform at 37°C using [^{14}C]-labeled compounds ([^{14}C]-Mannitol and [^{14}C]-Inulin) at 0.25 µCi/mL in HBSS. For all studies, astrocytes and pericytes ranged between passage number 6 to 12, iCell® Endothelial Cells ranged between passages 4-10, and HBEC-5i cells from passages 20-27. Cells were first washed in PBS, then incubated in HBSS for 30 minutes prior to initiating the study. Filter supports were moved from well-to-well at each time point to maintain sink conditions. Studies were conducted by pulling 100 µL samples at 15, 30, 45, 60, and 90 minute time points. Samples were analyzed via liquid scintillation counting by adding 4 mL of scintillation fluid to each sample. Apparent permeability coefficients (cm/sec) were calculated using the following equation

$$P_{app} = \frac{dM/dt}{C_0 * A}$$

(eq. 1)

where dM/dt represents the rate of compound movement across the cell layer, C_0 is the initial concentration of compound in the donor chamber, and A is the surface area of the filter support.

2.4 Results

2.4.1 *iCell® BBB Cultures*

Several culturing conditions were evaluated for iCell® endothelial cell BBB models. The optimal time for permeability studies was determined based on TEER trends observed over the length of culture. Tricultures containing 30,000 cells/cm^2 resulted in the highest TEER values at both 2 and 8 days post endothelial cell plating (67 ± 9 and 64 ± 5 Ω·cm^2) (Fig. 2.2).

Paracellular permeability coefficients of [^{14}C]-inulin and [^{14}C]-mannitol across the iCell endothelial BBB cultures were also evaluated (Table 2.1). All the evaluations were performed in triplicate with the exception of those noted otherwise for each of the markers in the conditions described. We did notice that several triculture samples were compromised due to cell rolling; therefore, data from these replicates was excluded from analysis and replaced.

Due to the expense (e.g., limited passaging of the iPSC cells, media costs, and sensitivity as reflected by rolling) of the continued culture of the iCell® endothelial cells, the use of our previously optimized hCMEC/D3 medium was explored. Supplemented EBM-2 was used at the time of endothelial cell plating and maintained throughout the duration of culture. Based on mannitol permeability the cultures in EBM-2 presented a higher paracellular tightness based upon

the reduced mannitol permeability (CDI medium: 1.82 ± 0.02 x 10^{-5} cm/sec, EBM-2: 1.54 ± 0.02 x 10^{-5} cm/sec) (Fig. 2.3).

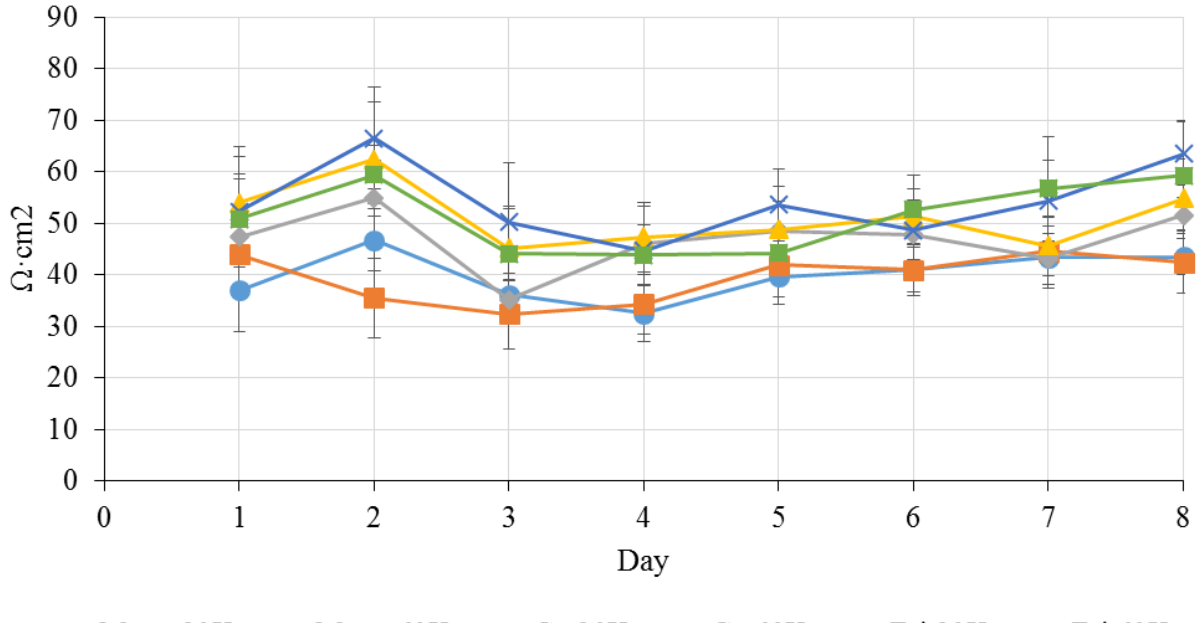

Figure 2.2. Transendothelial electrical resistance (TEER) trends for iCell® endothelial cell BBB monoculture (mono), astrocyte coculture (Co) and the astrocyte-pericyte triculture (Tri) models over the course of culturing. All TEER measurements were made in culture medium. Error bars represent one standard deviation (n=3).

Table 2.1. iCell Endothelial Cell BBB Culture Paracellular Permeability

BBB Culture – (iCell®/cm²)	P_{app} [^{14}C]-Inulin (x 10^{-5} cm/sec)	P_{app} [^{14}C]-Mannitol (x 10^{-5} cm/sec)
Monoculture – 30,000	0.96 ± 0.07	1.74 ± 0.03
Monoculture – 60,000	0.94 ± 0.11	1.77 ± 0.14
Coculture – 30,000	0.95 ± 0.03	1.72 ± 0.09
Coculture – 60,000	1.11 ± 0.30	2.08 ± 0.27
Triculture – 30,000	-	1.78 ± 0.13
Triculture – 60,000	0.97 ± 0.28	1.71 (n=1)

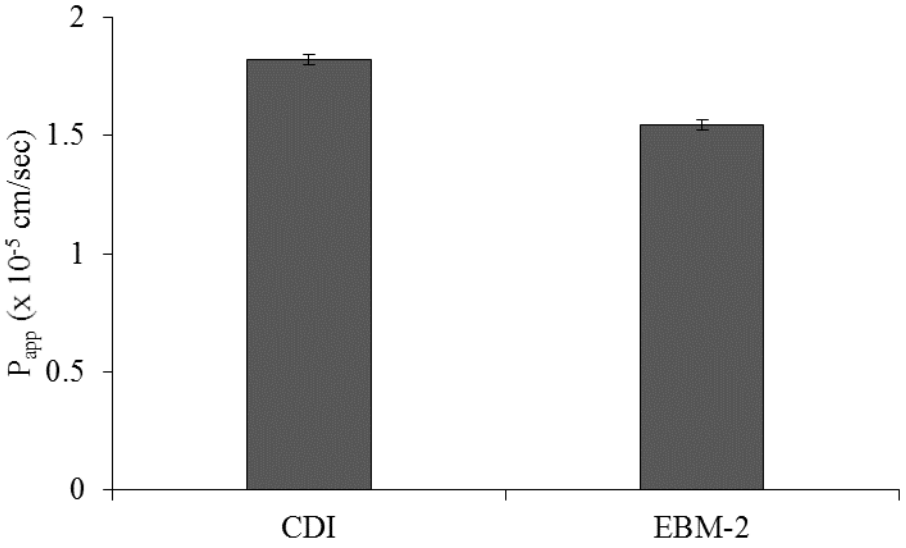

Figure 2.3. Apparent permeability of [^{14}C]-mannitol across the iCell® endothelial cell direct contact triculture maintained in CDI recommended medium and supplemented EBM-2. Error bars represent one standard deviation (n=3). Not significant based on Student's *t*-test ($p>0.05$).

2.4.2 *HBEC-5i BBB Cultures*

HBEC-5i optimization began with a monoculture BMEC experiment on the filter support. A range of seeding densities were evaluated followed by determining the optimal length of culture time (Table 2.2). Cultures were optimized based on paracellular permeability of [^{14}C]-mannitol resulting in 75,000 cells/cm^2 cultured for 7 days being selected as the optimal density and culture time for the endothelial cell layer.

The HBEC-5i direct contact coculture was optimized using both astrocytes and pericytes as the layer of supporting cells beneath the endothelium in comparison to the monoculture with culturing for 5 or 7 days post endothelial cell plating. Results revealed that despite the addition of pericytes or astrocytes, cells should still be cultured for an additional 7 days post HBEC-5i plating when compared to 5 days in culture. Astrocyte cocultures showed the lowest [^{14}C]-mannitol permeability after 7 days of endothelial culture ($1.86 \pm 0.14 \times 10^{-5}$ cm/sec) in comparison to the

pericyte coculture (2.59 ± 0.26 x 10^{-5} cm/sec) and HBEC-5i monoculture (2.24 ± 0.22 x 10^{-5} cm/sec) (Fig. 2.4).

Table 2.2. HBEC-5i Monoculture Density and Culture Time Optimization

HBEC-5i Density (cells/cm^2)	Day	P_{app} [^{14}C]-Mannitol (x 10^{-5} cm/sec)
50,000	7	2.64 ± 0.23
75,000	3	2.47 ± 0.14
75,000	4	2.46 ± 0.12
75,000	5	2.32 ± 0.21
75,000	6	2.39 ± 0.07
75,000	**7**	**2.24 ± 0.23**
100,000	7	2.43 ± 0.03
125,000	7	2.30 ± 0.17

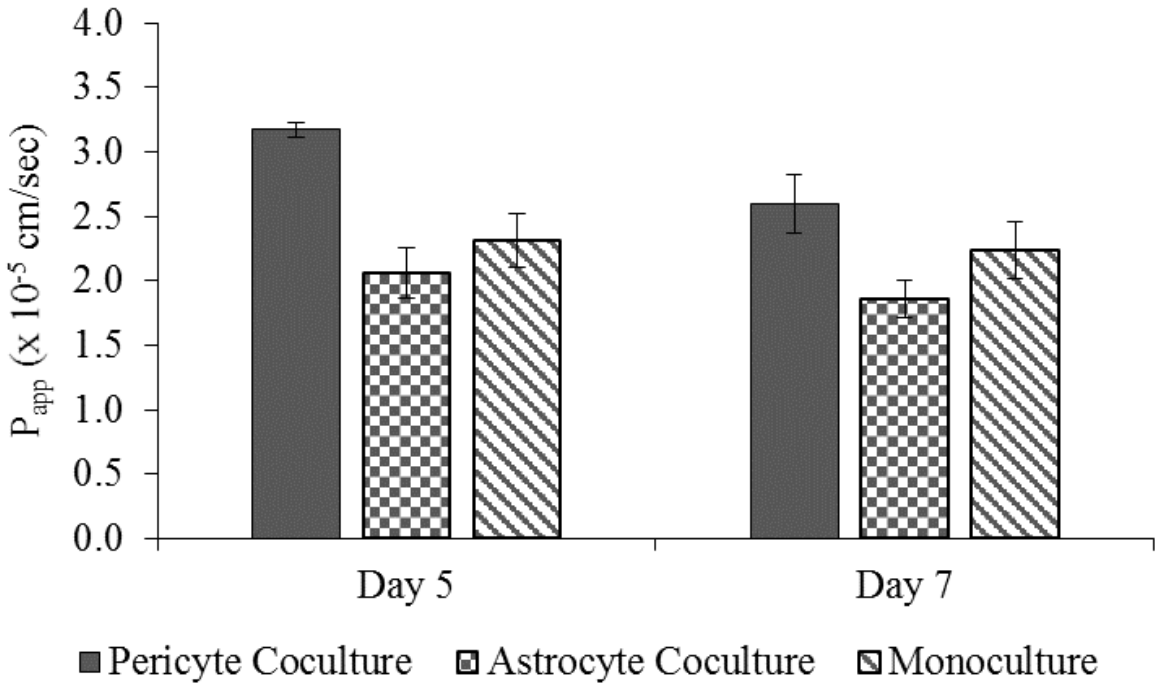

Figure 2.4. Apparent permeability of [^{14}C]-mannitol across HBEC-5i cocultures and monocultures based on days post HBEC-5i plating. Error bars represent one standard deviation (n=3).

The HBEC-5i direct contact triculture was plated based on the results of the previously in-house established BBB models. Here, the direct contact triculture was tested using both the recommended complete DMEM/F-12 and the supplemented EBM-2 at both 5 and 7 days post HBEC-5i plating, and compared based on [^{14}C]-mannitol permeability (Fig. 2.5). Apparent permeability of [^{14}C]-mannitol was lowest in the HBEC-5i 7 day triculture in DMEM/F-12 (2.05 ± 0.02 x 10^{-5} cm/sec) and highest in the day 7 EBM-2 model (2.40 ± 0.31 x 10^{-5} cm/sec). Unfortunately, these results showed worse paracellular tightness in the triculture when compared to the astrocyte coculture, which suggested that further optimization was required.

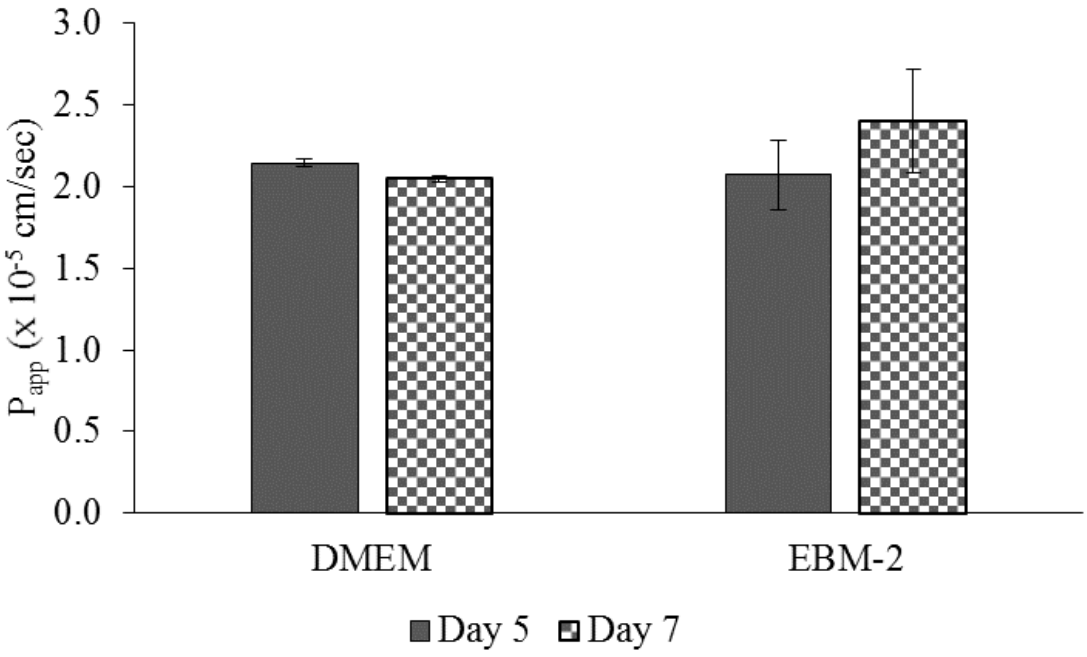

Figure 2.5. Apparent permeability of [^{14}C]-mannitol across the HBEC-5i day 5 and 7 tricultures maintained in supplemented DMEM/F-12 or EBM-2. Error bars represent one standard deviation (n=3).

2.5 Discussion

The first efforts made to develop the direct contact coculture and triculture models were done using the well-established hCMEC/D3 cell line. The hCMEC/D3 cell is the one of choice for

robust screening and optimization of *in vitro* models due to its capacity for extending culturing, expression of some key tight junction proteins, and extensive characterization.[14–19,32] However, there are drawbacks to using the hCMEC/D3, and given the trends of the BBB field moving towards cells derived from iPSC sources, we explored the iPSC derived iCell® endothelial cell and immortalized HBEC-5i cell lines as alternatives.[23,24,27,30]

The iCell® endothelial cells proved to be amenable to the direct contact systems. The cells were able to be seeded atop a lawn of astrocytes and pericytes to generate the intended layering of the cell types. Additionally, the resulting TEER values of the iCell® BBB models were comparative to those of the hCMEC/D3 model, but a significant difference between the different culture models were not observed.[10,13] This is concerning given the reliance on TEER trends for the assessment of barrier formation without disruption of the cells. However, TEER is a highly variable measurement and can be affected by medium composition, temperature, and placement of electrodes, therefore TEER measurements were supplemented with paracellular permeability studies utilizing established marker compounds to evaluate the barrier tightness.[33] Paracellular permeability of [^{14}C]-inulin and [^{14}C]-mannitol were in the range of what has been seen for our previously developed direct contact coculture and triculture models.[13] However, the addition of both astrocytes and pericytes did not result in the expected decrease in permeability of these markers in comparison to the iCell® monoculture as has been previously observed in the hCMEC/D3 models we have utilized. Although the relative permeability of the paracellular markers in the iCell® coculture and triculture model is similar to that of the hCMEC/D3, we did not observe the same synergistic effects on tightness with the addition of supporting cells in direct contact. An additional point of concern for the iCell® model was the tendency for the cell in the coculture and triculture systems to become compromised during culture (data not shown). Upon

visual inspection, a concerning amount of co- and triculture replicates would "roll" where the cells would pull up from the filter and grow as a mass rather than a flat layer of cells. This could possibly be mitigated by investigating alternative matrix proteins that could be used to seed the cells on the filter support to limit the tendency for the cells to lift from the filter. There are no other current reports for iCell® BBB models, but based on BBB models generated using non-commercial iPSC derived endothelium, we would expect the increase in barrier tightness of the iCell® models compared to the previously established hCMEC/D3 to be more substantial.[10,21,23,24] Given the limited improvement of the iCell® model over the hCMEC/D3 models, the costs associated with culturing the cells were prohibitive to continuing optimization.

Immortalized cell lines are robust and typically lower cost compared to primary and iPSC derived cell sources. Based on our experience with the hCMEC/D3 cell line we explored using the immortalized HBEC-5i as an alternative cell line. These cells are singly transfected as opposed to the doubly transfected hCMEC/D3, suggesting that the transfection may be less transforming and the cell line may be better suited for further transfection.[14,25,26] Although the HBEC-5i cell line has predominantly been used for cerebral malaria investigation, the recent work on the cell line as a BBB model is encouraging for use as an immortalized endothelium alternative.[27–31]

Early monoculture screening of the HBEC-5i cell line showed that it was not a tighter model than the hCMEC/D3 or iCell® models, but it was worth investigating its use in the multicellular models given the relative increases we have seen in tightness for the hCMEC/D3 when adding the supporting cells of the NVU in direct contact.[13] In the coculture models we observed decreases in paracellular permeability of [^{14}C]-mannitol suggesting that the presence of astrocytes in direct contact with the HBEC-5i cell layer increases the expression of tight junction proteins leading to a tighter model. To our concern, this phenomenon was not replicated in the

direct contact triculture model of the HBEC-5i cells. Given the high number of factors that contribute to the production of the direct contact triculture (*e.g.* seeding density of three cell types, culture time, and matrix proteins) it is possible that the model could be optimized to the HBEC-5i cell line.

2.6 Conclusion

The basis of this work was to continue the development and optimization of the direct contact coculture and triculture models for use in BBB permeability screening. The limitations of the hCMEC/D3 cells was a contributing factor in the search for an alternative endothelial cell line. Use of iPSC derived cell sources is of high interest in the field, however we could not replicate the same encouraging results using the commercially available iCell® endothelial cells as others were able to achieve using laboratory developed cells. We were able to show that the HBEC-5i cell line is a promising alternative for an immortalized cell source—demonstrating reproducible results in the direct contact coculture model. Ultimately, the work presented above has paved the path for the future work presented in this thesis. Many factors were identified and explored that all contribute to *in vitro* model performance. The work here is the foundation for the future optimization of the direct contact triculture model using the HBEC-5i cell line through a design of experiments based approach as presented in Chapters 3 and 4.

2.7 References

1. Kesselheim AS, Hwang TJ, Franklin JM. Two decades of new drug development for central nervous system disorders. *Nat Rev Drug Discov* 2015;**14**:815–6. https://doi.org/10.1038/nrd4793.

2. Abbott NJ, Rönnbäck L, Hansson E. Astrocyte-endothelial interactions at the blood-brain barrier. *Nat Rev Neurosci* 2006;**7**:41–53. https://doi.org/10.1038/nrn1824.

3. Abbott NJ, Patabendige AAK, Dolman DEM, Yusof SR, Begley DJ. Structure and function of the blood-brain barrier. *Neurobiol Dis* 2010;**37**:13–25. https://doi.org/10.1016/j.nbd.2009.07.030.

4. Bauer H-C, Krizbai IA, Bauer H, Traweger A. 'You Shall Not Pass'-tight junctions of the blood brain barrier. *Front Neurosci* 2014;**8**:392. https://doi.org/10.3389/fnins.2014.00392.

5. Löscher W, Potschka H. Blood-brain barrier active efflux transporters: ATP-binding cassette gene family. *NeuroRx J Am Soc Exp Neurother* 2005;**2**:86–98. https://doi.org/10.1602/neurorx.2.1.86.

6. Haseloff RF, Blasig IE, Bauer HC, Bauer H. In search of the astrocytic factor(s) modulating blood-brain barrier functions in brain capillary endothelial cells in vitro. *Cell Mol Neurobiol* 2005;**25**:25–39.

7. Zozulya A, Weidenfeller C, Galla H-J. Pericyte-endothelial cell interaction increases MMP-9 secretion at the blood-brain barrier in vitro. *Brain Res* 2008;**1189**:1–11. https://doi.org/10.1016/j.brainres.2007.10.099.

8. Wang Y, Wang N, Cai B, Wang G-Y, Li J, Piao X-X. In vitro model of the blood-brain barrier established by co-culture of primary cerebral microvascular endothelial and astrocyte cells. *Neural Regen Res* 2015;**10**:2011–7. https://doi.org/10.4103/1673-5374.172320.

9. Thomsen LB, Burkhart A, Moos T. A Triple Culture Model of the Blood-Brain Barrier Using Porcine Brain Endothelial cells, Astrocytes and Pericytes. *PloS One* 2015;**10**:e0134765. https://doi.org/10.1371/journal.pone.0134765.

10. Helms HC, Abbott NJ, Burek M, Cecchelli R, Couraud P-O, Deli MA, *et al.* In vitro models of the blood-brain barrier: An overview of commonly used brain endothelial cell culture models and guidelines for their use. *J Cereb Blood Flow Metab Off J Int Soc Cereb Blood Flow Metab* 2016;**36**:862–90. https://doi.org/10.1177/0271678X16630991.

11. Bouchaud C, Le Bert M, Dupouey P. Are close contacts between astrocytes and endothelial cells a prerequisite condition of a blood-brain barrier? The rat subfornical organ as an example. *Biol Cell* 1989;**67**:159–65.

12. Winkler EA, Bell RD, Zlokovic BV. Central nervous system pericytes in health and disease. *Nat Neurosci* 2011;**14**:1398–405. https://doi.org/10.1038/nn.2946.

13. Kulczar C, Lubin KE, Lefebvre S, Miller DW, Knipp GT. Development of a direct contact astrocyte-human cerebral microvessel endothelial cells blood-brain barrier coculture model. *J Pharm Pharmacol* 2017;**69**:1684–96. https://doi.org/10.1111/jphp.12803.

14. Weksler BB, Subileau EA, Perrière N, Charneau P, Holloway K, Leveque M, *et al.* Blood-brain barrier-specific properties of a human adult brain endothelial cell line. *FASEB J Off Publ Fed Am Soc Exp Biol* 2005;**19**:1872–4. https://doi.org/10.1096/fj.04-3458fje.

15. Carl SM, Lindley DJ, Das D, Couraud PO, Weksler BB, Romero I, *et al.* ABC and SLC transporter expression and proton oligopeptide transporter (POT) mediated permeation across the human blood--brain barrier cell line, hCMEC/D3 [corrected]. *Mol Pharm* 2010;**7**:1057–68. https://doi.org/10.1021/mp900178j.

16. Weksler B, Romero IA, Couraud P-O. The hCMEC/D3 cell line as a model of the human blood brain barrier. *Fluids Barriers CNS* 2013;**10**:16. https://doi.org/10.1186/2045-8118-10-16.

17. Eigenmann DE, Xue G, Kim KS, Moses AV, Hamburger M, Oufir M. Comparative study of four immortalized human brain capillary endothelial cell lines, hCMEC/D3, hBMEC, TY10, and BB19, and optimization of culture conditions, for an in vitro blood–brain barrier model for drug permeability studies. *Fluids Barriers CNS* 2013;**10**:33. https://doi.org/10.1186/2045-8118-10-33.

18. Urich E, Lazic SE, Molnos J, Wells I, Freskgård P-O. Transcriptional profiling of human brain endothelial cells reveals key properties crucial for predictive in vitro blood-brain barrier models. *PloS One* 2012;**7**:e38149. https://doi.org/10.1371/journal.pone.0038149.

19. Tai LM, Reddy PS, Lopez-Ramirez MA, Davies HA, Male DK, Male ADK, *et al.* Polarized P-glycoprotein expression by the immortalised human brain endothelial cell line, hCMEC/D3, restricts apical-to-basolateral permeability to rhodamine 123. *Brain Res* 2009;**1292**:14–24. https://doi.org/10.1016/j.brainres.2009.07.039.

20. Biemans EALM, Jäkel L, de Waal RMW, Kuiperij HB, Verbeek MM. Limitations of the hCMEC/D3 cell line as a model for Aβ clearance by the human blood-brain barrier. *J Neurosci Res* 2017;**95**:1513–22. https://doi.org/10.1002/jnr.23964.

21. Stebbins MJ, Wilson HK, Canfield SG, Qian T, Palecek SP, Shusta EV. Differentiation and characterization of human pluripotent stem cell-derived brain microvascular endothelial cells. *Methods San Diego Calif* 2016;**101**:93–102. https://doi.org/10.1016/j.ymeth.2015.10.016.

22. Lippmann ES, Weidenfeller C, Svendsen CN, Shusta EV. Blood-brain barrier modeling with co-cultured neural progenitor cell-derived astrocytes and neurons. *J Neurochem* 2011;**119**:507–20. https://doi.org/10.1111/j.1471-4159.2011.07434.x.

23. Lippmann ES, Azarin SM, Kay JE, Nessler RA, Wilson HK, Al-Ahmad A, *et al.* Derivation of blood-brain barrier endothelial cells from human pluripotent stem cells. *Nat Biotechnol* 2012;**30**:783–91. https://doi.org/10.1038/nbt.2247.

24. Lippmann ES, Al-Ahmad A, Palecek SP, Shusta EV. Modeling the blood–brain barrier using stem cell sources. *Fluids Barriers CNS* 2013;**10**:2. https://doi.org/10.1186/2045-8118-10-2.

25. Dorovini-Zis K, Prameya R, Bowman PD. Culture and characterization of microvascular endothelial cells derived from human brain. *Lab Investig J Tech Methods Pathol* 1991;**64**:425–36.

26. Wassmer SC, Cianciolo GJ, Combes V, Grau GE. Inhibition of Endothelial Activation: A New Way to Treat Cerebral Malaria? *PLoS Med* 2005;**2**:. https://doi.org/10.1371/journal.pmed.0020245.

27. Wassmer SC, Combes V, Candal FJ, Juhan-Vague I, Grau GE. Platelets Potentiate Brain Endothelial Alterations Induced by Plasmodium falciparum. *Infect Immun* 2006;**74**:645–53. https://doi.org/10.1128/IAI.74.1.645-653.2006.

28. Jambou R, Combes V, Jambou M-J, Weksler BB, Couraud P-O, Grau GE. Plasmodium falciparum adhesion on human brain microvascular endothelial cells involves transmigration-like cup formation and induces opening of intercellular junctions. *PLoS Pathog* 2010;**6**:e1001021. https://doi.org/10.1371/journal.ppat.1001021.

29. Jiang W, Huang W, Chen Y, Zou M, Peng D, Chen D. *HIV-1 Transactivator Protein Induces ZO-1 and Neprilysin Dysfunction in Brain Endothelial Cells via the Ras Signaling Pathway*. Oxidative Medicine and Cellular Longevity. 2017. https://doi.org/10.1155/2017/3160360.

30. Puech C, Hodin S, Forest V, He Z, Mismetti P, Delavenne X, *et al.* Assessment of HBEC-5i endothelial cell line cultivated in astrocyte conditioned medium as a human blood-brain barrier model for ABC drug transport studies. *Int J Pharm* 2018;**551**:281–9. https://doi.org/10.1016/j.ijpharm.2018.09.040.

31. Puech C, Delavenne X, He Z, Forest V, Mismetti P, Perek N. Direct oral anticoagulants are associated with limited damage of endothelial cells of the blood-brain barrier mediated by the thrombin/PAR-1 pathway. *Brain Res* 2019. https://doi.org/10.1016/j.brainres.2019.05.024.

32. Schrade A, Sade H, Couraud P-O, Romero IA, Weksler BB, Niewoehner J. Expression and localization of claudins-3 and -12 in transformed human brain endothelium. *Fluids Barriers CNS* 2012;**9**:6. https://doi.org/10.1186/2045-8118-9-6.

33. Srinivasan B, Kolli AR, Esch MB, Abaci HE, Shuler ML, Hickman JJ. TEER measurement techniques for in vitro barrier model systems. *J Lab Autom* 2015;**20**:107–26. https://doi.org/10.1177/2211068214561025.

CHAPTER 3. DESIGN OF EXPERIEMENT BASED OPTIMIZATION OF AN IN VITRO DIRECT CONTACT TRICULTURE BLOOD BRAIN BARRIER MODEL FOR PERMEABILITY SCREENING

3.1 Abstract

The restrictive properties of the blood brain barrier (BBB) are largely influenced by the presence of supporting cells (astrocytes and pericytes) of the neurovascular unit (NVU), which underlie the brain microvessel endothelial cells (BMEC) in close proximity. *In vivo* relevant direct contact between astrocytes, pericytes, and BMECS to our knowledge has not been established in conventional Transwell® based *in vitro* screening models of the BBB. We have previously established a direct contact triculture model to mimic the *in vivo* NVU by developing direct layered contact of astrocytes, pericytes, and BMECs layered on the apical surface of a permeable filter support with hCMEC/D3 cells. Due to some concerns regarding the loss of phenotypic similarity with increasing passages, the hCMEC/D3 cell line was replaced. Here we describe the utilization of primary human astrocytes and pericytes cultured with the human brain endothelial cells (HBEC-5i), where culturing conditions were optimized using a design of experiments (DOE) based approach to arrive at optimized conditions using the multi-factor cell based system. We have demonstrated that a DOE approach is a useful tool to expedite optimization of biologically based systems and facilitates understanding of factor interactions in these models. The direct contact model has been shown to provide increased NVU-like restricted permeation comparative to HBEC-5i monoculture and direct contact coculture models, suggesting that the presence of both astrocytes and pericytes in physiologically relevant contact with the endothelium further enhances the restrictive NVU phenotype. Additionally, the model was demonstrated to be capable of differentiating between BBB positive and negative permeants, as identified in *in vitro* and *in vivo*

studies, suggesting that it may be an enhanced better discriminating screening model for potential neurotherapeutics and possible neurotoxicants.

3.2 Introduction

There is a continuing need for screening models that will facilitate the development of therapeutic agents aimed at mitigating brain disorders, particularly as there is a rapidly increasing prevalence of neurodegenerative and neurodevelopmental diseases.[1] The costs associated with developing neurotherapeutics is significant in a large part due to the high rates of attrition in later stages of development.[2] The implementation of a low cost, predictive, and physiologically relevant *in vitro* screening model to more rigorously facilitate hit and lead candidate selection providing greater *in vivo* correlative rank ordering of potential compounds or drug delivery systems for further development is imperative.

Many have theorized that the high rates of attrition are predominantly due to the in ability of drug candidates to cross the blood brain barrier (BBB).[1–3] The BBB has traditionally been believed to be comprised of brain microvessel endothelial cells (BMECs) that line the capillaries of the brain to maintain a homeostatic environment. The BBB separates the brain parenchyma from the systemic circulation and prevents permeation of potential xenobiotics into the brain milieu.[4,5] The BBB endothelium is unique in comparison to the periphery due to the high expression of efflux proteins, drug transporters, metabolizing enzymes, and the presence of restrictive tight junctions.[6,7] Tight junctions in the brain are formed between adjacent BEMCs by a complex of transmembrane intracellular cleft spanning proteins such as occludin and claudins 3 and 5, which anchor to cytosolic scaffolding proteins supported by the actin cytoskeleton.[8–10] The presence of restrictive tight junctions limits the permeation of small hydrophilic compounds,

forcing compounds to move transcellularly in order to cross the BBB. The high expression levels of non-substrate specific ATP-binding cassette (ABC) transporters such as P-glycoprotein (P-gp) and Breast Cancer Resistance Protein (BCRP) results in a high degree of efflux for molecules that attempt to cross the BBB through the transcellular pathway.[11] The presence of efflux transporters may limit the permeation of potential neurotoxicants, while also presenting a challenge for drug delivery as a number of intended neurotherapeutics tend to be lipophilic, favoring multidrug-resistant isoform efflux.[12] Due to their unique presence in the BBB, restrictive tight junctions and functional efflux proteins are key validation characteristics when establishing an *in vitro* BBB screening model.

The *in vivo* BBB phenotype is also largely modulated by the presence of supporting cellular and non-cellular components including astrocytes, pericytes, neurons, and the basal lamina. Together, these components make up the neurovascular unit (NVU), which are each essential for the function of the BBB *in vivo*. Astrocytes fully surround the endothelium and are linked to each other via gap junctions.[13] Single astrocytes have been shown to interact with up to four different neurons and five blood vessels, making them the cellular link between the endothelium and brain parenchyma.[14–16] Astrocytes participate in ion and water regulation due to the localization of these channels in the astrocytic endfeet and has been linked to the expression of basal lamina proteins.[10,17] Additionally, astrocytes influence BMEC growth, modulation through extracellular signaling, play an important metabolic role, and assist in the functional maintenance through the secretion of soluble factors which have been shown to be essential for NVU homeostasis.[18–21] Towards the latter point, several *in vitro* and *in vivo* studies have demonstrated that changes in BBB integrity may result from a deficiency of certain astrocytic soluble factors.[18–21] Pericytes are found enveloped in the basal lamina of the NVU between the astrocytes and endothelium. However,

pericyte distribution is not continuous and in general cover approximately one third of the BMEC basal layer, with higher densities observed regiospecifically within the brain.[22] Pericytes are believed to play a similar role as astrocytes in NVU modulation through the secretion of soluble factors, but are unique in their role in NVU formation and maintenance, specifically during development.[23,24] Pericyte-endothelial crosstalk occurs through a number of signal cascades including platelet-derived growth factor B (PDGF-B) and transforming growth factor-β (TGF-β), as well as others.[25] Interactions between the pericytes and endothelium occurs within the basal lamina due to the relative location of embedded pericytes in the shared basement membrane, potentially suggesting that the composition of the extracellular matrix plays a role in BBB development and maintenance. The basal lamina is a non-cellular component of the NVU and is responsible for maintaining integrity of the BBB by anchoring the cellular components. There are a significant number basement membrane proteins that include fibronectin, collagen IV, laminins, and vitronectin that form the matrix which is approximately 20 nm thick *in vivo*.[6,26,27] Given the multiple components that make up the NVU, cellular and non-cellular, we propose that the BBB should be viewed as the NVU as a whole rather than simply the contributions of the BMECs.

In vitro screening models have traditionally been used to evaluate the potential of new chemical entities to cross the BBB, with much of the emphasis of these models being placed on the endothelial cell type. The BMEC used is often primary or immortalized and of animal or human origin, each presenting its own advantages for use in *in vitro* models.[28,29] Although animal sources are typically lower cost, have significantly higher access, and can be easier to isolate, physiological and phenotypic differences between the human and animal NVU make human cell sources preferred for drug permeability screening due to the presumed physiological relevance to the patient. Primary cells, directly isolated from patients, often present a phenotype most similar to *in*

vivo, but are often difficult to acquire due to ethical reasons, require intricate isolation protocols, and present concerns with patient specific differences.[30,31] Therefore, much of the emphasis has been placed on establishing and characterizing human immortalized cell lines for robust screening methods.

Since its establishment in 2005, the human cerebral microvessel endothelial cell line (hCMEC/D3) has been the most widely used immortalized endothelial cell line for BBB *in vitro* models.[32,33] Although it is widely used, studies (as well as our observations, unpublished results) have revealed that hCMEC/D3 cells can have relatively "leaky" tight junctions and demonstrate a functional reduction in efflux transporter expression with passaging.[28,34–36] The hCMEC/D3 cells were also isolated from a single patient who suffered from epilepsy and was immortalized by a co-transfection of hTERT oncogene and SV40. An alternative immortalized human brain endothelium is the HBEC-5i cell line that was singly transfected with SV40 and originates from a patient pool of cerebral cortex fragments, lacking pathological abnormalities.[37,38] The HBEC-5i has been used predominantly in the study of cerebral malaria; however, these studies have established the potential for this cell line to be used for BBB *in vitro* permeability screening.[38–41] These cells have been observed to express a high number of electron-dense tight junctions as seen under electron scanning microscopy, as well as provide high transendothelial electrical resistance (TEER) and low permeability comparable to other immortalized BMECs.[38] Recently, the HBEC-5i cell line has been used for *in vitro* modeling of the BBB showing functional expression of ABC transporters and stable barrier properties over multiple days of culture, suggesting that they are a viable alternative to the hCMEC/D3 cell line and other immortalized BMEC sources.[42,43]

Given the interaction of multiple cell types in the NVU to maintain the BBB phenotype, many *in vitro* models include astrocytes and pericytes in conjunction with BMECs.[28,44–48]

Typically, these models involve seeding the endothelium on the apical surface of the filter and the supporting NVU cells in the basolateral chamber or on the reverse side of the filter.[49–53] Seeding supporting NVU cells on the reverse side of the filter support displays improved barrier properties in the cultured BMECs by reducing the distance between the cell types and further enhances the BBB phenotype in the cultured endothelium.[53,54] However, the direct cell-cell contact is limited due to the thickness of the filter support and opposable culturing surfaces, where growth through the filter pores provide limited interactions. Studies in our laboratory have demonstrated that seeding endothelium directly layered atop a lawn of cultured astrocytes results in direct cell-cell contacts that enhance barrier properties in comparison to indirect culturing methods.[55] In this study we have further developed and optimized the direct contact, layered coculture model to a triculture system with the inclusion of pericytes to further increase the physiological relevance of the *in vitro* model. The direct contact, layered triculture model is cultured by seeding astrocytes, followed by pericytes, then the endothelium all on the apical side of a filter support to reflect the *in vivo* configuration and cell-cell contacts of the NVU (Fig. 3.1). In our previous studies, we have utilized a One Factor at a Time approach to optimize culturing variables in a laborious and time-consuming manner. Given the multiple factors that influence the performance of this model, we have now utilized a design of experiments (DOE) approach to determine optimal culturing conditions by assessing the influence of multiple variables on barrier properties in a single experiment. This study has demonstrated that a DOE based approach, typically utilized in non-biological process optimization, can be used to optimize other multi-factor cell-based *in vitro* systems by assessing variable influence on model performance. Additionally, the results of this study demonstrate the importance of direct cell contact in *in vitro* models and suggests that increasing physiological

relevance of *in vitro* models to mimic the *in vivo* NVU can further enhance screening tools for neurotherapeutic development.

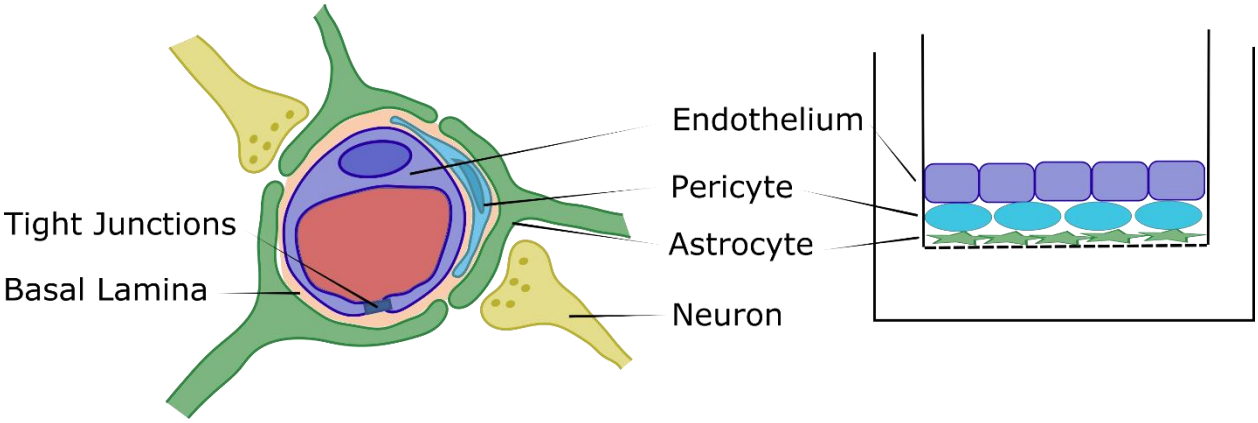

Figure 3.1. Cross section depiction of the neurovascular unit (NVU) with the endothelium (BMECs) lining the capillary, pericytes embedded within the basal lamina, astrocytes having nearly full coverage of the BMECs and surrounding pericytes, and neurons in close contact with the astrocytes (left). The direct contact triculture model on the apical surface of a Transwell® filter support mimicking the *in vivo* NVU. Astrocytes are seeded first on the filter, followed by pericytes, then BMECs to generate a fully apical, direct contact triculture model (right).

3.3 Materials and Methods

3.3.1 *Materials*

Transwell® filters of 12 mm 0.4 µm pore size, T-75 culture flasks, Matrigel®, mouse laminin, and type I rat tail collagen were purchased from Corning (Corning, NY, USA). Hank's balanced salt solution (HBSS) and Dulbecco's Modified Eagle Medium/Nutrient Mixture F-12 (DMEM/F-12) were obtained from Gibco (Carlsbad, CA, USA). Fetal bovine serum (FBS), hydrocortisone, lithium chloride, retinoic acid, rhodamine 123 (R123), elacridar, digoxin, carbamazepine, colchicine, clozapine, caffeine, and prazosin hydrochloride were purchased from MilliporeSigma (St. Louis, MO, USA). HEPES (2-[4-(2-hydroxyethyl)piperazin-1-yl]ethanesulfonic acid) and calcium chloride dihydrate were obtained from J.T. Baker

(Phillipsburg, NJ, USA). Dexamethasone was obtained from MP Biomedicals (Santa Ana, CA, USA). Endothelial cell growth supplement (ECGS) was purchased from Alfa Aesar (Haverhill, MA, USA). Fluorescein isothiocyanate (FITC) labeled 4 kD dextran was purchased from Chondrex (Redmond, WA, USA). Poly-L-lysine (PLL) was purchased from Trevigen (Gaithersburg, MD, USA). Radiolabeled compounds [14C]-mannitol, -sucrose, -inulin, -PEG-4000, and [3H]-L-histidine were purchased from Moravek Biochemicals Inc. (Brea, CA, USA). Human astrocytes, human brain vascular pericytes, astrocyte medium, pericyte medium, and astrocyte and pericyte growth factors were all obtained from ScienCell Research Laboratories (Carlsbad CA, USA). HBEC-5i cells were purchased from ATCC (Manassas, VA, USA).

3.3.2 *Cell Culture*

Human Brain Endothelial Cells (HBEC-5i) were maintained in T-75 culture flasks pre-coated with Type I rat tail collagen with medium changes every 3 days and culturing at 80-90% confluency. The cells were utilized in the studies between passages 22 and 30. HBEC-5i culture medium was made up of Dulbecco's Modified Eagle Medium/Nutrient Mixture F-12 (DMEM/F-12) supplemented with 10% FBS, 15 mM HEPES, and 40 ug/mL endothelial cell growth supplement (ECGS). Human astrocytes and human brain vascular pericytes are maintained in T-75 culture flasks pre-coated with poly-L-lysine with medium changes every 3 days and subculturing at 80-90% confluency. For the studies presented herein, the astrocytes and pericytes were utilized between passage 4 and 10. Astrocyte culture medium was made up of Astrocyte Medium supplemented with 5% FBS, astrocyte growth supplement, and penicillin/streptomycin. Pericyte culture medium was made up of Pericyte Medium supplemented with 5% FBS, pericyte growth supplement, and penicillin/streptomycin.

3.3.3 *Experimental Design for Optimization*

Optimization of plating conditions (cell seeding densities, extracellular matrix protein, and length of culture) and medium additives were performed in sequential design of experiment (DOE) analyses. For plating studies JMP® 13.2 from SAS statistical software was used to determine the plating conditions of each experimental run for a total of 39 combinations by utilizing a 5 factor, 2 level, custom design (DOE_P). Each run was done in a single replicate with DOE_P selected conditions to determine best levels for each variable and then the combined optimized conditions were further confirmed in subsequent experiments in triplicate. Table 3.1 lists the various factors and the respective levels of each.

Table 3.1. Plating Factors and Conditions for DOE_P

Factor	Selected Range*
Astrocyte Seeding Density	20,000 – 60,000 cells/cm^2
Pericyte Seeding Density	20,000 – 60,000 cells/cm^2
HBEC-5i Seeding Density	50,000 – 110,000 cells/cm^2
Study Day	Day 5 – 9
Extracellular Matrix	Collagen I, Matrigel, Laminin

* 3 levels each factor

Similarly, medium optimization was performed in two analyses using a custom design DOE to determine medium conditions that resulted in the tightest barrier properties. The first analysis (DOE_{M1}) was performed using HEPES, hydrocortisone, dexamethasone, LiCl, calcium, and retinoic acid—observing permeability at 9 days post endothelial cell plating (Table 3.2). A second analysis (DOE_{M2}) was performed, based on the results of the first, using hydrocortisone, dexamethasone, LiCl, and retinoic acid at both 5 and 7 days post endothelial cell plating (Table

3.3). Exact conditions for each of the three analyses can be found in Supplemental Material (Table 3.S1-3.S3).

Table 3.2. Medium Optimization with Evaluation on Day 9 (DOE_{M1})

Factor	Selected Range*
HEPES	15 – 25 mM
Hydrocortisone	0 – 1.4 µM
Dexamethasone	0 – 10 µM
Lithium Chloride	0 – 10 mM
Calcium	0 – 1 mM
Retinoic Acid	0 – 10 µM
Study Day	Day 9

* 2 levels each factor (presence of absence of given additive)

Table 3.3. Medium Optimization with Evaluation on Day 5 and 7 (DOE_{M2})

Factor+	Selected Range*
Hydrocortisone	0 – 1.4 µM
Dexamethasone	0 – 10 µM
Lithium Chloride	0 – 10 mM
Retinoic Acid	0 – 10 µM
Study Day	Day 5 or 7

* 2 levels each factor (presence of absence of given additive)

+ All medium supplemented with 15 mM HEPES

3.3.4 *Plating Direct Contact Triculture on Transwell® Filter Support*

For the DOE_P studies, filters were pre-coated with poly-L-lysine (PLL) by pre-coating 12 mm, 0.4 µm pore Transwell® inserts with 5 µg/cm^2 PLL. Astrocytes were plated at seeding densities of 20,000, 40,000, or 60,000 cells/cm^2 and allowed to grow for 48 hours. After 48 hours

of astrocyte growth, astrocyte medium was removed and pericytes were seeded atop the astrocyte lawn at seeding densities of 20,000, 40,000, or 60,000 cells/cm^2 and allowed to grow for 48 hours. After 48 hours of pericyte growth, apical medium was replaced with the specified ECM protein solution. Astrocyte-pericyte lawn filters were coated with one of the following ECM proteins at the respective concentrations: Matrigel® 25 μL/cm^2 (2.5 μg/cm^2), Laminin 5 μg/cm^2, or Type I Rat Tail Collagen 5 μg/cm^2. To coat inserts, Matrigel®, Laminin, or collagen I aliquots were diluted in HBSS with Ca^{2+} and Mg^{2+} and 0.5 mL dispensed onto to each respective 12 mm insert. Inserts were left to incubate with the respective ECM protein for 45 min at 37 °C. After incubation, the ECM solution was removed and HBEC-5i cells were plated at seeding densities of 50,000, 80,000, or 110,000 cells/cm^2 and allowed to grow for 5, 7, or 9 days prior to permeability measurements. Cultures were maintained in complete HBEC-5i medium with medium changes every other day following endothelial cell plating. Transendothelial electrical resistance (TEER) was measured every 24 hours after HBEC-5i plating using 4 mm Chopstick electrode with EVOM2 Volt/Ohm Meter (World Preclinical Instruments), and normalized based on resistance across blank filter supports.

In $DOE_{M1/2}$ studies, culturing methodology described above was used with the modification that the complete HBEC-5i culture medium was supplemented with additional factors and introduced to cultures 24 hours post endothelial plating with medium changes every other day until the day of study. Medium for $DOE_{M1/2}$ was prepared from concentrated stock solutions of 1 M HEPES in water, 4.6 mM hydrocortisone in ethanol, 3.8 mM dexamethasone in DMSO, 11.8 M LiCl in water, 1.7 M $CaCl_2$ in water, and 33.3 mM retinoic acid in DMSO. Total percentage of each solvent was kept constant across all medium conditions.

3.3.5 *Plating Monoculture and Direct Contact Coculture on Transwell® Filter Support*

Monoculture (HBEC-5i alone) and direct contact coculture (astrocyte-HBEC-5i and pericyte-HBEC-5i) models were used for comparison with the direct contact triculture. For monoculture studies, 12 mm, 0.4 μm pore Transwell® inserts were pre-coated with 25 μL/cm^2 Matrigel®. HBEC-5i cells were plated on Matrigel® coated filters at a density of 80,000 cells/cm^2 and cultured for 9 days with medium changed every other day. Direct contact cocultures were plated according to methods developed by Kulczar *et al.* with some modifications.[55] Transwell® filters were pre-coated with 5 μg/cm^2 PLL followed by seeding of astrocytes or pericytes at 20,000 cells/cm^2 and allowed to grow for 48 hours. At 48 hours post astrocyte or pericyte plating, HBEC-5i cells at 80,000 cells/cm^2 were seeded directly atop the lawn of pre-seeded cells and cultured for an additional 9 days with medium changed every other day.

3.3.6 *Permeability Assays*

To optimize conditions permeability was measured using 4 kD FITC-dextran at an initial concentration of 0.25 mg/mL in HBSS with Ca^{2+} and Mg^{2+}. Tricultures were washed and left to equilibrate in HBSS at 37 °C for 30 minutes prior to the start of the permeability assay. Permeability was performed at 37 °C on a rocking platform maintaining sink conditions and sampling at 15, 30, 45, 60, and 90 minutes. Samples of 100 μL from each basolateral chamber were removed at each time point and placed into a 96-well black flat-bottomed well plate for fluorescence reading. Samples were analyzed using a BioTek Synergy 4 plate reader at excitation of 485 nm and emission of 530 nm. Apparent permeability (P_{app}) was calculated using the following equation 1 (eq. 1)

$$P_{app} = \frac{dM/dT}{C_0 \times A}$$

(eq. 1)

where dM/dT is the amount of Dextran that moves across the filter over time, Co is the initial concentration in the donor (apical) chamber, and A is the surface area of the filter support. The effective permeability (P_{eff}, permeability contributions of cell layer alone) of each condition was determined using the following equation 2 (eq. 2)

$$\frac{1}{P_{app}} = \frac{1}{P_{eff}} + \frac{1}{P_{filter}}$$

(eq. 2)

where the P_{filter} value used is that of the ECM used in the given condition.

Apparent permeability of additional paracellular markers of varying sizes ([^{14}C]-mannitol, [^{14}C]-sucrose, [^{14}C]-inulin, and [^{14}C]-PEG-4000) was determined in the optimized direct contact triculture. Permeability assays were performed as stated above with an initial concentration of 0.25 µCi/mL in HBSS for all markers and analysis performed by liquid scintillation counting.

A range of BBB positive and negative permeants were used to further evaluate barrier properties of the optimized model. The permeability of [^{3}H]-L-histidine, carbamazepine, colchicine, digoxin, clozapine, and prazosin was determined by preparing 10 mM stock solutions of each compound in DMSO, with the exception of [^{3}H]-L-histidine. For each study, the final concentration of DMSO was equivalent at 1% (v/v). Permeability of [^{3}H]-L-histidine was determined using the same method as stated above for radiolabeled paracellular markers. Working solutions of non-radiolabeled compounds were prepared at a concentration of 25 µM in HBSS with permeability measurements performed as stated above and sampling at 30, 60, 90, 120, and

150 minutes. Analysis for these compounds was performed using high performance liquid chromatography (HPLC). Permeability was calculated according to equation 1.

The function of P-gp in the triculture model was determined using P-gp substrate rhodamine 123 (R123) in the presence and absence of the inhibitor elacridar. Stock solutions of R123 (2 mM) and elacridar (10 mM) were prepared in DMSO. Working solutions of 10 µM R123 and 2 µM elacridar were prepared in HBSS with 1% DMSO. For inhibition studies, tricultures plated on permeable filter supports were pre-incubated with 2 µM elacridar for 45 minutes prior to the addition of R123. Samples were removed at 30, 60, 90, and 120 minute time points and analysis was performed using the BioTek Synergy 4 plate reader at excitation of 485 nm and emission of 530 nm. Permeability was calculated according to equation 1.

3.3.7 *High Performance Liquid Chromatography*

Analysis of carbamazepine, caffeine, colchicine, digoxin, clozapine, and prazosin was performed on an Agilent 1100 reverse phase HPLC with variable wavelength detection (VWD). All samples were run isochratically through an Ascentis® C-18 15 x 4.6 mm, 5 µm column, at 25 µL injection volume, using water and acetonitrile (ACN) for all mobile phase. Carbamazepine analysis was performed using a column temperature of 40 °C, mobile phase of 65:35, water:ACN, at a 1.5 mL/min flow rate, and absorbance measurement at 284 nm. Caffeine analysis was at ambient temperature, a mobile phase of 90:10, water:ACN, at a 1.0 mL/min flow rate, and absorbance measurement at 275 nm. Colchicine analysis was performed using a column temperature of 40 °C, mobile phase of 75:25, water:ACN, at a 1.5 mL/min flow rate, and absorbance measurement at 354 nm. Digoxin was analyzed using a column temperature of 40 °C, a mobile phase of 70:30, water:ACN, at a 1.1 mL/min flow rate, and absorbance measurement at 218 nm. Clozapine analysis was performed using a column temperature of 40 °C, mobile phase of

45:55, water:ACN, at a 1.5 mL/min flow rate, and absorbance measurement at 254 nm. Prazosin analysis was performed using a column temperature of 40 °C, mobile phase of 65:35, water:ACN, at a 1.5 mL/min flow rate, and absorbance measurement at 254 nm.

3.3.8 *Statistical Analysis*

JMP 13.2 statistical software was used to generate custom experimental designs based on categorical and discrete continuous factors. Analysis of each DOE was done by fitting models based on the P_{eff} of 4 kD dextran response to standard least squares to determine optimal conditions. In comparison studies, all conditions were performed in triplicate (n=3) and subjected to Student's *t*-test or one-way ANOVA with Tukey Kramer post-hoc test. A p-value of 0.05 was considered to be statistically significant.

3.4 Results

3.4.1 *Plating Optimization (DOE_P)*

Traditionally, a one factor at a time (OFAT) approach is used for assessing the impact of variable changes in biologically based models and processes, where one variable (e.g. cell density) is optimized in the presence of several other unoptimized variables in an inefficient and laborious manner. A design of experiments based approach allows for the influence of multiple factors to be observed on a measured response to arrive at an optimal level for each given variable. Furthermore, it allows one to more rapidly identify optimized growth conditions in a time and labor efficient manner. Based on previous studies establishing a direct contact triculture (unpublished results) and our direct contact coculture model, informed selection of the seeding densities of all three cell types, ECM used to aid endothelial attachment, and length of culture of the endothelium were the

selected factors.[55] Optimal plating conditions were determined using P_{eff} values to account for the differences associated with ECM coatings. Conditions 8 (60 HA, 60 HBVP, 110 EC, Laminin, Day 9) and 20 (20 HA, 20 HBVP, 110 EC, Laminin, Day 9) exhibited the lowest Peff values at 3.2 x 10^{-6} cm/sec (Fig. 3.2).

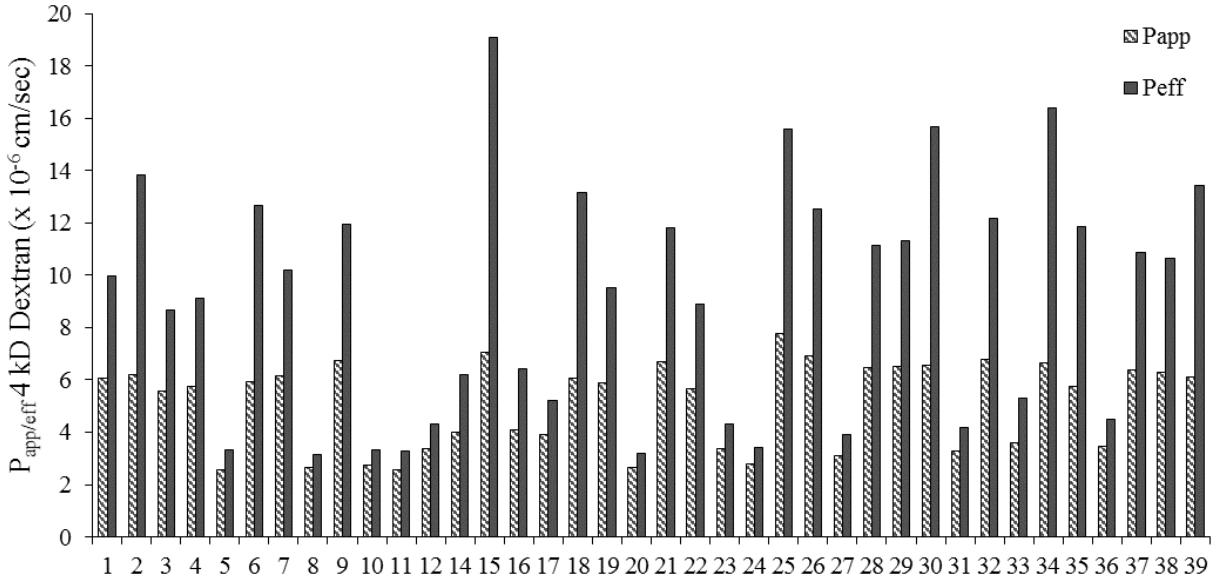

Figure 3.2. P_{app} and P_{eff} of 4 kD FITC-Dextran across different direct contact triculture conditions of DOE_P. All conditions were performed as n=1. Condition 13 was compromised and permeability was not performed, data point was excluded from statistical analysis.

Based on the trends in the data, study day has the largest impact on paracellular permeability resulting in significantly lower 4 kD dextran permeability at day 9 compared to days 5 and 7. When separating the data by study day and factor there are observable trends in the permeability, including the effects of astrocyte and pericyte cell density. With extended culturing, higher seeding densities of astrocytes appears to result in higher permeability of the dextran, however this observation is not significant (Fig. 3.3). HBEC-5i seeding density also shows trends towards lower permeability at higher seeding densities; however, this trend is not as strong at day 9 when the cells have had sufficient time to reach confluency.

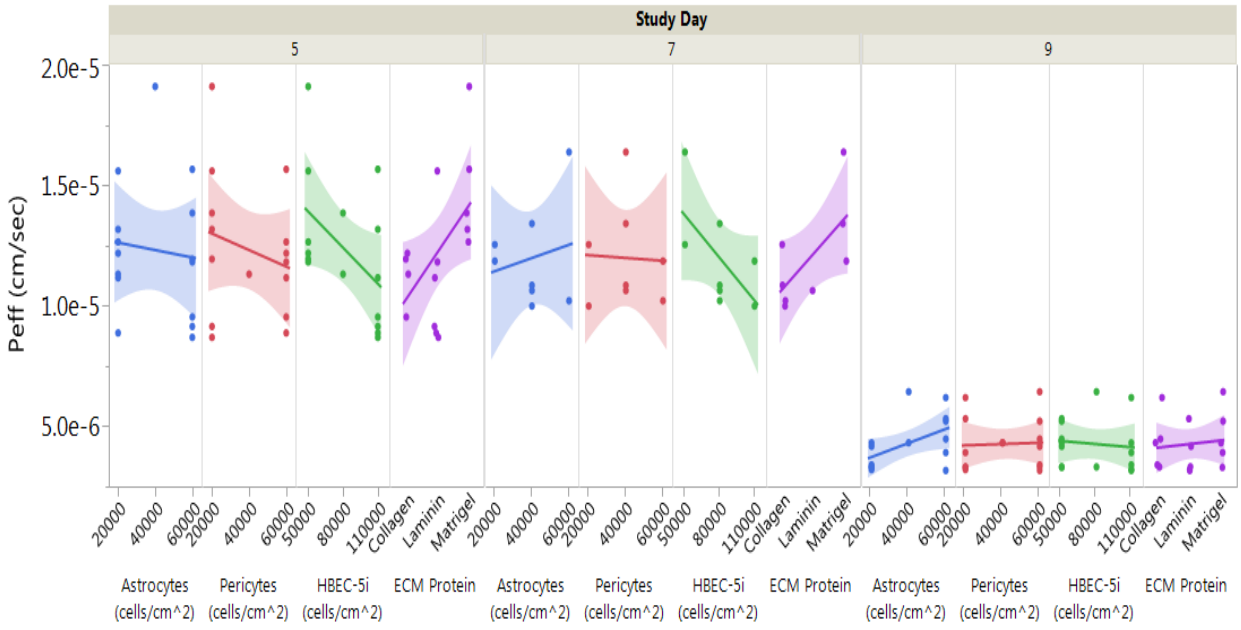

Figure 3.3. P_{eff} of 4 kD FITC-Dextran for DOE_P separated by factor and further by day of study showing relative trends of factor levels at increasing length of culture. All conditions are represented by single data points across the graph, n=1.

Using JMP 13.2 software, a prediction profiler was generated based on the obtained P_{eff} values for the given conditions. By maximizing the Desirability to achieve the lowest possible permeability, the optimal conditions were determined to be 20,000 cells/cm^2 for both astrocytes and pericytes, 80,000 cells/cm^2 HBEC-5i cells, Matrigel® as the ECM protein, and culturing for 9 days post endothelial cell plating (Fig. 3.4). These conditions would optimally generate a predicted P_{eff} value of 2.4 x 10^{-6} cm/sec for 4 kD dextran. Upon repeating the analysis at selected optimal conditions, the P_{eff} of a 4 kD dextran showed to be reproducible resulting in a similar permeability value (P_{eff}; 3.7 x 10^{-6} cm/sec ± 0.04, n = 3).

3.4.2 *Medium Optimization ($DOE_{M1/2}$)*

Selection of medium additives were chosen based on literature and previous studies in our laboratory to be added to HBEC-5i medium based on their reported influences on barrier tightness

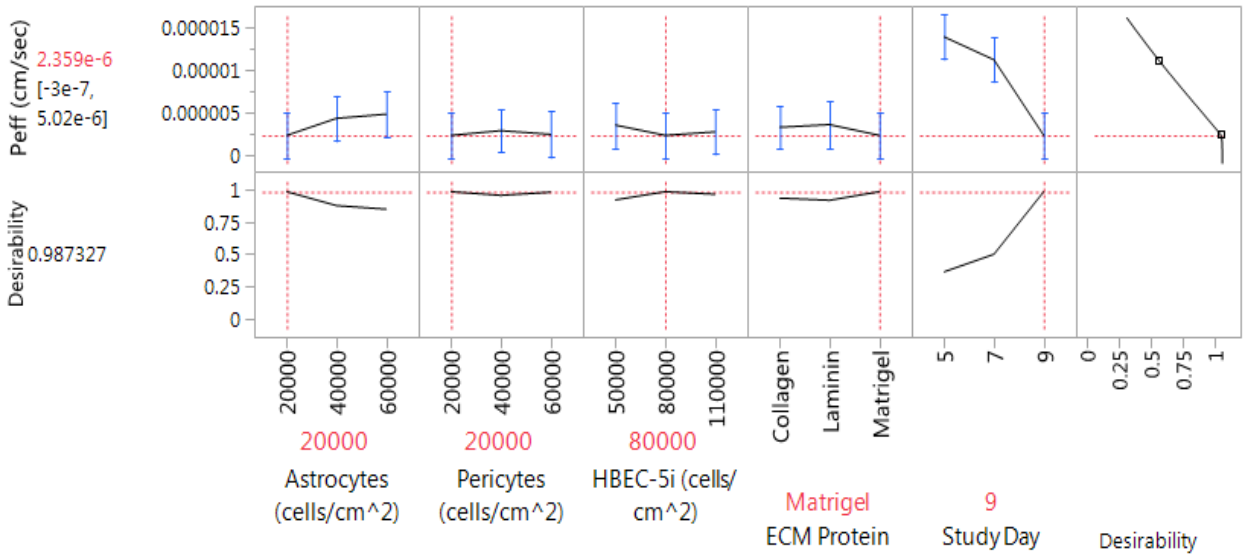

Figure 3.4. JMP 13.2 Prediction Profiler generated based on maximizing desirability for P_{eff} based on DOE_P. Optimal plating conditions 20,000 cells/cm^2 astrocytes and pericytes, 80,000 cells/cm^2 HBEC-5i, Matrigel, and 9 days of endothelial growth. Predicted P_{eff} of 2.4 x 10^{-6} cm/sec for optimal conditions.

both *in vitro* and *in vivo*.[55–62] Unmodified HBEC-5i medium contains 15 mM HEPES; therefore, higher levels of HEPES were included to assess the impact that a higher buffering capacity would have on barrier tightness. Hydrocortisone was selected for its influence on inflammatory responses as a glucocorticoid and potential to prevent tight junction break down.[56] Lithium chloride has been shown to influence claudin expression through stimulation of the Wnt/β-catenin pathway.[57] Calcium was studied as a medium additive due to its influence on adherens and tight junction protein expression to increase barrier tightness, where studies have shown that low extracellular calcium levels can lead to an increase in paracellular permeability.[58,59] Like hydrocortisone, dexamethasone acts to inhibit inflammatory responses and upregulate tight junctions; however, it is a synthetic alternative to the naturally occurring hydrocortisone.[60] Lastly, retinoic acid is naturally secreted by glial cells and has revealed significant increases in paracellular tightness in *in vitro* BBB models.[61,62]

The first analysis of medium optimization (DOE_{M1}) was performed at optimal plating conditions determined from DOE_P: 20,000 cells/cm^2 for astrocytes and pericytes, 80,000 cells/cm^2 HBEC-5i, Matrigel, after 9 days of endothelial growth. HEPES, hydrocortisone, dexamethasone, lithium chloride, calcium, and retinoic acid were chosen as medium additives due their reported influence on tight junction expression and induction of barrier properties in *in vitro* BBB models. The lowest achieved 4 kD dextran P_{eff} of DOE_{M1} was 6.3 x 10^{-6} cm/sec, suggesting that, under these conditions, the additives did not provide further tightening of the model. Strong trends are not apparent for any of the additives with the exception of higher levels of HEPES resulting in higher permeability values. The optimal medium condition was determined to be 15 mM HEPES, 1 mM calcium, and 10 µM retinoic acid, but the influence of these factors on barrier tightness was not significant (Fig. 3.5).

Based on these results a second analysis (DOE_{M2}) was performed to assess the influence of the additives in earlier days of culture. These studies were conducted in the presence or absence of hydrocortisone, dexamethasone, lithium chloride, and retinoic acid at 5 and 7 days post endothelial cell culture, HEPES was held constant at 15 mM and calcium was removed from

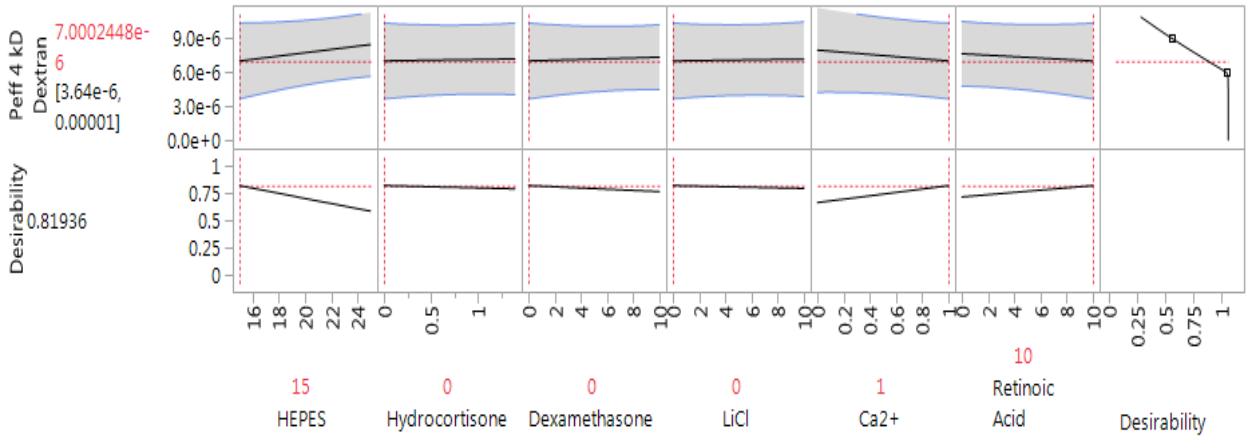

Figure 3.5. JMP 13.2 Prediction Profiler generated based on maximizing desirability for P_{eff} of DOE_{M1}. Optimal medium conditions 15 mM HEPES, 1 mM Ca^{2+}, and 10 µM retinoic acid at 9 days of endothelial growth. Predicted P_{eff} of 7.0 x 10^{-6} cm/sec for optimal conditions.

DOE_{M2}. The lowest 4 kD dextran P_{eff} of DOE_{M2} was 8.3 x 10^{-6} cm/sec, suggesting that the additives do not provide increased barrier tightness based on the optimized plating conditions of DOE_P. Optimal conditions for medium was determined to be 10 µM dexamethasone, 10 µM retinoic acid, 10 mM LiCl, through 7 days of endothelial cell culture; however, these conditions were not used for continued assessment of the optimized model due to the lack of improvement over unmodified medium (Fig. 3.6).

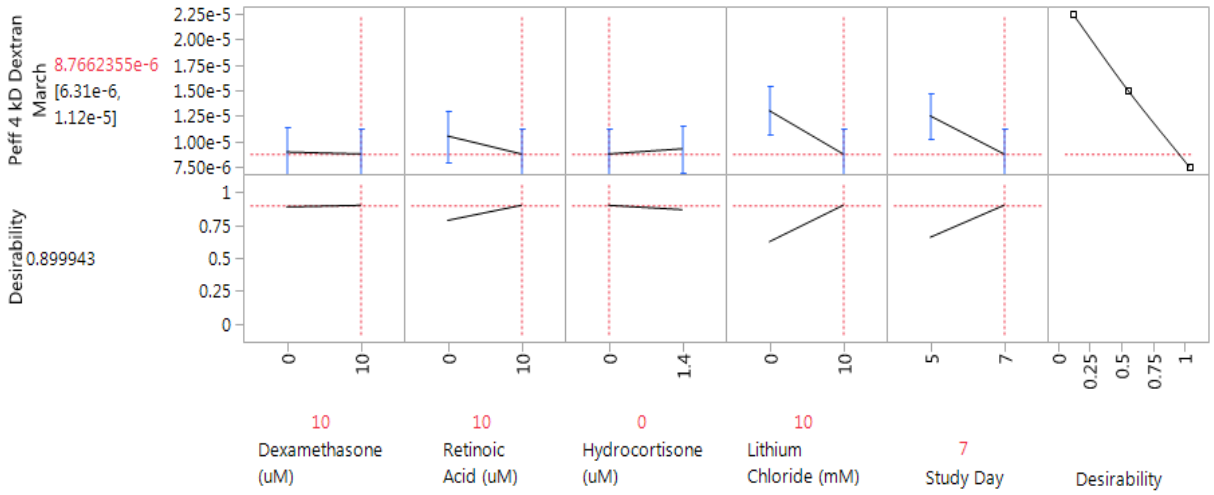

Figure 3.6. JMP 13.2 Prediction Profiler generated based on maximizing desirability for P_{eff} of DOE_{M2}. Optimal medium conditions 10 µM dexamethasone, 10 µM retinoic acid, 10 mM LiCl, through 7 days of endothelial culture. Predicted P_{eff} of 8.8 x 10^{-6} cm/sec for optimal conditions.

3.4.3 *Comparison to Mono- and Cocultures*

The optimized direct contact triculture was compared to a monoculture of HBEC-5i cells alone and direct contact cocultures of HEBC-5i cells plated atop a lawn of astrocytes or pericytes (Fig. 3.7). Effective permeability of the 4 kD FITC-dextran was used for comparison between the different models. In comparison to the optimized direct contact triculture (3.7 x 10^{-6} ± 0.0 cm/sec) the HBEC-5i monoculture had the highest observed permeability (19.7 x 10^{-6} ± 3.0 cm/sec; $p < 0.01$), followed by the perictye-HBEC-5i coculture (15.1 x 10^{-6} ± 3.7 cm/sec; $p < 0.05$), and the astrocyte-HBEC-5i coculture (12.8 x 10^{-6} ± 2.1 cm/sec; $p < 0.05$). Given the significant differences

observed between the direct contact triculture and the monoculture and coculture models, the inclusion of all three cell types offers increased barrier tightness for the *in vitro* model.

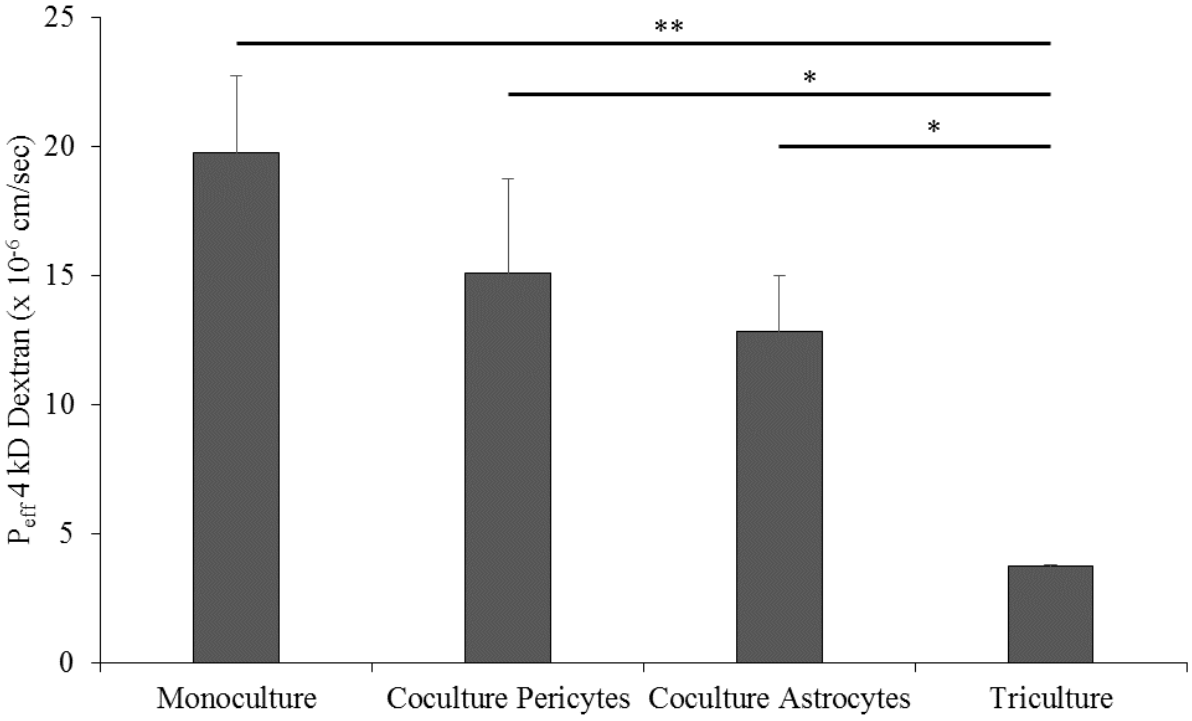

Figure 3.7. Effective permeability (P_{eff}) of 4 kD FITC-dextran across an HBEC-5i monoculture, pericyte-HBEC-5i direct contact coculture, astrocyte-HBEC-5i direct contact coculture, and optimized direct contact triculture. Statistical analysis was performed with one-way ANOVA and Tukey-Kramer post-hoc test. Error bars represent one standard deviation (n=3). *, $p < 0.05$ and **, $p < 0.01$.

3.4.4 *Direct Contact Triculture BBB Marker Compounds*

Paracellular markers possessing a broad range of hydrodynamic radii were used to evaluate the functional tightness of the optimized model (Fig. 3.8).[63–65] The lowest apparent paracellular permeability observed was that of PEG-4000 ($0.78 \times 10^{-5} \pm 0.00$ cm/sec, 15.9 Å) followed by inulin ($P_{app} = 1.55 \times 10^{-5} \pm 0.01$ cm/sec, 10 Å), mannitol ($P_{app} = 1.99 \times 10^{-5} \pm 0.01$ cm/sec, 4.3 Å), and sucrose ($P_{app} = 2.18 \times 10^{-5} \pm 0.02$ cm/sec, 5.2 Å). The apparent paracellular permeability of the hydrophilic markers shows the model is able to distinguish between markers of varying sizes.

However, based on the hydrodynamic radius, sucrose should have a lower permeability as the larger compound in comparison to mannitol.

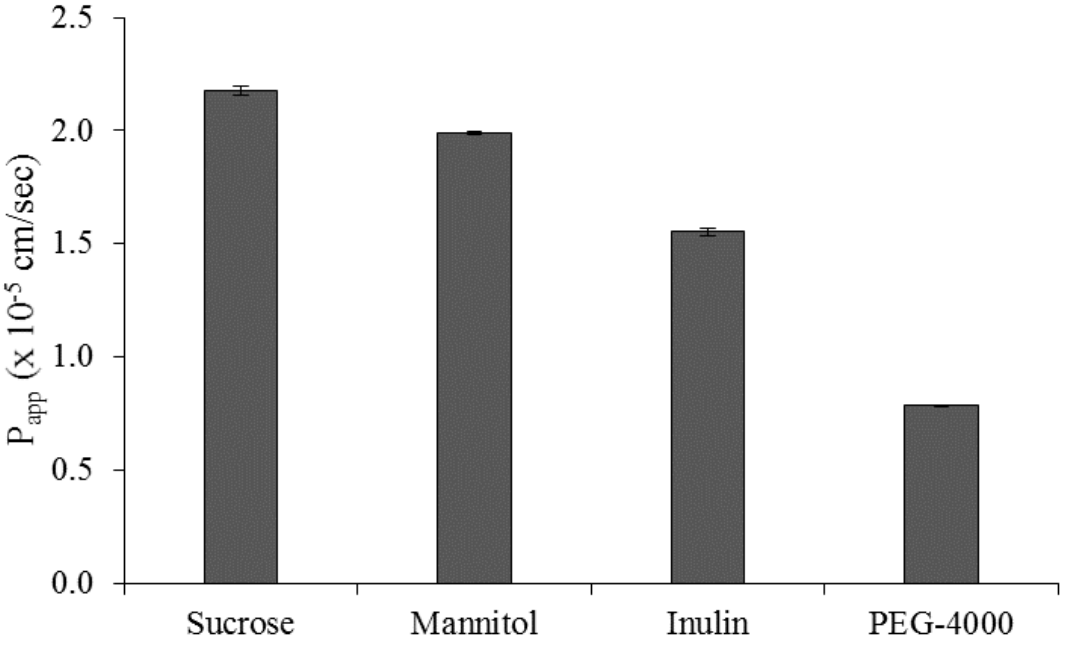

Figure 3.8. Apparent permeability of radiolabeled paracellular markers [^{14}C]-sucrose. [^{14}C]-mannitol, [^{14}C]-inulin, and [^{14}C]-PEG-4000 across the optimized direct contact triculture. Error bars represent one standard deviation.

P-gp function in the direct contact triculture was assessed using P-gp substrate R123 alone and in the presence of P-gp inhibitor elacridar (Fig. 3.9). In the absence of inhibitor, the P_{app} of R123 was 18.52 x 10^{-5} ± 0.58 cm/sec. The presence of elacridar significantly increased the P_{app} of R123 (P_{app} = 21.14 x 10^{-6} ± 0.46 cm/sec; $p<0.01$) across the direct contact triculture. Additional P-gp substrates were utilized as marker compounds such as digoxin (P_{app} = 9.21 x 10^{-6} ± 0.31 cm/sec) and colchicine (P_{app} = 18.67 x 10^{-6} ± 2.75 cm/sec). Prazosin, a BCRP substrate, was used to assess the function of other efflux transporters in the direct contact model (P_{app} = 6.16 x 10^{-6} ± 0.11 cm/sec) (Fig. 3.10).

The antipsychotic drug clozapine showed an apparent permeability value of 8.15 x 10^{-6} ± 0.58 cm/sec. The amino acid L-histidine was used to assess facilitative transport across the *in vitro* model with an observed apparent permeability of 52.61 x 10^{-6} ± 0.70 cm/sec, as reported previously.[64] Carbamazepine is an antiepileptic drug and a BBB positive permeant with an observed apparent permeability of 27.71 x 10^{-6} ± 1.13 cm/sec in the optimized model. Caffeine, a small hydrophilic molecule, also had BBB positive permeation with an obtained apparent permeability of 28.93 x 10^{-6} ± 1.15 cm/sec (Fig. 3.10).

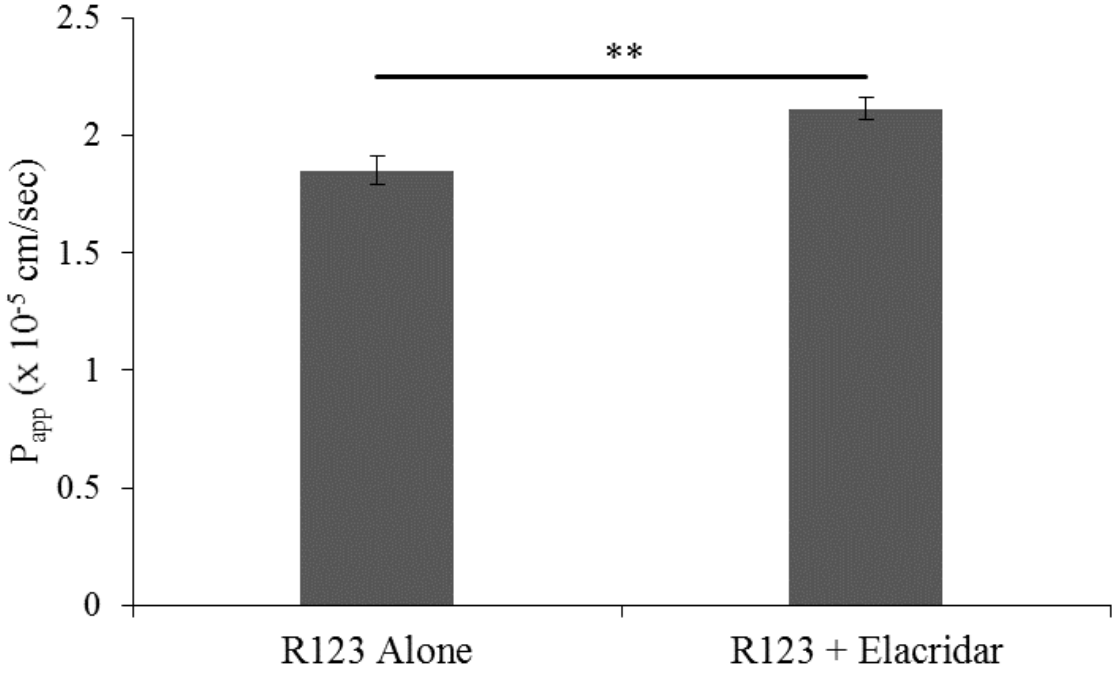

Figure 3.9. Apparent permeability of P-gp substrate rhodamine 123 (R123) in the presence and absence of P-gp inhibitor elacridar across the optimized direct contact triculture. Assays were run in triplicate and subjected to Student's *t*-test. Significant difference is indicated by *, $p < 0.05$ and **, $p < 0.01$. Error bars represent one standard deviation (n=3).

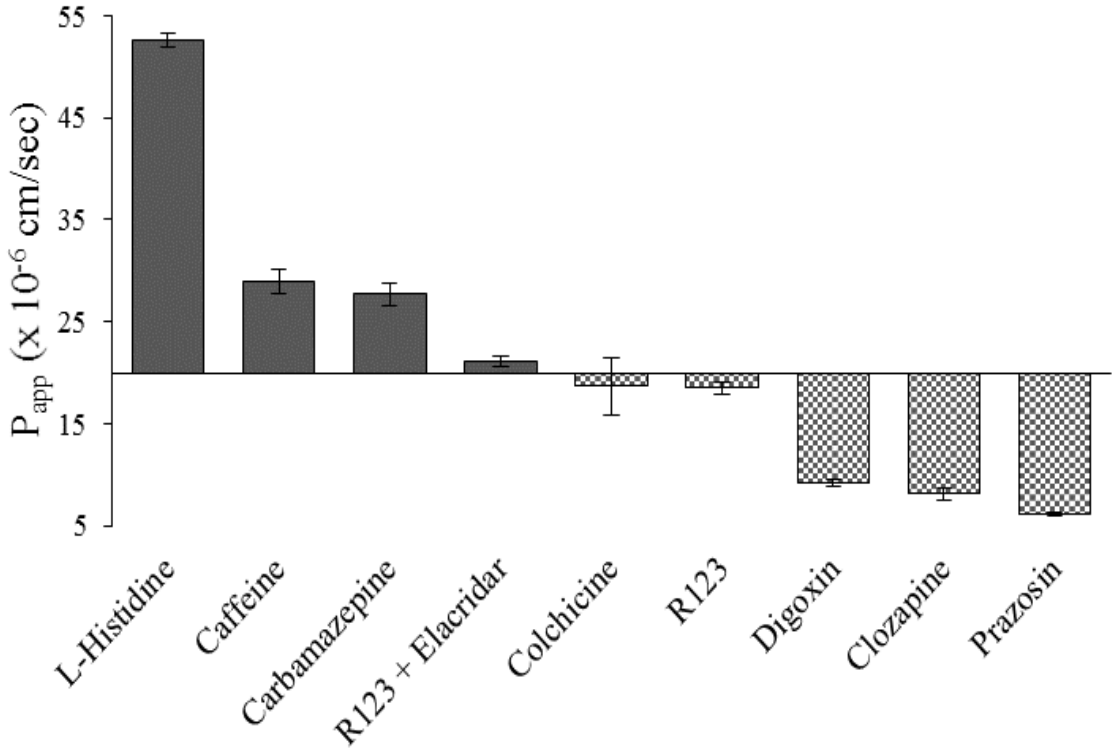

Figure 3.10. Apparent permeability of BBB positive (L-histidine, carbamazepine, and rhodamine 123 in the presence of P-gp inhibitor elacridar) and negative (colchicine, rhodamine 123, digoxin, clozapine, and prazosin) permeants across the optimized direct contact triculture. Assays were performed in triplicate. Error bars represent one standard deviation (n=3).

3.5 Discussion

The HBEC-5i cell line has not been as extensively used for *in vitro* BBB permeability modeling comparative to other BMEC cell sources (e.g. hCMEC/D3). However, it has been shown to have good expression levels of brain endothelial markers such as vascular cell adhesion molecule (VCAM-1) and intercellular adhesion molecule (ICAM-1) essential for immune cell trafficking, CD51 (α_V-integrin) that is involved in extracellular matrix adhesion, as well as tight junction proteins zonula occluden 1 (ZO-1) and claudin-5.[38,42] Transporter expression and function of BCRP, P-gp, MRP-1, and MRP-2 has also been recently evaluated and shown to be comparable

to other immortalized brain endothelium.[42] Conversely, this cell line has also been indicated to be lacking in expression of platelet endothelial cell adhesion molecule (PECAM-1, CD31) and CD36.[38] Given the expression of endothelial markers and transporters that have been investigated by others, we selected the HBEC-5i cell line as the BMEC for the direct contact triculture over using the hCMEC/D3 cell line that we utilized in the development of the direct contact coculture.[55]

In vitro models of the BBB are increasingly being developed to provide physiological relevance through co- and triculture indirect contact methods with astrocytes and pericytes that comprise the NVU to further enhance barrier properties. However, the direct cell-cell contacts of astrocytes and pericytes with the endothelium *in vivo* are often overlooked in these multi-cellular models that are currently being utilized.[28,44–48] We have previously shown that the direct contact between astrocytes and the endothelium in a coculture model increases the barrier properties compared to endothelial monocultures and indirect plating methods.[55] Although astrocytes are often used in *in vitro* models as a supporting cell, pericytes also play an important role in influencing and regulating the BBB phenotype through a number of signaling cascades.[24,66,67] Since each supporting cell acts in a functionally different manner on the BMECs, incorporating both astrocytes and pericytes in direct contact cell based models should better enable synergistic effects of the NVU to be represented *in vitro*.

A design of experiments approach was taken to develop and optimize the direct contact triculture in order to adequately understand the interactions each variable would have on the performance of the model. As opposed to an OFAT approach, DOE takes into account the implications of changing multiple variables to come to optimal conditions in a significantly more efficient manner in terms of time invested and resources required. In optimizing the triculture we arrived at optimal conditions with reproducible results in a time frame of two months as opposed

to our previous optimization efforts that spanned the course of multiple years. The results of DOE_P revealed optimal plating conditions of 20,000 cells/cm^2 for both astrocytes and pericytes, 80,000 cells/cm^2 for HBEC-5i, Matrigel® as the ECM to promote endothelial adhesion, and culturing the endothelium for 9 days after seeding. The comparison of 4 kD dextran permeability to other reported data revealed that our optimized model infers that the model is among the tightest we

Table 3.2. P_{eff} Values of 4 kD Dextran for Different BBB Models

Model/Endothelial Cell Line	Peff (10^{-6} cm/sec)
DOE Direct Contact Triculture, HBEC-5i	3.7
Monoculture (HA conditioned medium), HBEC-5i	3.6[a]
Monoculture, hCMEC/D3	8.8[b], 5.4[c]
Isolated endothelial cells, rat	1.0[d]
In vivo microvessels, rat	0.92[e]

a Puech, C., *et al.*, Int J Pharm (2018) 551(1) 281-289, **b** Förster, C., *et al.*, J Physiol (2008) 589(7) 1937-1949, **c** Weksler, B., *et al.*, FASEB J. (2005) 19(13) 1872-1874, **d** Watson, P.M.D., *et al.*, BMC Neuroscience (2013) 14:59, **e** Yuan, W.. *et al.*, Microvasc Res (2009) 77(2) 166-173

found reported, suggesting that culturing multiple NVU cell types in direct contact synergistically increases barrier tightness (Table 3.4).

In addition to selecting an optimized set of plating conditions, the DOE approach facilitated an understanding of how changing factor levels may impact the model performance. At higher densities of astrocytes and pericytes a decrease in paracellular tightness was observed with extended culture time. This phenomenon is likely due to the length of time these cells are in culture, with the astrocytes and pericytes possibly becoming senescent by the day of study. Additionally, higher seeding densities of endothelial cells resulted in lower paracellular permeation rates at day 5 and 7, which may be expected by the increased ability of the cells to form a confluent layer at fewer days of culture. However, that trend is less drastic after 9 days of culture suggesting that

seeding density does not play as significant of a role at confluency, but rather time in culture is necessary to allow for differentiation and adequate tight junction formation.

An effort to optimize culture medium (DOE_{M1} and DOE_{M2}) was made to further increase barrier properties of the model through the inclusion of additives that have been shown to enhance the BBB phenotype in *in vitro* and *in vivo* studies. Between both assessments it was revealed that the length of culture time for the endothelium still had the largest impact on model performance regardless of additives (Fig. 3.6). Based on this finding it is possible that due to the influence the additives have on the endothelium the HBEC-5i cells are differentiating before reaching confluency, and this is not sustainable through the length of culture. This phenomenon could also explain why the effects of additives appear to be more extreme in DOE_{M2}, culturing for 5 or 7 days post endothelial plating, as the differentiation effects may be occurring earlier and not maintained through culture times for DOE_{M1}. A way to improve on this would be to include HBEC-5i seeding density as a factor in further assessments of medium additives. With the trends of DOE_P establishing the positive impacts higher seeding densities have on model tightness, seeding at a higher density (greater than the optimized 80,000 cells/cm^2) with differentiation inducing medium supplements may result in the tightest barrier formed and additionally reduce culturing time. An alternative would be to continue with optimized conditions of DOE_P and include time of addition as a factor in further studies by introducing additives after the HBEC-5i have been in culture for more than 24 hours.

The influence of the medium additives may also extend beyond paracellular tightness. Hydrocortisone has been shown to increase barrier tightness through the upregulation of tight junction proteins, but has also been demonstrated to induce efflux transporter expression.[42,68,69] Expression and function of ABC efflux transporters, specifically BCRP and P-gp, was also

demonstrated to be influenced by the release of tumor necrosis factor-α (TNF-α) and subsequent inflammatory responses.[42,69,70] However, hydrocortisone is a glucocorticoid that has been demonstrated to impact P-gp and BCRP expression by inducing anti-inflammatory responses. Therefore, in addition to the impact on paracellular tightness, the induction of efflux transporter expression should also be assessed by evaluating the time of addition of hydrocortisone to the culture medium.

The increase in physiological relevance of adding additional cell types of the NVU in direct contact with BBB endothelium provides increased barrier restrictive properties in comparison to the endothelium alone. Additionally, including both supporting cell types (astrocytes and pericytes) in direct contact with HBEC-5i cells results in increased barrier tightness compared to direct contact cocultures (astrocyte- and pericyte-HBEC 5i combinations alone). This finding suggests that including both the astrocytes and pericytes in *in vitro* models further synergistically enhances the properties of the BBB in addition to better representing the *in vivo* NVU. The inductive effects of astrocytes and pericytes and their roles in BBB maintenance have been well established; however, many of the models used for *in vitro* BBB permeability screening do not consider the direct contact the different cell types have with one another *in vivo*. By seeding astrocytes, pericytes, and the endothelium directly atop one another this model better mimics the 20 nm distance between the cell types due to the presence of the basal lamina that is seen *in vivo*.[22] Although indirect plating methods with cell types cultured on opposite sides of a 10 μm thick filter support also provide increased barrier properties over endothelial monocultures, the direct contact triculture is more physiologically relevant to the *in vivo* NVU and does not require manipulation of the Transwell® system and potentially is more amenable to automation for higher capacity throughput screening assays.

Paracellular permeants of increasing hydrodynamic radius were selected to evaluate the tight junction formation in the direct contact model. With increasing marker size there is a related decrease in paracellular permeability due to the size of the molecule in relation to the pore size of the tight junctions formed between adjacent endothelial cells. Permeability of [^{14}C]-PEG-4000 (15.9 Å) is the lowest of all markers used as expected followed by [^{14}C]-inulin (10 Å). In studies with the optimized direct contact triculture model the permeability of [^{14}C]-sucrose (5.2 Å) is faster than that of the smaller [^{14}C]-mannitol (4.3 Å), which is opposite of what would be expected based on molecule size alone.[63–65] One possible explanation is that the relative size of the two markers is small in comparison to the pore size of the model that elucidating differences in their respective permeation rates would not be observable. Alternatively, sucrose, a disaccharide of a fructose and glucose molecule linked via glycosidic bond, may serve as a substrate for active or facilitative nutrient transporters. For example, glucose permeation across the BBB has been reported to be modulated by several nutrient transporters, in particular the facilitative Glucose Transporter 1 (GLUT1) that is highly expressed in both BMECs and astrocytes.[71,72] Several neurotherapeutics utilize a pro-drug approach where the agent is conjugated to glucose in an effort to enhance brain parenchymal exposure via GLUT1.[71,73] Based on the structure of sucrose, the idea that there is some degree of nutrient transporter activity of the purported paracellular marker via the GLUT1 transporter is feasible. Therefore, we posit that the observed permeation rate for sucrose would be higher due to a potential transporter contribution that is not available for [^{14}C]-mannitol in the optimized direct contact triculture. This theory is further exacerbated by the presence of astrocytes and pericytes on the apical side of the Transwell® in the direct contact triculture since both of these cell types have reported expression of GLUT1, which may further increase the permeation of [^{14}C]-sucrose in the apical to basolateral direction in comparison to *in vitro* models that culture these

cells on the underside of the filter or in the basolateral chamber. The exact cause of the higher [^{14}C]-sucrose permeability can be further investigated using GLUT1 or related transporter inhibitors or transfected HBEC-5i cells with modified expression of glucose transporters.

The functional activity of efflux transporters in BMECs is a key characteristic of the BBB, with the most prevalent isoform being P-gp. P-gp and related multidrug resistance conferring efflux transporters function to prevent xenobiotics from permeating into the brain parenchyma with a broad substrate affinity and capacity. Rhodamine-123 (R123) is a commonly used P-gp substrate to assess functional activity in the presence or absence of an inhibitor. Elacridar is a third generation P-gp inhibitor and has been reported to have among the highest specificity and potency for P-gp inhibition within the class of agents.[74] We observed that the presence of elacridar resulted in an increase in R123 permeability across the direct contact triculture, suggesting that P-gp is functionally present in the optimized model. In these studies R123 permeation was only assessed in the apical to basolateral direction. Additional studies to elucidate P-gp function can include bi-directional permeability assessment as well as cellular accumulation; however, given the multiple cell types in direct contact the assessment of P-gp function an expression would require more in depth studies. This is particularly true given the fact that astrocytes have also been reported to express P-gp, which may further obfuscate P-gp assessment of the endothelium alone.[75]

In addition to limiting paracellular permeation of hydrophilic solutes and potentially P-gp substrates, we theorized that a well-established *in vitro* model of the NVU should have an enhanced ability to differentiate between *in vivo* demonstrated high and low brain permeating compounds. *In vitro* permeability screening models capable of predicting *in vivo* permeation rates in order to rank new chemical entities is essential to facilitate compound advancement with translation as the aim. A number of positive and negative permeants were selected to assess the utility of the direct

contact triculture. Amino acids and related analogues (e.g. γ-aminobutyric acid or GABA) play a critical role in maintaining brain homeostasis and modulating function. Here we selected L-histidine as an amino acid that is actively transported in a stereospecific manner across the BBB by amino acid transporters and potentially Peptide Histidine Transporter 1.[76] However, L-histidine is a small water soluble molecule that can potentially permeate *in vitro* models to a significant extent via the paracellular pathway. Hence, the paracellular route may contribute to a higher permeation rate of L-histidine in comparison to other transporter specific markers. Caffeine was also selected as a small hydrophilic psychostimulant that has been demonstrated to permeate the *in vivo* BBB, and we demonstrated its permeation across the direct contact triculture model.[77] Carbamazepine was selected as it is an anticonvulsant commonly used as a BBB positive marker and to our knowledge has not been shown to possess significant P-gp affinity.[78,79] In addition to R123, permeability of P-gp substrates colchicine and digoxin were assessed in the optimized model. The differences in permeation rates for separate P-gp substrates can be attributed to the broad substrate affinities and capacities of the efflux transporters and their relative expression levels. Further studies can be performed to assess the effect of P-gp inhibition on the permeation of these substrates as well as inhibition of other efflux transporters such as BCRP as there is also fairly significant substrate overlap across several efflux transporter isoforms. Clozapine is an antipsychotic that has been shown to be highly metabolized and may potentially inhibit P-gp.[68,80] Clozapine metabolites have also been demonstrated to have high BBB permeation, where additional studies using LC-mass spectrometry analysis and longer incubation time could be performed to elucidate the metabolic fate in the optimized triculture model.[80] Although no metabolite peaks were observed in this study, a more rigorous separation analysis would be warranted to further investigate this possibility. Lastly, prazosin is a BCRP substrate that proved

to have the lowest permeability of the selected markers. The low permeation of prazosin across the *in vitro* triculture model potentially suggests that functional BCRP activity is greater than that of P-gp or other efflux transporters, however further studies need to be performed to delineate the effects. The observed ranking of high and low BBB permeating compounds is ordered in a similar fashion to what has been seen by other both *in vitro* and *in vivo*. The observed permeability of a small library of compounds across the optimized direct contact triculture model suggests that it is a useful tool for further assessment of BBB permeation of new chemical entities as well understanding of the synergistic effects of direct cell-cell contacts.

Herein, we have established an enhanced physiologically relevant *in vitro* model of the BBB by culturing the astrocytes, pericytes, and HBEC-5i cells in a layered, direct contact manner resemblant of the *in vivo* NVU. We provide supporting evidence that the apical layering removes the physical barrier observed in conventional triculture models and supports the potential of synergistic interactions occurring to provide a phenotype closer to the NVU. In addition, to our knowledge we are one of the first laboratories to utilize a three stage multifactorial DOE based approach expedite optimization of a BBB *in vitro* model. Additional DOE based studies maybe performed to develop analogous models to mimic different pathologies of the brain, for example neurodevelopmental changes or neurodegenerative effects on the BBB with primary or proliferative cell lines.

3.6 Conclusion

The blood brain barrier *in vitro* screening approaches have traditionally focused on tightening the brain microvessel endothelium that line the capillaries, separate the blood from the neuronal environment, and maintain homeostasis. While screening models in the presence of

astrocytes and pericytes in indirect contact to the BMECs have been developed, we postulated that direct contact of these cells, as found *in vivo*, would more adequately enhance *in vitro-in vivo* comparative studies. The direct layered culturing approach should enhance the synergistic effects by removing physical barriers and providing proximity so that secreted soluble factors and their effects on the regulation of the BMEC phenotype should be enhanced without added dilution and diffusion. Additionally, the ability for the model to rank established high and low brain permeating compounds eludes to its potential for BBB permeability screening of new chemical entities. This study also demonstrates the feasibility of using an informed DOE based approach to expedite culture development and can be further expanded for additional applications. Taken together, the direct contact triculture developed within appears to provide increased barrier properties that we theorize is attributable through facilitating adequate crosstalk between the three major cell types of the NVU. The findings of this work open the door for continued investigation of the roles of each NVU cell type and its influence on barrier properties, as well as the establishment of a fully human, physiologically relevant *in vitro* model that can be used for moderate throughput screening to rank order potential neurotherapeutic compounds.

3.7 Supplemental Material

Table 3.S1. Conditions and P_{eff} of 4 kD Dextran for DOE_P

Condition	HA (cells/cm^2)	HBVP (cells/cm^2)	HBEC-5i (cells/cm^2)	ECM	Day	Peff (cm/sec)
1	40000	20000	110000	Collagen	7	9.99E-06
2	60000	20000	80000	Matrigel	5	1.38E-05
3	60000	20000	110000	Laminin	5	8.69E-06
4	60000	20000	110000	Laminin	5	9.14E-06
5	20000	20000	80000	Collagen	9	3.32E-06
6	20000	60000	50000	Matrigel	5	1.26E-05
7	60000	60000	80000	Collagen	7	1.02E-05
8	60000	60000	110000	Laminin	9	3.17E-06
9	60000	20000	50000	Collagen	5	1.19E-05
10	20000	60000	50000	Laminin	9	3.32E-06
11	20000	20000	50000	Matrigel	9	3.30E-06
12	20000	40000	110000	Matrigel	9	4.31E-06
13	20000	20000	110000	Collagen	5	-
14	60000	20000	110000	Collagen	9	6.19E-06
15	40000	20000	50000	Matrigel	5	1.91E-05
16	40000	60000	80000	Matrigel	9	6.43E-06
17	60000	60000	50000	Matrigel	9	5.22E-06
18	20000	20000	110000	Matrigel	5	1.32E-05
19	60000	60000	110000	Collagen	5	9.54E-06
20	20000	20000	110000	Laminin	9	3.20E-06
21	60000	60000	50000	Laminin	5	1.18E-05
22	20000	60000	110000	Laminin	5	8.87E-06
23	40000	40000	50000	Collagen	9	4.32E-06
24	20000	60000	110000	Collagen	9	3.40E-06
25	20000	20000	50000	Laminin	5	1.56E-05
26	20000	20000	50000	Collagen	7	1.25E-05
27	60000	20000	110000	Matrigel	9	3.91E-06
28	20000	60000	110000	Laminin	5	1.12E-05
29	20000	40000	80000	Collagen	5	1.13E-05
30	60000	60000	110000	Matrigel	5	1.57E-05
31	20000	60000	50000	Laminin	9	4.17E-06
32	20000	60000	50000	Collagen	5	1.22E-05
33	60000	20000	50000	Laminin	9	5.32E-06
34	60000	40000	50000	Matrigel	7	1.64E-05
35	20000	60000	110000	Matrigel	7	1.19E-05
36	60000	60000	50000	Collagen	9	4.47E-06
37	40000	40000	80000	Collagen	7	1.08E-05
38	40000	40000	80000	Laminin	7	1.06E-05
39	40000	40000	80000	Matrigel	7	1.34E-05

Table 3.S2. Conditions and P_{eff} of 4 kD Dextran for DOE_{M1}

Condition	HEPES (mM)	HC (µM)	DEX (µM)	LiCl (mM)	Ca^{2+} (mM)	RA (µM)	Peff (cm/sec)
1	25	0	0	10	1	0	8.66E-06
2	15	1.4	10	10	1	10	9.12E-06
3	25	1.4	10	0	0	10	1.11E-05
4	15	0	0	0	1	0	7.29E-06
5	25	0	10	10	0	0	8.37E-06
6	25	0	10	10	1	10	1.07E-05
7	15	0	0	10	1	10	-1.87E-04
8	15	0	10	10	1	0	3.67E-05
9	15	0	0	10	0	0	1.20E-05
10	25	1.4	0	0	0	0	1.18E-05
11	25	0	10	0	1	0	1.09E-05
12	15	1.4	10	0	1	0	9.10E-06
13	15	1.4	10	10	0	0	7.10E-06
14	25	0	0	0	0	10	8.54E-06
15	15	0	10	0	0	0	1.66E-05
16	25	1.4	0	0	1	10	6.32E-06
17	25	1.4	0	10	0	10	1.10E-05
18	15	0	10	10	0	10	7.70E-06
19	25	1.4	10	10	1	0	1.82E-05
20	25	1.4	0	10	0	10	9.79E-05
21	15	1.4	0	10	1	0	7.29E-06
22	20	0.7	5	5	0.5	5	6.71E-06
23	15	1.4	0	0	0	10	2.00E-05
24	15	0	10	0	1	10	6.87E-06

Table 3.S3. Conditions and P_{eff} of 4 kD Dextran for DOE_{M2}

Condition	HC (μM)	DEX (μM)	LiCl (mM)	RA (μM)	Study Day	Peff (cm/sec)
1	1.4	0	10	0	7	9.47e-6
2	0	0	0	10	5	1.913e-5
3	1.4	10	10	10	7	8.29e-6
4	1.4	10	0	10	5	2.07e-5
5	1.4	10	0	0	7	1.47e-5
6	0	0	10	10	7	1.17e-5
7	1.4	10	10	0	5	1.65e-5
8	1.4	0	0	0	5	2.05e-5
9	0	0	0	0	7	1.33e-5
10	0	10	10	0	7	1.01e-5
11	1.4	0	10	10	5	1.08e-5
12	0	10	10	10	5	1.15e-5
13	1.4	0	10	10	5	1.16e-5
14	1.4	0	10	0	7	1.13e-5
15	0	10	0	10	7	1.08e-5
16	1.4	10	10	10	7	1.06e-5
17	1.4	10	0	10	5	1.31e-5
18	0	10	0	0	5	1.67e-5
19	1.4	10	10	0	5	1.72e-5
20	1.4	0	0	10	7	1.32e-5
21	0	10	10	10	5	1.32e-5
22	0	0	10	0	5	1.34e-5
23	1.4	10	0	0	7	1.68e-5
24	0	0	0	10	7	1.56e-5

3.8 References

1. Pardridge WM. Why is the global CNS pharmaceutical market so under-penetrated? *Drug Discov Today* 2002;**7**:5–7. https://doi.org/10.1016/S1359-6446(01)02082-7.
2. Gribkoff VK, Kaczmarek LK. The Need for New Approaches in CNS Drug Discovery: Why Drugs Have Failed, and What Can Be Done to Improve Outcomes. *Neuropharmacology* 2017;**120**:11–9. https://doi.org/10.1016/j.neuropharm.2016.03.021.
3. Kesselheim AS, Hwang TJ, Franklin JM. Two decades of new drug development for central nervous system disorders. *Nat Rev Drug Discov* 2015;**14**:815–6. https://doi.org/10.1038/nrd4793.
4. Abbott NJ, Patabendige AAK, Dolman DEM, Yusof SR, Begley DJ. Structure and function of the blood-brain barrier. *Neurobiol Dis* 2010;**37**:13–25. https://doi.org/10.1016/j.nbd.2009.07.030.
5. Abbott NJ. Blood-brain barrier structure and function and the challenges for CNS drug delivery. *J Inherit Metab Dis* 2013;**36**:437–49. https://doi.org/10.1007/s10545-013-9608-0.
6. Serlin Y, Shelef I, Knyazer B, Friedman A. Anatomy and Physiology of the Blood-Brain Barrier. *Semin Cell Dev Biol* 2015;**38**:2–6. https://doi.org/10.1016/j.semcdb.2015.01.002.
7. Weiss N, Miller F, Cazaubon S, Couraud P-O. The blood-brain barrier in brain homeostasis and neurological diseases. *Biochim Biophys Acta BBA - Biomembr* 2009;**1788**:842–57. https://doi.org/10.1016/j.bbamem.2008.10.022.
8. Bauer H-C, Krizbai IA, Bauer H, Traweger A. ‘You Shall Not Pass’-tight junctions of the blood brain barrier. *Front Neurosci* 2014;**8**:392. https://doi.org/10.3389/fnins.2014.00392.

9. Haseloff RF, Dithmer S, Winkler L, Wolburg H, Blasig IE. Transmembrane proteins of the tight junctions at the blood-brain barrier: structural and functional aspects. *Semin Cell Dev Biol* 2015;**38**:16–25. https://doi.org/10.1016/j.semcdb.2014.11.004.

10. Wolburg H, Lippoldt A. Tight junctions of the blood-brain barrier: development, composition and regulation. *Vascul Pharmacol* 2002;**38**:323–37.

11. Löscher W, Potschka H. Blood-brain barrier active efflux transporters: ATP-binding cassette gene family. *NeuroRx J Am Soc Exp Neurother* 2005;**2**:86–98. https://doi.org/10.1602/neurorx.2.1.86.

12. Polli JW, Olson KL, Chism JP, John-Williams LS, Yeager RL, Woodard SM, *et al.* An Unexpected Synergist Role of P-Glycoprotein and Breast Cancer Resistance Protein on the Central Nervous System Penetration of the Tyrosine Kinase Inhibitor Lapatinib (N-{3-Chloro-4-[(3-fluorobenzyl)oxy]phenyl}-6-[5-({[2-(methylsulfonyl)ethyl]amino}methyl)-2-furyl]-4-quinazolinamine; GW572016). *Drug Metab Dispos* 2009;**37**:439–42. https://doi.org/10.1124/dmd.108.024646.

13. Abbott NJ, Rönnbäck L, Hansson E. Astrocyte-endothelial interactions at the blood-brain barrier. *Nat Rev Neurosci* 2006;**7**:41–53. https://doi.org/10.1038/nrn1824.

14. Bouchaud C, Le Bert M, Dupouey P. Are close contacts between astrocytes and endothelial cells a prerequisite condition of a blood-brain barrier? The rat subfornical organ as an example. *Biol Cell* 1989;**67**:159–65.

15. Bushong EA, Martone ME, Jones YZ, Ellisman MH. Protoplasmic astrocytes in CA1 stratum radiatum occupy separate anatomical domains. *J Neurosci Off J Soc Neurosci* 2002;**22**:183–92.

16. Halassa MM, Fellin T, Takano H, Dong J-H, Haydon PG. Synaptic islands defined by the territory of a single astrocyte. *J Neurosci Off J Soc Neurosci* 2007;**27**:6473–7. https://doi.org/10.1523/JNEUROSCI.1419-07.2007.

17. Wolburg H, Wolburg-Buchholz K, Fallier-Becker P, Noell S, Mack AF. Chapter one - Structure and Functions of Aquaporin-4-Based Orthogonal Arrays of Particles. In: Jeon KW, editor. *Int. Rev. Cell Mol. Biol.*, vol. 287. Academic Press; 2011. p. 1–41.

18. Haseloff RF, Blasig IE, Bauer HC, Bauer H. In search of the astrocytic factor(s) modulating blood-brain barrier functions in brain capillary endothelial cells in vitro. *Cell Mol Neurobiol* 2005;**25**:25–39.

19. Lee S-W, Kim WJ, Choi YK, Song HS, Son MJ, Gelman IH, *et al.* SSeCKS regulates angiogenesis and tight junction formation in blood-brain barrier. *Nat Med* 2003;**9**:900–6. https://doi.org/10.1038/nm889.

20. Argaw AT, Gurfein BT, Zhang Y, Zameer A, John GR. VEGF-mediated disruption of endothelial CLN-5 promotes blood-brain barrier breakdown. *Proc Natl Acad Sci U S A* 2009;**106**:1977–82. https://doi.org/10.1073/pnas.0808698106.

21. Alvarez JI, Katayama T, Prat A. Glial influence on the Blood Brain Barrier. *Glia* 2013;**61**:1939–58. https://doi.org/10.1002/glia.22575.

22. Mathiisen TM, Lehre KP, Danbolt NC, Ottersen OP. The perivascular astroglial sheath provides a complete covering of the brain microvessels: An electron microscopic 3D reconstruction. *Glia* 2010;**58**:1094–103. https://doi.org/10.1002/glia.20990.

23. Winkler EA, Bell RD, Zlokovic BV. Central nervous system pericytes in health and disease. *Nat Neurosci* 2011;**14**:1398–405. https://doi.org/10.1038/nn.2946.

24. Daneman R, Zhou L, Kebede AA, Barres BA. Pericytes are required for blood-brain barrier integrity during embryogenesis. *Nature* 2010;**468**:562–6. https://doi.org/10.1038/nature09513.

25. Gaengel K, Genové G, Armulik A, Betsholtz C. Endothelial-mural cell signaling in vascular development and angiogenesis. *Arterioscler Thromb Vasc Biol* 2009;**29**:630–8. https://doi.org/10.1161/ATVBAHA.107.161521.

26. Hawkins BT, Davis TP. The Blood-Brain Barrier/Neurovascular Unit in Health and Disease. *Pharmacol Rev* 2005;**57**:173–85. https://doi.org/10.1124/pr.57.2.4.

27. Baeten KM, Akassoglou K. Extracellular Matrix and Matrix Receptors in Blood-Brain Barrier Formation and Stroke. *Dev Neurobiol* 2011;**71**:1018–39. https://doi.org/10.1002/dneu.20954.

28. Helms HC, Abbott NJ, Burek M, Cecchelli R, Couraud P-O, Deli MA, *et al.* In vitro models of the blood-brain barrier: An overview of commonly used brain endothelial cell culture models and guidelines for their use. *J Cereb Blood Flow Metab Off J Int Soc Cereb Blood Flow Metab* 2016;**36**:862–90. https://doi.org/10.1177/0271678X16630991.

29. NAIK P, CUCULLO L. In Vitro Blood–Brain Barrier Models: Current and Perspective Technologies. *J Pharm Sci* 2012;**101**:1337–54. https://doi.org/10.1002/jps.23022.

30. Bernas MJ, Cardoso FL, Daley SK, Weinand ME, Campos AR, Ferreira AJG, *et al.* Establishment of primary cultures of human brain microvascular endothelial cells to provide an in vitro cellular model of the blood-brain barrier. *Nat Protoc* 2010;**5**:1265–72. https://doi.org/10.1038/nprot.2010.76.

31. Lacombe O, Videau O, Chevillon D, Guyot A-C, Contreras C, Blondel S, *et al.* In vitro primary human and animal cell-based blood-brain barrier models as a screening tool in drug discovery. *Mol Pharm* 2011;**8**:651–63. https://doi.org/10.1021/mp1004614.

32. Weksler BB, Subileau EA, Perrière N, Charneau P, Holloway K, Leveque M, *et al.* Blood-brain barrier-specific properties of a human adult brain endothelial cell line. *FASEB J Off Publ Fed Am Soc Exp Biol* 2005;**19**:1872–4. https://doi.org/10.1096/fj.04-3458fje.

33. Weksler B, Romero IA, Couraud P-O. The hCMEC/D3 cell line as a model of the human blood brain barrier. *Fluids Barriers CNS* 2013;**10**:16. https://doi.org/10.1186/2045-8118-10-16.

34. Tai LM, Reddy PS, Lopez-Ramirez MA, Davies HA, Male DK, Male ADK, *et al.* Polarized P-glycoprotein expression by the immortalised human brain endothelial cell line, hCMEC/D3, restricts apical-to-basolateral permeability to rhodamine 123. *Brain Res* 2009;**1292**:14–24. https://doi.org/10.1016/j.brainres.2009.07.039.

35. Biemans EALM, Jäkel L, de Waal RMW, Kuiperij HB, Verbeek MM. Limitations of the hCMEC/D3 cell line as a model for Aβ clearance by the human blood- brain barrier. *J Neurosci Res* 2017;**95**:1513–22. https://doi.org/10.1002/jnr.23964.

36. Urich E, Lazic SE, Molnos J, Wells I, Freskgård P-O. Transcriptional profiling of human brain endothelial cells reveals key properties crucial for predictive in vitro blood-brain barrier models. *PloS One* 2012;**7**:e38149. https://doi.org/10.1371/journal.pone.0038149.

37. Dorovini-Zis K, Prameya R, Bowman PD. Culture and characterization of microvascular endothelial cells derived from human brain. *Lab Investig J Tech Methods Pathol* 1991;**64**:425–36.

38. Wassmer SC, Combes V, Candal FJ, Juhan-Vague I, Grau GE. Platelets Potentiate Brain Endothelial Alterations Induced by Plasmodium falciparum. *Infect Immun* 2006;**74**:645–53. https://doi.org/10.1128/IAI.74.1.645-653.2006.

39. Wassmer SC, Cianciolo GJ, Combes V, Grau GE. Inhibition of Endothelial Activation: A New Way to Treat Cerebral Malaria? *PLoS Med* 2005;**2**:. https://doi.org/10.1371/journal.pmed.0020245.

40. Jambou R, Combes V, Jambou M-J, Weksler BB, Couraud P-O, Grau GE. Plasmodium falciparum adhesion on human brain microvascular endothelial cells involves transmigration-like cup formation and induces opening of intercellular junctions. *PLoS Pathog* 2010;**6**:e1001021. https://doi.org/10.1371/journal.ppat.1001021.

41. Jiang W, Huang W, Chen Y, Zou M, Peng D, Chen D. *HIV-1 Transactivator Protein Induces ZO-1 and Neprilysin Dysfunction in Brain Endothelial Cells via the Ras Signaling Pathway*. Oxidative Medicine and Cellular Longevity. 2017. https://doi.org/10.1155/2017/3160360.

42. Puech C, Hodin S, Forest V, He Z, Mismetti P, Delavenne X, *et al.* Assessment of HBEC-5i endothelial cell line cultivated in astrocyte conditioned medium as a human blood-brain barrier model for ABC drug transport studies. *Int J Pharm* 2018;**551**:281–9. https://doi.org/10.1016/j.ijpharm.2018.09.040.

43. Puech C, Delavenne X, He Z, Forest V, Mismetti P, Perek N. Direct oral anticoagulants are associated with limited damage of endothelial cells of the blood-brain barrier mediated by the thrombin/PAR-1 pathway. *Brain Res* 2019. https://doi.org/10.1016/j.brainres.2019.05.024.

44. Dohgu S, Takata F, Yamauchi A, Nakagawa S, Egawa T, Naito M, *et al.* Brain pericytes contribute to the induction and up-regulation of blood-brain barrier functions through transforming growth factor-beta production. *Brain Res* 2005;**1038**:208–15. https://doi.org/10.1016/j.brainres.2005.01.027.

45. Zozulya A, Weidenfeller C, Galla H-J. Pericyte-endothelial cell interaction increases MMP-9 secretion at the blood-brain barrier in vitro. *Brain Res* 2008;**1189**:1–11. https://doi.org/10.1016/j.brainres.2007.10.099.

46. Demeuse P, Kerkhofs A, Struys-Ponsar C, Knoops B, Remacle C, van den Bosch de Aguilar P. Compartmentalized coculture of rat brain endothelial cells and astrocytes: a syngenic model to study the blood–brain barrier. *J Neurosci Methods* 2002;**121**:21–31. https://doi.org/10.1016/S0165-0270(02)00225-X.

47. Thanabalasundaram G, El-Gindi J, Lischper M, Galla H-J. Methods to assess pericyte-endothelial cell interactions in a coculture model. *Methods Mol Biol Clifton NJ* 2011;**686**:379–99. https://doi.org/10.1007/978-1-60761-938-3_19.

48. Li G, Simon MJ, Cancel LM, Shi Z-D, Ji X, Tarbell JM, *et al.* Permeability of endothelial and astrocyte cocultures: in vitro blood-brain barrier models for drug delivery studies. *Ann Biomed Eng* 2010;**38**:2499–511. https://doi.org/10.1007/s10439-010-0023-5.

49. Thomsen LB, Burkhart A, Moos T. A Triple Culture Model of the Blood-Brain Barrier Using Porcine Brain Endothelial cells, Astrocytes and Pericytes. *PloS One* 2015;**10**:e0134765. https://doi.org/10.1371/journal.pone.0134765.

50. Wuest DM, Wing AM, Lee KH. Membrane configuration optimization for a murine in vitro blood–brain barrier model. *J Neurosci Methods* 2013;**212**:211–21. https://doi.org/10.1016/j.jneumeth.2012.10.016.

51. Hatherell K, Couraud P-O, Romero IA, Weksler B, Pilkington GJ. Development of a three-dimensional, all-human in vitro model of the blood–brain barrier using mono-, co-, and tri-cultivation Transwell models. *J Neurosci Methods* 2011;**199**:223–9. https://doi.org/10.1016/j.jneumeth.2011.05.012.

52. McConnell HL, Kersch CN, Woltjer RL, Neuwelt EA. The Translational Significance of the Neurovascular Unit. *J Biol Chem* 2017;**292**:762–70. https://doi.org/10.1074/jbc.R116.760215.

53. Malina KC-K, Cooper I, Teichberg VI. Closing the gap between the in-vivo and in-vitro blood–brain barrier tightness. *Brain Res* 2009;**1284**:12–21. https://doi.org/10.1016/j.brainres.2009.05.072.

54. Gaston JD, Bischel LL, Fitzgerald LA, Cusick KD, Ringeisen BR, Pirlo RK. Gene Expression Changes in Long-Term In Vitro Human Blood-Brain Barrier Models and Their Dependence on a Transwell Scaffold Material. *J Healthc Eng* 2017;**2017**:. https://doi.org/10.1155/2017/5740975.

55. Kulczar C, Lubin KE, Lefebvre S, Miller DW, Knipp GT. Development of a direct contact astrocyte-human cerebral microvessel endothelial cells blood-brain barrier coculture model. *J Pharm Pharmacol* 2017;**69**:1684–96. https://doi.org/10.1111/jphp.12803.

56. Förster C, Burek M, Romero IA, Weksler B, Couraud P-O, Drenckhahn D. Differential effects of hydrocortisone and TNFα on tight junction proteins in an in vitro model of the human blood–brain barrier. *J Physiol* 2008;**586**:1937–49. https://doi.org/10.1113/jphysiol.2007.146852.

57. Paolinelli R, Corada M, Ferrarini L, Devraj K, Artus C, Czupalla CJ, *et al.* Wnt Activation of Immortalized Brain Endothelial Cells as a Tool for Generating a Standardized Model of

the Blood Brain Barrier In Vitro. *PLOS ONE* 2013;**8**:e70233. https://doi.org/10.1371/journal.pone.0070233.

58. Brown RC, Davis TP. Calcium modulation of adherens and tight junction function: a potential mechanism for blood-brain barrier disruption after stroke. *Stroke* 2002;**33**:1706–11.

59. De Bock M, Culot M, Wang N, da Costa A, Decrock E, Bol M, *et al.* Low extracellular Ca2+ conditions induce an increase in brain endothelial permeability that involves intercellular Ca2+ waves. *Brain Res* 2012;**1487**:78–87. https://doi.org/10.1016/j.brainres.2012.06.046.

60. Hue CD, Cho FS, Cao S, "Dale" Bass CR, Meaney DF, Morrison III B. Dexamethasone potentiates in vitro blood-brain barrier recovery after primary blast injury by glucocorticoid receptor-mediated upregulation of ZO-1 tight junction protein. *J Cereb Blood Flow Metab* 2015;**35**:1191–8. https://doi.org/10.1038/jcbfm.2015.38.

61. Lippmann ES, Al-Ahmad A, Azarin SM, Palecek SP, Shusta EV. A retinoic acid-enhanced, multicellular human blood-brain barrier model derived from stem cell sources. *Sci Rep* 2014;**4**:4160. https://doi.org/10.1038/srep04160.

62. Mizee MR, Wooldrik D, Lakeman KAM, Hof B van het, Drexhage JAR, Geerts D, *et al.* Retinoic Acid Induces Blood–Brain Barrier Development. *J Neurosci* 2013;**33**:1660–71. https://doi.org/10.1523/JNEUROSCI.1338-12.2013.

63. Ghandehari H, Smith PL, Ellens H, Yeh PY, Kopecek J. Size-dependent permeability of hydrophilic probes across rabbit colonic epithelium. *J Pharmacol Exp Ther* 1997;**280**:747–53.

64. Carl SM, Lindley DJ, Das D, Couraud PO, Weksler BB, Romero I, *et al.* ABC and SLC transporter expression and proton oligopeptide transporter (POT) mediated permeation across the human blood--brain barrier cell line, hCMEC/D3 [corrected]. *Mol Pharm* 2010;**7**:1057–68. https://doi.org/10.1021/mp900178j.

65. Sorensen M, Steenberg B, Knipp GT, Wang W, Steffansen B, Frokjaer S, *et al.* The effect of beta-turn structure on the permeation of peptides across monolayers of bovine brain microvessel endothelial cells. *Pharm Res* 1997;**14**:1341–8. https://doi.org/10.1023/A:1012104301773.

66. Lai C-H, Kuo K-H. The critical component to establish in vitro BBB model: Pericyte. *Brain Res Brain Res Rev* 2005;**50**:258–65. https://doi.org/10.1016/j.brainresrev.2005.07.004.

67. Armulik A, Genové G, Mäe M, Nisancioglu MH, Wallgard E, Niaudet C, *et al.* Pericytes regulate the blood-brain barrier. *Nature* 2010;**468**:557–61. https://doi.org/10.1038/nature09522.

68. Maines LW, Antonetti DA, Wolpert EB, Smith CD. Evaluation of the role of P-glycoprotein in the uptake of paroxetine, clozapine, phenytoin and carbamazapine by bovine retinal endothelial cells. *Neuropharmacology* 2005;**49**:610–7. https://doi.org/10.1016/j.neuropharm.2005.04.028.

69. Wedel- Parlow MV, Wölte P, Galla H-J. Regulation of major efflux transporters under inflammatory conditions at the blood-brain barrier in vitro. *J Neurochem* 2009;**111**:111–8. https://doi.org/10.1111/j.1471-4159.2009.06305.x.

70. Eisenblätter T, Galla H-J. A new multidrug resistance protein at the blood-brain barrier. *Biochem Biophys Res Commun* 2002;**293**:1273–8. https://doi.org/10.1016/S0006-291X(02)00376-5.

71. Patching SG. Glucose Transporters at the Blood-Brain Barrier: Function, Regulation and Gateways for Drug Delivery. *Mol Neurobiol* 2017;**54**:1046–77. https://doi.org/10.1007/s12035-015-9672-6.

72. Morgello S, Uson RR, Schwartz EJ, Haber RS. The human blood-brain barrier glucose transporter (GLUT1) is a glucose transporter of gray matter astrocytes. *Glia* 1995;**14**:43–54. https://doi.org/10.1002/glia.440140107.

73. Xiuli G, Meiyu G, Guanhua D. Glucose Transporter 1, Distribution in the Brain and in Neural Disorders: Its Relationship With Transport of Neuroactive Drugs Through the Blood-Brain Barrier. *Biochem Genet* 2005;**43**:175–87. https://doi.org/10.1007/s10528-005-1510-5.

74. Amin MdL. P-glycoprotein Inhibition for Optimal Drug Delivery. *Drug Target Insights* 2013;**7**:27–34. https://doi.org/10.4137/DTI.S12519.

75. Zhang L, Ong WY, Lee T. Induction of P-glycoprotein expression in astrocytes following intracerebroventricular kainate injections. *Exp Brain Res* 1999;**126**:509–16.

76. Yamakami J, Sakurai E, Sakurada T, Maeda K, Hikichi N. Stereoselective blood-brain barrier transport of histidine in rats. *Brain Res* 1998;**812**:105–12.

77. Chen X, Ghribi O, Geiger JD. Caffeine protects against disruptions of the blood-brain barrier in animal models of Alzheimer's and Parkinson's disease. *J Alzheimers Dis JAD* 2010;**20**:S127–41. https://doi.org/10.3233/JAD-2010-1376.

78. Grewal GK, Kukal S, Kanojia N, Madan K, Saso L, Kukreti R. In Vitro Assessment of the Effect of Antiepileptic Drugs on Expression and Function of ABC Transporters and Their Interactions with ABCC2. *Mol Basel Switz* 2017;**22**:. https://doi.org/10.3390/molecules22101484.

79. Potschka H, Fedrowitz M, Löscher W. Brain access and anticonvulsant efficacy of carbamazepine, lamotrigine, and felbamate in ABCC2/MRP2-deficient TR- rats. *Epilepsia* 2003;**44**:1479–86.

80. Hellman K, Aadal Nielsen P, Ek F, Olsson R. An ex Vivo Model for Evaluating Blood–Brain Barrier Permeability, Efflux, and Drug Metabolism. *ACS Chem Neurosci* 2016;**7**:668–80. https://doi.org/10.1021/acschemneuro.6b00024.

CHAPTER 4. DEVELOPMENT OF AN IN VITRO MODEL OF THE NEUROVASCULAR UNIT FOR BBB PERMEABILITY LINKED NEUROACTIVITY SCREENING

4.1 Abstract

Many potential neurotherapeutic agents fail in the later stages of development due to a lack of efficacy or associated neurotoxicity, which many be attributable to the restrictive permeation properties of the blood brain barrier (BBB). We posit that the development of a physiologically relevant screening tool that mimics the *in vivo* BBB by incorporating the cells found in the neurovascular unit (NVU) can help to mitigate attrition rates of these compounds by enhancing the translational potential for permeability and potential neuroactivity screening in the early discovery and development stages. In order to achieve such an ambitious goal, reflection and incorporation that enables the cell-cell signaling and key interactions governing *in vivo* response in the *in vitro* screens are requisite. We have previously discussed (Chapters 2 and 3) the development of a direct contact triculture model of the BBB that incorporates astrocytes, pericytes, and brain microvessel endothelial cells (BMECs) in direct layered contact on a permeable filter support to screen for BBB permeability. Herein, we describe our efforts to further enhance this model by seeding a human neuron resembling cell line, SH-SY5Y cells, in the basolateral chamber underlying the BBB triculture to potentially enable permeability linked neuronal response. We have demonstrated that the incorporation of the four cell types of the NVU in close contact both increases phenotypic expression of BBB characteristics as well as increases overall neuron viability due to the potential facilitation of cell-cell signaling. A range of marker compounds have been used to demonstrate the neuroactivity of compounds as it relates to the respective BBB permeability. The *in vitro* NVU neuronal model provides a succinct tool that is predictive of both

BBB permeability as well as neuroactivity, resulting in the generation of an enhanced physiologically relevant screening tool that can be implemented in early hit and lead candidate rank ordering for large compound libraries.

4.2 Introduction

Currently, the clinical translation of neurotherapeutics significantly lags behind the rapid increase in neurological disorders being seen worldwide, thus it is imperative that new methodologies are established to help facilitate the pharmaceutical development of these agents. Many have theorized that a majority of to the difficulties associated with translation of these agents arises because of the highly restrictive nature of the blood brain barrier (BBB) *in vivo* where preclinical *in vitro* screens that do not provide physiological semblance and rigor for lead candidate selection and optimization. Compound design and selection has traditionally focused on selected physiochemical properties (e.g., MW< 400, high lipophilicity, and poor solubility) that have been conventionally considered as favorable for the ability to traverse the BBB. In addition, a significant focus has also been placed on demonstrating lower affinity and capacity for efflux transporters like P-gp to increase parenchymal exposure. Often overlooked is the role of metabolism in the BBB or the potential that compounds possessing these physicochemical properties may also cross in excess and potentially elicit neurotoxic effects.[1,2] We have hypothesized that by developing an *in vitro* BBB model where neuroactivity could also be assessed would better evaluate risks in earlier stages that would aid in Go/No Go decision making.

Approaches to developing more physiologically relevant cell based models of the BBB, where the properties of the brain microvessel endothelial cells (BMECs) are emphasized has been the industrial standard to attempt mitigation of attritions rates. However, these efforts typically

lead to *in vitro* models that are somewhat predictive, but lack *in vivo* relevancy in the configuration of cells in the model and are predicated on the fact that they are more readily amenable to higher throughput screening demands associated with large compound libraries.[3] Additionally, these models emphasize BBB permeability and do not incorporate neuroactivity, associated toxicity or induction of neuronal function, into the *in vitro* screening.

When developing an *in vitro* model for BBB permeability or neuroactivity screening the structure and the multiple cell types of the *in vivo* neurovascular unit (NVU) should be considered. We postulate that the conventional *in vitro* BBB phenotypic screening methodologies place too much emphasis on the BMECs, where the synergistic interaction between supporting cells (astrocytes, pericytes, and neurons) that leads to the *in vivo* phenotype and neuroactivity are not integrated. In fact, most neuroactivity screens are performed separately in neuron only models, despite the recognition that cell-cell signaling between all four cell types governs *in vivo* response. Thus, BBB permeability screening model predictability will be limited unless permeability and neuroactivity can be integrated into an enriched *in vitro* model system representing the *in vivo* structure of the NVU.[4–9]

Specifically, the *in vivo* NVU is comprised of BMECs that express restrictive tight junctions, ubiquitous efflux transporters, and highly specific drug transporters, which together contribute the physical barrier and selective transport of solutes into the brain parenchyma.[10] Surrounding the endothelium are pericytes and astrocytes, which fully envelop the BMECs and synergistically improve the BBB phenotype through the secretion of soluble factors that modulate BMEC protein and transporter expression, function, and even regulate capillary blood flow.[7,11–16] These three cell types, in conjunction with the non-cellular basal lamina and neurons, make up the NVU and should be considered in BBB permeability models as well as neuroactivity screening

tools. For example, it has been established that neurons in contact with nearby astrocytes lead to neuronal-glial interactions and signaling, which is further propagated to the rest of the NVU to meet the metabolic demands of the brain parenchyma.[17–19] A number of vasoactive molecules are released by both astrocytes and neurons in response to synaptic glutamate to influence cerebral blood flow via vasoconstriction or dilation by pericytes and smooth muscle cells.[15,20,21] Cerebral blood flow is also regionally modulated based on neural activity, and there is evidence that the pericytes act to regulate vasoconstriction.[20]

Given the cellular signaling between the neurons and the other NVU cell types, *in vitro* screening models that would be comprised of all four would best provide a predictive and physiologically relevant cell-based permeability linked neuroactivity assessment of potential drug candidates. Additionally, a synergistic model would also serve as an effective screen for many therapeutic agents theorized to possess potential neurotoxic off target effects driven by brain parenchymal exposure based on several scenarios including direct neuronal effects, significant accumulation, or disruption of the BBB.[22] Therefore, including the BBB in neuroactivity screening tools enhances the utility of the model.[22,23] Traditionally, *in vitro* neuroactivity screening is performed on cultures of neuronal cells independent from BBB permeability and assessed based on neuronal health and neurite outgrowth or retraction in response to incubation with chemical entities.[22,24,25] Although these assays allow for high throughput screening of large compound libraries and assessment of direct neuronal effects, they do not mimic the state of neuroactivity *in vivo* as these models neglect the permeation barrier of the BBB, gradual accumulation of the compound in the brain parenchyma, and potential implications of therapeutic metabolites. Work has been done to assess neuroactivity of compounds linked to BBB permeability and determine relative toxicity of a compound based on associated effects on BMECs as well as neurons, with

neuroactivity measured based drug accumulated in the receiver chamber of a permeation assay.[26,27] Although these works measure relative neuroactivity effect of a compound as it relates to BBB permeability, we believe that it is possible to further increase the *in vivo* relevancy of the model.

The study herein describes the development and early optimization of an *in vitro* NVU permeability-linked neuroactivity screening model. The model is predicated on utilizing the novel, direct contact BBB triculture for permeability assessment across human BMECs, pericytes, and astrocytes layered atop one another on a permeable filter support. The resulting flux of the compound then leads to exposure in the basal chamber, where human neuroblastoma cells (SH-SY5Y) that serve as a neuron surrogate are seeded and time dependent response can be evaluated, depicted in Figure 4.1. The SH-SY5Y cell line was utilized here due to their use in neurotoxicity studies, however it should be noted that this is proof of concept and the limitations of the SH-SY5Y cells are taken into account.[26,28,29] To determine feasibility, BBB permeability linked neuroactivity was investigated utilizing marker compounds that were selected based upon reports

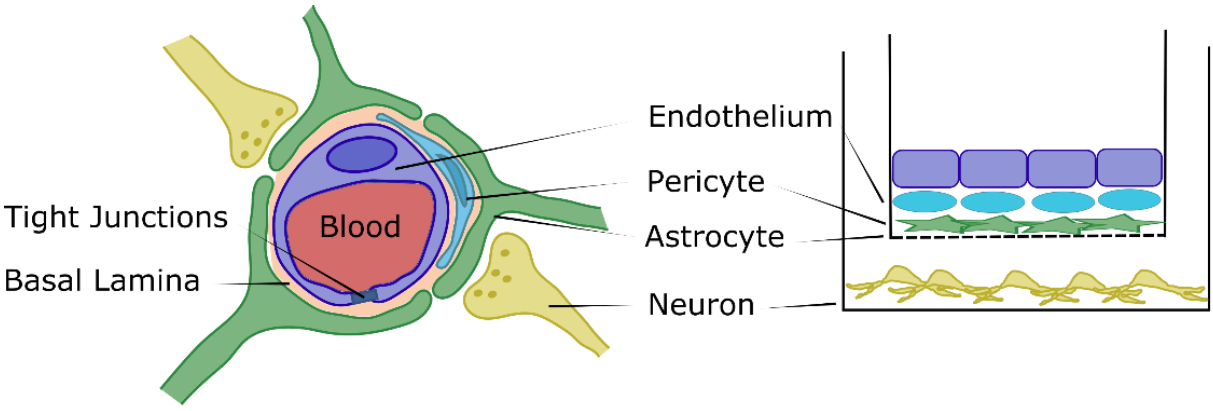

Figure 4.1. Cross sectional depiction of the neurovascular unit (NVU) with the endothelium (BMECs) lining the capillary, pericytes embedded within the basal lamina, astrocytes having nearly full coverage of the BMECs and surrounding pericytes, and neurons in close contact with the astrocytes (left). The direct contact triculture model on the apical surface of a Transwell® filter support with neurons in the basolateral chamber mimicking the *in vivo* NVU. Astrocytes are seeded first on the filter, followed by pericytes, then BMECs to generate a fully apical, direct contact triculture model and neurons seeded in the basolateral chamber to generate the *in vitro* NVU model for BBB permeability and neuroactivity screening (right).

indicating their effects on neuronal health and neurite outgrowth and the response to drug accumulation in the receiver chamber was determined. The model developed here encompasses the *in vivo* reality of an intended neurotherapeutic agent and its associated neuronal effects resulting in a physiologically relevant screening tool that may potentially be utilized to assess large libraries for hit and lead candidate selection.

4.3 Materials and Methods

4.3.1 *Materials*

Human brain astrocytes and vascular pericytes, astrocyte medium, pericyte medium, and astrocyte and pericyte growth factors were all obtained from ScienCell Research Laboratories (Carlsbad CA, USA). HBEC-5i cells were purchased from ATCC (Manassas, VA, USA). SH-SY5Y neurons were graciously provided by Dr. Jean-Christophe Rochet (Purdue University, Department of Medicinal Chemistry and Molecular Pharmacology, West Lafayette, IN, USA). Transwell® filters of 12 mm 0.4 µm pore size, T75 culture flasks, Matrigel®, type I rat tail collagen, NuSerum™, penicillin/streptomycin, and RPMI-1640 were purchased from Corning (Corning, NY, USA). Hank's balanced salt solution (HBSS) and Dulbecco's Modified Eagle Medium/Nutrient Mixture F-12 (DMEM/F-12) were obtained from Gibco (Carlsbad, CA, USA). Fetal bovine serum (FBS), hydrocortisone, rhodamine 123 (R123), elacridar, carbamazepine, colchicine, clozapine, caffeine, melatonin, digoxin, cyclosporin A, and prazosin hydrochloride were purchased from MilliporeSigma (St. Louis, MO, USA). Lapatinib was purchased from Attix Pharmaceuticals (Ontario, Canada). Radiolabeled [^{14}C]-sucrose was obtained from Moravek Biochemicals Inc. (Brea, CA, USA). HEPES (2-[4-(2-hydroxyethyl)piperazin-1-yl]ethanesulfonic acid) and calcium chloride dehydrate were obtained from J.T. Baker (Phillipsburg, NJ, USA).

Dexamethasone and MTT (3-(4,5-dimethylthiazolyl-2)-2,5-diphenyl tetrazolium bromide) were obtained from MP Biomedicals (Santa Ana, CA, USA). Endothelial cell growth supplement (ECGS) was purchased from Alfa Aesar (Haverhill, MA, USA). Fluorescein isothiocyanate (FITC) labeled 4 kD and 40 kD dextrans were purchased from Chondrex (Redmond, WA, USA). Fluorescein isothiocyanate (FITC) labeled 10 kD dextran was purchased from TCI America (Portland, OR, USA). Poly-L-lysine (PLL) was purchased from Trevigen (Gaithersburg, MD, USA). Neurite Outgrowth Staining Kit was purchased from Molecular Probes (Eugene, OR, USA).

4.3.2 *Cell Culture*

Human Brain Endothelial Cells (HBEC-5i) were maintained in T-75 culture flasks pre-coated with Type I rat tail collagen with medium changes every 3 days and subculturing at 80-90% confluency—cells were utilized between passage 22 and 30. HBEC-5i culture medium was made up of Dulbecco's Modified Eagle Medium/Nutrient Mixture F-12 (DMEM/F-12) supplemented with 10% FBS, 15 mM HEPES, and 40 ug/mL endothelial cell growth supplement (ECGS). Human astrocytes and human brain vascular pericytes are maintained in T-75 culture flasks pre-coated with poly-L-lysine with medium changes every 3 days and passaging at 80-90% confluency, where the cells were utilized between passages 4 and 10. Astrocyte culture medium was made up of Astrocyte Medium supplemented with 5% FBS, astrocyte growth supplement, and penicillin/streptomycin. Pericyte culture medium was comprised of Pericyte Medium supplemented with 5% FBS, pericyte growth supplement, and penicillin/streptomycin. Human neuroblastoma cell line, SH-SY5Y, was maintained in T-75 culture flasks with medium changes every 3 days and passaging at 80-90% confluency. SH-SY5Y cells were grown in RPMI 1640 with L-glutamine and 25 mM HEPES supplemented with 10% NuSerum^{TM} and 1% penicillin/streptomycin. SH-SY5Y cells were used between passage 10 and 17 in all experiments.

4.3.3 *Optimizing Plating of Neurons with Direct Contact Triculture*

Seeding density and time of introduction of with the direct contact triculture with the SH-SY5Y neurons was optimized using a full factorial design of the two factors (Table 4.1). Plating methods of the BBB triculture is explained in the following section. Neurons were plated in a separate 12-well plate at 25,000, 50,000, or 75,000 cells/cm^2 24 hours prior to placing the direct contact triculture atop the neurons. Neurons were cultured with the apical triculture starting at 3 or 7 days post endothelial cells plating, and cultured until day 9 post endothelium plating. Cultures were maintained at 37°C and 5% CO_2 with complete endothelial medium in the apical chamber and neuronal medium in the basolateral chamber with medium changes every other day. Optimized conditions were selected based on paracellular permeability of a 4 kD fluorescein labeled dextran.

4.3.4 *Plating Direct Contact Triculture with Neurons in the Basolateral Chamber*

Seeding of the direct contact triculture was done following the optimized procedure outlined in Chapter 3 of this thesis. Briefly, 12mm, 0.4 µm pore polyester Transwell® filters were pre-coated with 5 µg/cm^2 poly-L-lysine. Astrocytes were seeded at a density of 20,000 cells/cm^2 and allowed to grow for 48 hours prior to seeding pericytes atop the astrocyte cell layer at a density of 20,000 cells/cm^2. After 48 hours of pericyte growth, Matrigel® at a density of 25 µL/cm^2 in HBSS was added to the astrocyte-pericyte lawn and allowed to incubate at 37°C for 45 minutes. Matrigel® was removed and HBEC-5i cells were seeded directly atop the astrocyte-pericyte ECM coated lawn at a density of 80,000 cells/cm^2 and maintained. SH-SY5Y cells were introduced to the direct contact triculture 3 days post endothelial cell plating. Neurons were seeded 24 hours prior to incorporation in a 12-well plate at a density of 25,000 cells/cm^2. Filter supports containing the direct contact triculture were placed above the culture neurons in the basolateral chamber of

the well plate. Cultures were maintained with complete endothelial medium on the apical side of the filter and complete neuronal medium in the basolateral chamber. Cultures were utilized for assessing permeability and neuroactivity screening at 9 days post endothelial cell seeding.

4.3.5 *Permeability Assays*

Prior to commencing all assays, cells were washed (2x) with PBS to remove residual medium and then left to incubate in HBSS for 30 minutes at 37°C to equilibrate. Apparent permeability of paracellular markers 4 kD, 10 kD, and 40 kD FITC-dextran, and [^{14}C]-sucrose was performed at 37°C on a rocking platform with samples pulled at 15, 30, 45, 60, and 90 minutes, where all studies were conducted under sink conditions. Dextran solutions and [^{14}C]-sucrose were prepared at initial concentrations of 250 μg/mL and 0.25 μCi respectively in HBSS containing 0.50% DMSO. Dextran solutions were analyzed using a BioTek Synergy 4 plate reader with excitation at 485 nm and emission at 530 nm while [^{14}C]-sucrose was assessed via scintigraphy.

The effective permeability coefficients of selected markers (caffeine, carbamazepine, melatonin, clozapine, digoxin, cyclosporine A, lapatinib, and prazosin) was performed at initial concentrations of 25 or 50 μM in HBSS containing 0.50% DMSO from 10 mM concentrated stock solutions in DMSO for each compound. Samples were removed at 30, 60, 90, 120, 150, and 180 minutes for determining permeation rates and the remaining neurons then washed for the evaluation of neuroactivity. All samples for these compounds were analyzed using high performance liquid chromatography (HPLC). Apparent permeability (P_{app}) and flux (J) were calculated using the following equation:

$$C_0 \cdot P_{apparent} = \frac{dM/dT}{A} = Flux$$

where dM/dT is the amount of material that moves across the filter over time, Co is the initial concentration in the donor (apical) chamber, and A is the surface area of the filter support.

Apparent permeability of P-glycoprotein (P-gp) substrate rhodamine 123 (R123) was measured in the presence and absence of elacridar, a P-gp inhibitor. Working solutions of R123 at 10 µM and elacridar at 2 µM were prepared in HBSS with 1% DMSO. Replicates in the presence of inhibitor were incubated with elacridar for 45 minutes prior to the start of R123 permeation, while samples without inhibitor were incubated in blank HBSS. Samples were collected at 30, 60, 90, and 120 minute intervals and assessed using a BioTek Synergy 4 plate reader at excitation of 485 nm and emission of 530 nm. Apparent permeability was measured using eq. 1 above.

4.3.6 *High Performance Liquid Chromatography*

All compounds were analyzed using an Agilent 1100 reversed phase HPLC equipped with a variable wavelength detector (VWD). All methods were run isochratically using water and acetonitrile (ACN) through an Ascentis® C-18 15 x 4.6 mm, 5 µm column at 25 µL injections. Caffeine mobile phase consisted of 90:10, water:ACN, flow rate of 1.0 mL/min run at ambient temperature and analysis at 275 nm. Carbamazepine was run with 65:35, water:ACN at 1.5 mL/min with a column temperature of 40°C and observed at 284 nm. Clozapine utilized a mobile phase of 45:55, water:ACN at 1.5 mL/min flow rate and 40°C column temperature with analysis at 254 nm. Colchicine analysis was performed using a mobile phase of 75:25, water:ACN at a flow rate of 1.5 mL/min, 40°C column temperature, and wavelength of 354 nm. Cyclosporin A was run using a mobile phase of 30:70, water:ACN at 1.5 mL/min flow rate, 40°C column temperature, and measured at 214 nm. Digoxin utilized a mobile phase of 30:70, water:ACN at a flow rate of 1.1 mL/min, 40°C column temperature, and observed at 218 nm. Lapatinib utilized a mobile phase of 40:60, water:ACN at a flow rate of 1.0 mL/min, a column temperature of 25°C, and VWD

detection at 232 nm. Melatonin was measured using a mobile phase of 75:25, water:ACN with a flow rate of 1.5 mL/min, 40°C column temperature, and measured at 222 nm. Prazosin was analyzed with a mobile phase of 65:35, water:ACN at a flow rate of 1.5 mL/min, a 40°C column, and wavelength of 254 nm.

4.3.7 *Neuroactivity Assessment*

Neuroactivity was assessed after 3 hour BBB permeability of marker compounds caffeine, carbamazepine, clozapine, digoxin, prazosin, and cyclosporin A using the dual fluorescent dye Molecular Probes® Neurite Outgrowth Staining Kit which provides neuronal viability and degree of neurite outgrowth differences in comparison to a control. Following incubation, drug was removed from the neuronal cells and neurons were washed with fresh HBSS. Staining solution containing cell viability indicator and cell membrane stain was prepared according to manufacturer recommendations in fresh HBSS and added to neuron samples. After cells were incubated with the stain for 20 minutes at room temperature the stain was removed, cells were gently washed with fresh HBSS, and background suppression solution was added for analysis. Fluorescence quantification was measured using a BioTek Neo2 plate reader where the viability stain was measured at excitation and emission of 483 nm and 525 nm, whereas the cell membrane stain was measured at excitation and emission wavelength of 535 nm and 590 nm. All samples were compared to a control containing vehicle alone (0.50% DMSO in HBSS) and cell free controls were used to account for background fluorescence. Qualitative images were obtained using the BioTek Cytation 3 with the 20x objective for bright field and fluorescent pictures. Green Fluorescent Protein (GFP) and Texas Red filters were used for to observe fluorescence in each sample.

4.3.8 *Triculture Cell Viability Assay*

The viability of the direct contact triculture at the completion of the neuroactivity measurements was inferred from the mitochondrial oxidation of 3-(4,5-dimethylthiazolyl-2)-2,5-diphenyl tetrazolium bromide (MTT) dye. At the end of BBB permeability linked neuroactivity studies triculture plated filters were moved to a blank chamber well and the apical solution was removed from the filter support then washed with fresh HBSS. The triculture was incubated with 450 µL of fresh HBSS and 50 µL of 5 mg/mL MTT stock solution in HBSS for 4 hours at 37°C, blank HBSS was kept in the basolateral chamber to ensure cells were not directly exposed to air. After incubation, MTT solution was removed and replaced with 300 µL of DMSO to lyse cells and solubilize the mitochondria-generated formazan salt. A sample volume of 50 µL was diluted an equal volume of fresh DMSO in a 96-well plate. Absorbance was measured at 560 nm using a BioTek Powerwave HT plate reader. Samples were compared to a control of triculture incubated with vehicle alone (0.50% DMSO in HBSS) over the course of permeability measurement.

Table 4.1. Optimization of the NVU Model

Condition	SH-SY5Y Density (x 10^3 cells/cm^2)	Incorporation Day*	% Papp (4 kD FITC-Dextran) change of control
1	25	3	- 11%
2	25	7	+ 2%
3	50	3	- 16%
4	50	7	+ 6%
5	75	3	- 3%
6	75	7	- 4%
Optimized Triculture Control+	-	-	-

* day post endothelial cell plating

+ all conditions performed at n=1, control at n=2

4.4 Results

4.4.1 *NVU Optimization*

A full factorial design was used to determine the optimal conditions using three levels of neuron density and two times of inclusion. Upon analysis, the seeding density and time of inclusion of the SH-SY5Y neurons with the DOE optimized direct contact triculture (Chapter 3) were determined to be the two most important factors that influence the barrier restrictiveness of the NVU model. Neuronal influence on BBB properties was assessed based on the change in paracellular permeability marker compound, 4 kD FITC-dextran. Results revealed that, regardless of cell density, introducing neurons to the basal chamber at day 7 post HBEC-5i plating had a lesser impact on barrier properties in contrast to introduction earlier in culture at day 3. Introducing neurons on day 3 at 25,000 and 50,000 cells/cm^2 resulted in the largest decreases in BBB

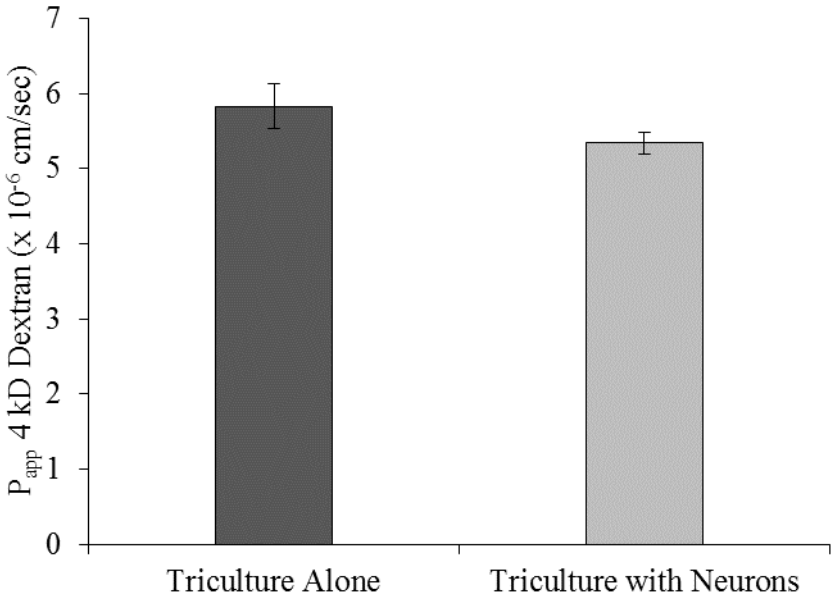

Figure 4.2. Apparent permeability (Papp) of a 4 kD FITC-dextran across the direct contact triculture alone (dark grey) and the optimized NVU model (light grey) with neurons in the basolateral chamber. Optimized conditions for the NVU model consists of 25,000 cells/cm^2 SH-SY5Y neurons introduced to the apical direct contact triculture 3 days post endothelial cell plating. Error bars represent one standard deviation (n=3).

permeation, 11% and 16% decreases respectively (Table 4.1). A neuron density of 25,000 cells/cm^2 introduced at day 3 post endothelial cell plating were the conditions chosen for all further studies to facilitate neuroactivity measurements. The selected optimized conditions were repeated to confirm the decrease in the permeation rate for 4 kD FITC-dextran with the addition of neurons in the basolateral chamber. The P_{app} observed for the triculture alone was $5.83 \pm 0.30 \times 10^{-6}$ cm/sec compared to $5.34 \pm 0.15 \times 10^{-6}$ cm/sec with neurons in the basolateral chamber resulting in an apparent decrease of 9% in permeability ($p > 0.05$) (Fig. 4.2).

4.4.2 *Neuron Viability and NVU Marker Compounds*

Viability and outgrowth of neurons throughout the length of coculture in the presence of the direct contact triculture was assessed. SH-SY5Y neuronal cells were cultured alone in a well

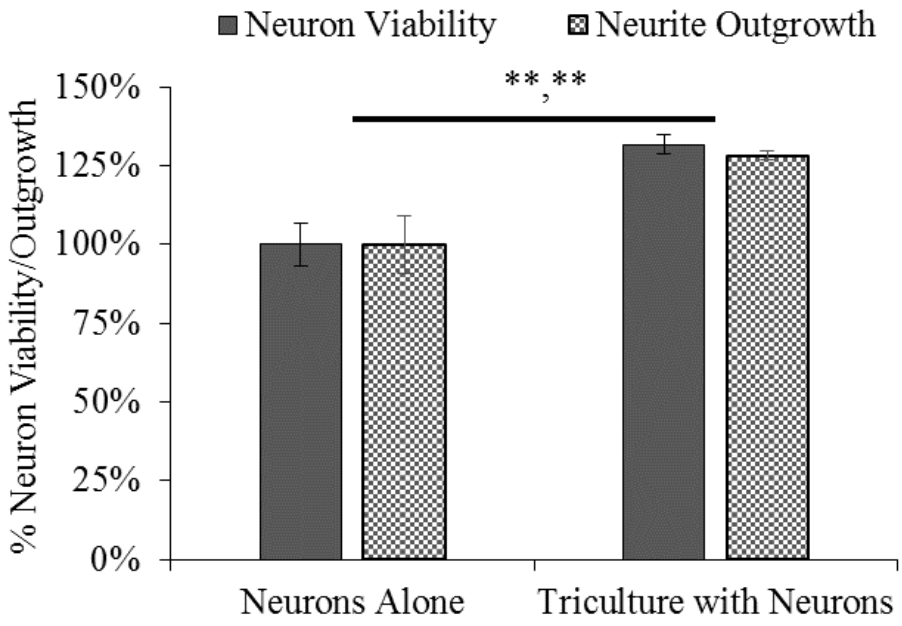

Figure 4.3. Viability and outgrowth of SH-SY5Y neurons in culture with and without the presence of the direct contact triculture as measured by the Neurite Outgrowth Staining Kit. Viability and outgrowth of SH-SY5Y cells cultured alone were normalized to 100% for comparison. Statistical significance was determined using Student's *t*-test between the two groups. Significance is labeled by (viability, outgrowth) where * $p<0.05$, ** $p<0.01$. Error bars represent one standard deviation (n=5).

plate for 8 days or for 24 hours alone then combined with the apical triculture for an additional 7 days. Viability and outgrowth of neurons cultured alone was normalized to the control values of 100 ± 7% and 9% respectively. In the presence of the triculture neuron viability increased by 32 ± 3% and outgrowth increased by 28 ± 1% in comparison to the neurons alone (Fig. 4.3). This was determined based on quantifying relative fluorescence intensity of the neuron viability and neurite outgrowth stain using the Molecular Probes® Neurite Outgrowth Staining Kit.

Four paracellular markers of increasing hydrodynamic radii were used to assess the tightness of the NVU model. Apparent permeability of [^{14}C]-sucrose (4.6 Å) was 13.61 ± 1.94 x 10^{-6} cm/sec, followed by 4 kD FITC-dextran (14 Å) at 4.85 ± 0.20 x 10^{-6} cm/sec, 10 kD FITC-dextran (23 Å) at 3.64 ± 0.20 x 10^{-6} cm/sec, and 40 kD FITC-dextran (45 Å) at 1.92 ± 0.05 x 10^{-6} cm/sec (Fig. 4.4).

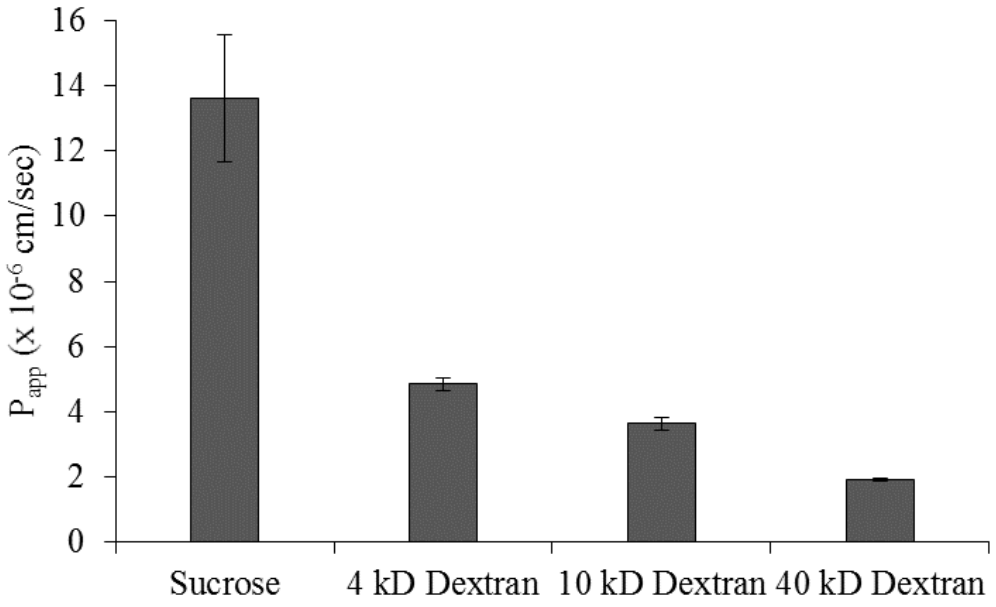

Figure 4.4. Apparent permeability of paracellular marker compounds [^{14}C]-sucrose and FITC-dextrans of 4 kD, 10 kD, and 40 kD across the optimized NVU model. Error bars represent one standard deviation (n=3).

The function of efflux transporter P-glycoprotein (P-gp) is **also** a key validation characteristic of any *in vitro* BBB model. P-gp function was assessed in the NVU model using P-gp substrate rhodamine (R123) in the presence and absence of P-gp inhibitor elacridar (Fig. 4.5). In the NVU model, the P_{app} of R123 alone was 12.12 ± 0.57 x 10^{-6} cm/sec versus 13.56 ± 0.50 x 10^{-6} cm/sec in the presence of elacridar ($p<0.05$). In comparison, the P_{app} of R123 alone and in the absence of elacridar across the BBB direct contact triculture alone was 18.52 ± 0.58 x 10^{-6} cm/sec and 21.14 ± 0.46 x 10^{-6} cm/sec respectively ($p<0.01$, data presented in Chapter 3). The triculture alone shows a greater increase in the P_{app} of R123 in the presence of inhibitor (14% increase) compared to the NVU model (12% increase), however the overall permeability of R123 with and without inhibitor is decreased in the NVU model compared to the triculture alone ($p<0.001$).

The apparent permeability across the NVU model was measured for a number of BBB high and low permeating compounds to validate the screening tool for use in ranking potential therapeutic agents based on permeation rates (Fig. 4.6). Caffeine (P_{app} = 30.70 ± 1.18 x 10^{-6} cm/sec), carbamazepine (P_{app} = 25.37 ± 2.80 x 10^{-6} cm/sec), melatonin (P_{app} = 18.29 ± 0.50 x 10^{-6} cm/sec), and R123 in the presence of elacridar (P_{app} = 13.56 ± 0.50 x 10^{-6} cm/sec) are positive BBB permeants. R123 alone (P_{app} = 12.12 ± 0.57 x 10^{-6} cm/sec), clozapine (P_{app} = 11.44 ± 0.78 x 10^{-6} cm/sec), digoxin (P_{app} = 8.78 ± 0.37 x 10^{-6} cm/sec), prazosin (P_{app} = 3.90 ± 0.35 x 10^{-6} cm/sec), and cyclosporine A (P_{app} = 2.61 ± 0.37 x 10^{-6} cm/sec) are BBB negative permeants. Lapatinib was also tested for permeability, but was undetectable in the receiver chamber after 3 hours (data not shown). The BBB permeants that were tested across both the optimized triculture without neurons (data presented in Chapter 3) and the NVU model were plotted for comparison. Of the markers screened, significant decreases in permeation rates across the NVU model were observed for R123 with elacridar ($p<0.001$), R123 alone ($p<0.001$), and prazosin ($p<0.01$) while a significant increase

in permeation was seen for clozapine ($p<0.01$) all in comparison to the optimized triculture alone (Fig. 4.7).

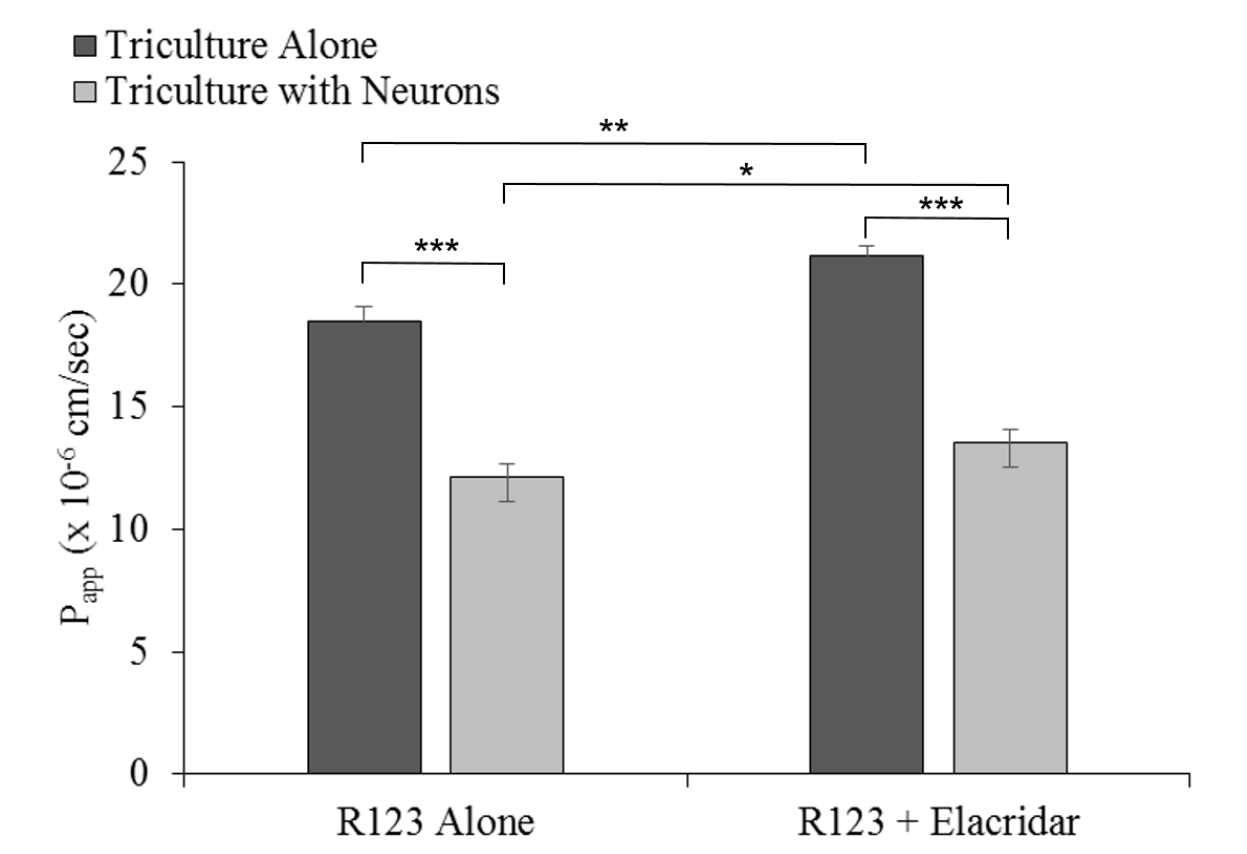

Figure 4.5. Apparent permeability of P-gp substrate rhodamine 123 (R123) in the presence and absence of elacridar, a P-gp inhibitor. Papp was measured across the triculture without neurons (dark grey) and the NVU model (light grey). One way ANOVA with a Tukey-Kramer post-hoc test was used to determine significance between R123 with and without elacridar for the triculture with neurons and without where * $p<0.05$, ** $p<0.01$, and *** $p<0.001$. Error bars represent one standard deviation (n=3).

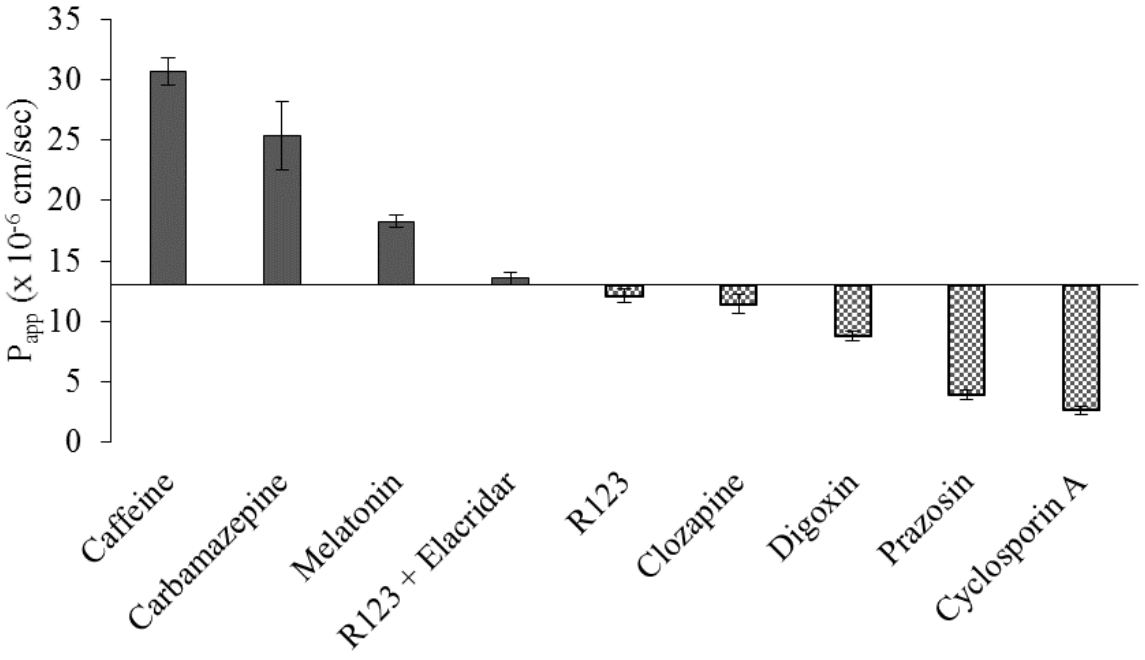

Figure 4.6. Apparent permeability of BBB positive (grey) and negative (patterned) permeants across the optimized NVU model. Assays were performed in triplicate where error bars represent one standard deviation (n=3-6).

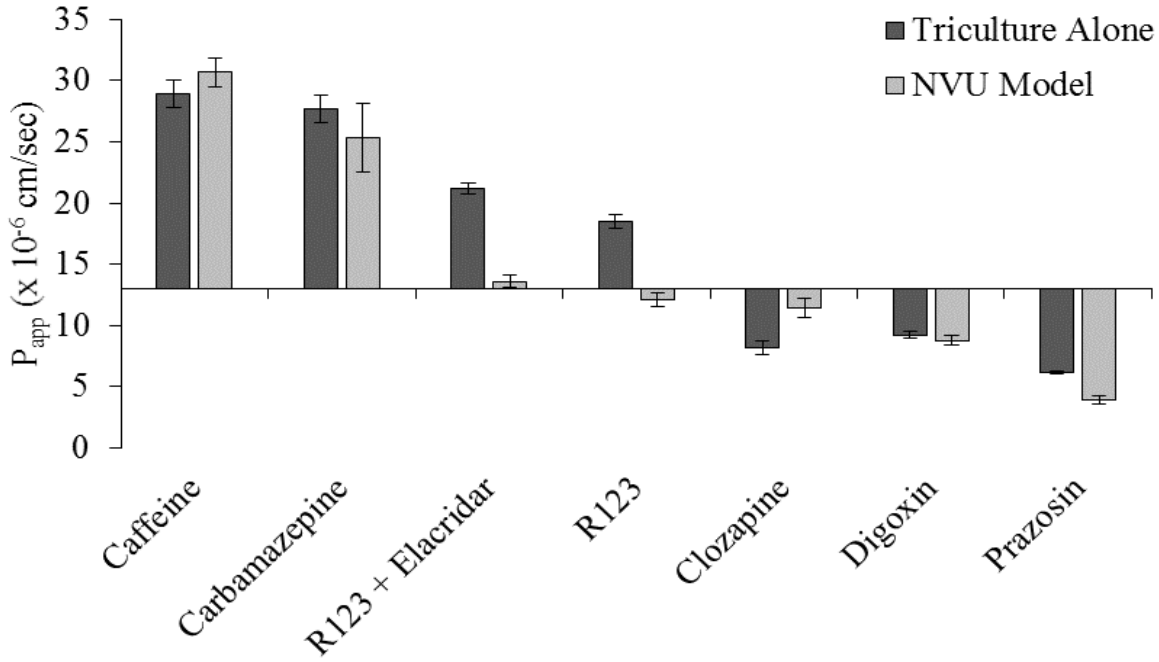

Figure 4.7. Apparent permeability of high and low permeating marker compounds across the optimized direct contact triculture (dark grey, presented in Chapter 3) and the optimized NVU model (light grey). Student's *t*-test was used to determine statistical significance between P_{app} of markers across the two models where * $p<0.05$, ** $p<0.01$, and *** $p<0.001$. Error bars represent one standard deviation (n=3-6).

4.4.3 *BBB Linked Neuroactivity*

Relative neuroactivity was measured following 3 hour BBB permeability at an initial concentration of 50 µM in the NVU model where drug accumulated in the receiver chamber containing SH-SY5Y neuronal cells over the course of permeation across the apical direct contact triculture (Fig. 4.8). This study was performed at n=4 and neuroactivity (neuronal viability and outgrowth) data is reported as a percent of control NVU SH-SY5Y cells with vehicle (0.50% DMSO) alone, and flux reported for each compound to represent the amount accumulated in the neuronal chamber. In comparison to the control (neuron viability was 100 ± 8%, where neurite outgrowth was 100 ± 26%) caffeine accumulation resulted in a significant increase in viability with a non-significant increase in outgrowth (159 ± 34%, $p<0.05$; 122 ± 26%; flux = 269 ± 14 pg/cm^2 · sec). Carbamazepine (96 ± 18%; 96 ± 9%; flux = 310 ± 9 pg/cm^2 · sec) demonstrated negligible changes in viability and outgrowth while clozapine (143 ± 20%; 111 ± 12%; flux = 372 ± 19 pg/cm^2 · sec) and prazosin (137 ± 19%; 106 ± 22%; flux = 166 ± 14 pg/cm^2 · sec) demonstrated insignificant increases in both viability and outgrowth in comparison to the control. Permeability linked neuroactivity of the SH-SY5Y cells in response to digoxin accumulation resulted in significant increases in both viability and outgrowth when compared to the control neuronal cells (157 ± 18%, $p<0.05$; 147 ± 15%, $p<0.05$; flux = 450 ± 19 pg/cm^2 · sec). Lastly, cyclosporin A accumulation resulted in the largest increase in neuronal viability and insignificant changes in neurite outgrowth (365 ± 30%, $p<0.001$; 106 ± 15%; flux = 127 ± 27 pg/cm^2 · sec).

Representative images of neuronal viability and outgrowth staining are presented for the control, digoxin, and cyclosporin A samples (Fig. 4.9). In comparison to the control (panel A), punctate neurite projections are observable in the fluorescent (red) and bright field images of digoxin SH-SY5Y neurons (panel B), while a qualitative intensified green fluorescence and diffuse outgrowth is observed for cyclosporin A neuronal cells (panel C). These qualitative observations correlate to the quantifiable data obtained from the relative fluorescence results (Fig. 4.8).

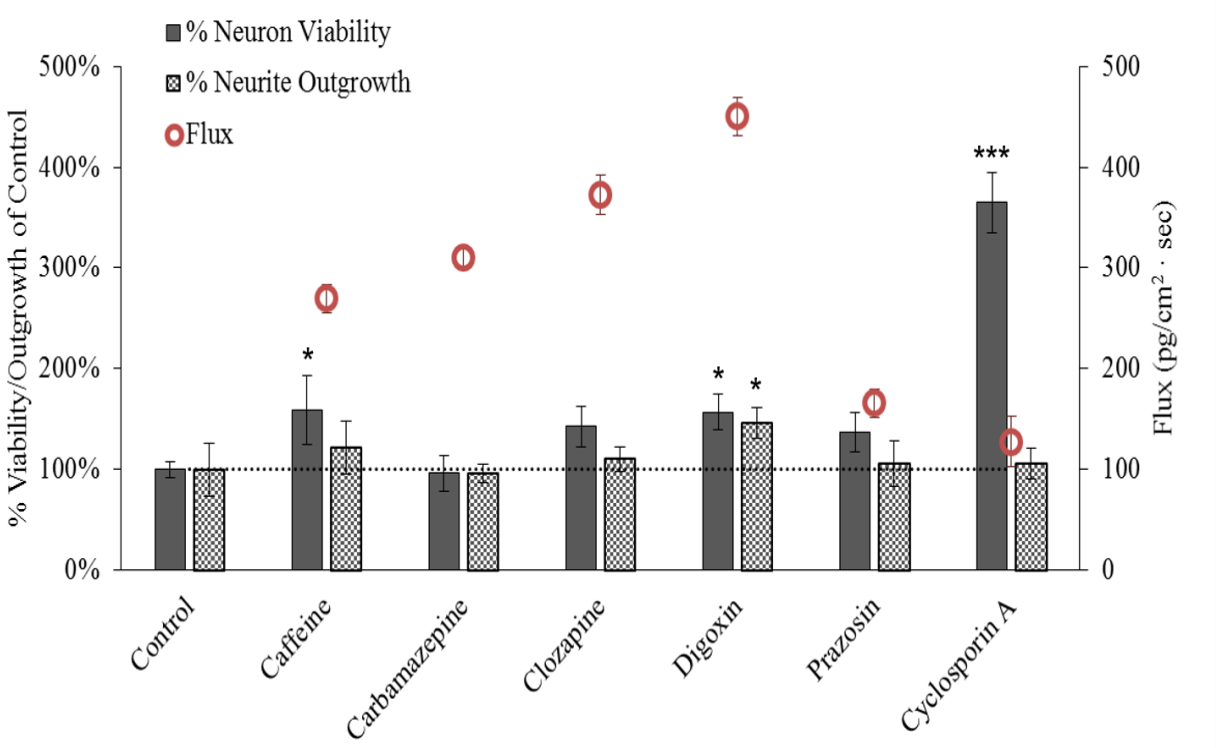

Figure 4.6. Neuroactivity of marker compounds after 3 hour permeability measured by neuronal viability (solid) and outgrowth (checkered) of SH-SY5Y cells represented as percentage of control NVU neuronal cells with vehicle (0.50% DMSO) alone and relative flux of each marker compound (red circle). Initial concentrations of 50 µM were placed in the apical chamber of the NVU model, SH-SY5Y neurons were stained for viability and outgrowth at the end of 3 hours of marker permeation. Viability stain was measured at ex: 483 nm and em: 525 nm and outgrowth stain was measured at ex: 535 nm and em: 590 nm. Markers are ordered based on highest to lowest permeation rate across the NVU model. Statistical significance was determined using a one way ANOVA followed by a Tukey-Kramer post-hoc test where * $p<0.05$, ** $p<0.01$, and *** $p<0.001$. Error bars represent one standard deviation (n=4).

4.4.4 *BBB Triculture Viability*

Viability of the apical triculture cells was inferred using an MTT assay to determine if observed neuronal effects or flux were due to changes in the integrity of the triculture cells. Inferred viability of the triculture cells is normalized to the triculture cells of the control NVU and reported as percent of the control (Fig. 4.10). The viability of the triculture following 3 hours of caffeine (104 ± 25%), carbamazepine (103 ± 5%), clozapine (99 ± 4%), digoxin (94 ± 5%), prazosin (82 ± 6%), and cyclosporin A (103 ± 2%) permeation resulted in no significant changes in comparison to the triculture of the control NVU (100 ± 2%, $p>0.05$).

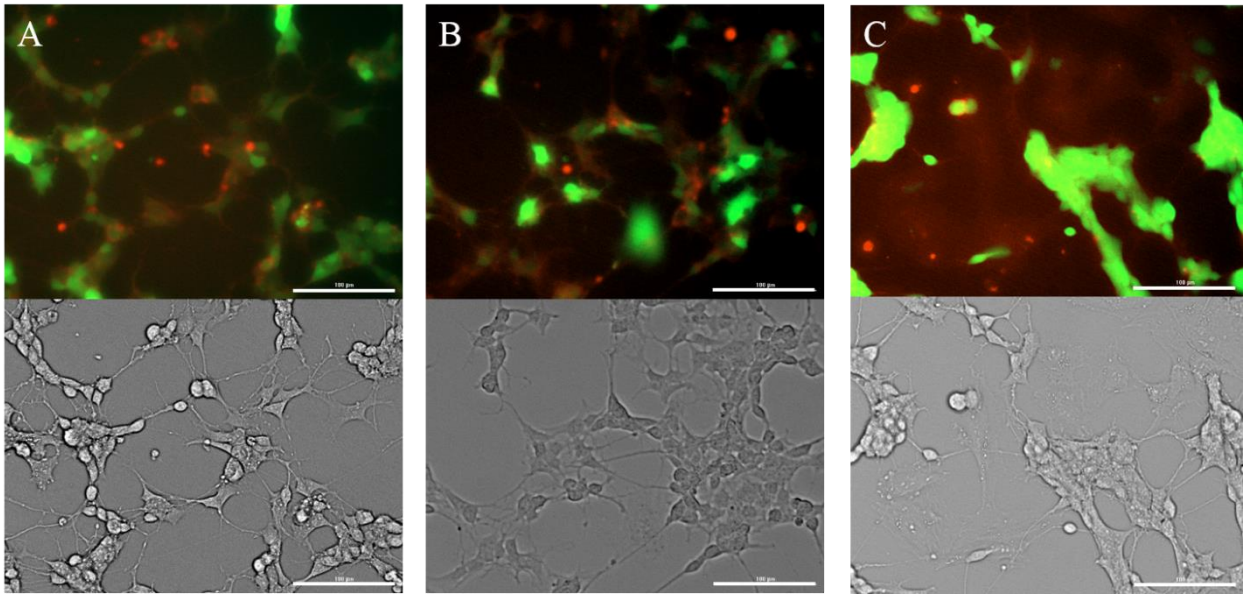

Figure 4.7. Qualitative fluorescence (top) and bright field (bottom) images of SH-SY5Y neuronal cells after 3 hours of (A) control vehicle (0.50% DMSO), (B) digoxin, and (C) cyclosporin A accumulation after permeation across the apical triculture in the optimized NVU model. Images were obtained using the BioTek Cytation 3 with 20x objective and Green Fluorescent Protein and Texas Red filters for neuronal viability and outgrowth respectively. Scale bars represent 100 µm.

4.5 Discussion

Using a previously optimized *in vitro* model of the BBB that encompasses the 3 major cell types of the NVU (Chapter 3), we have further improved upon the utility of the model by including

neurons as the fourth cellular component for use in both permeability and associated neuroactivity evaluation of a potential drug candidate. Although we encourage direct, physiologically relevant contact between the different cell types of the NVU, it is important to consider that for the utility of the NVU model it is necessary to separate the neurons for subsequent neuroactivity screening. However, as evidenced by our results, there is apparent cell-cell signaling between the neurons and the apical triculture based on the decrease in permeation of paracellular markers, an index of tightness, across the BMECs and an increase in both neuronal viability and outgrowth when in the presence of the triculture as compared to being cultured separately.

Seeding density of neurons in the basolateral chamber and the time of introduction of the apical BBB filter were chosen at the two key factors that would influence the characteristics of the model. Optimization was performed using a full factorial design to observe the impact of a low, medium, and high SH-SY5Y seeding density and two different times of BBB filter incorporation on the paracellular tightness of the model evaluated by permeation of a 4 kD FITC-dextran (Table 4.1). Results showed that allowing neurons and the apical triculture to coculture for a longer period of time, regardless of density, resulted in greater restrictiveness of the BMECs as compared to shorter coculturing times. This can be explained by the active cross-talk that occurs between the neurons and astrocytes *in vivo*.[19,21] The presence of neurons in companion wells has been shown to increase expression levels of occludin and claudin-5, essential tight junction proteins, in BMECs cultured on apical filter supports, which suggests that the presence of neurons in our NVU model may be increasing tight junction protein expression in the endothelium thus resulting in the reduced permeability of paracellular markers compared to the triculture alone.[8,30] However, the decrease in permeability of the 4 kD dextran in the NVU model is not significant, therefore it is difficult to say with certainty what effects the presence of the neuronal cells has on tight junction expression

in the absence of molecular based techniques (*i.e.* Western blot, mRNA expression). Secondly, lower densities of SH-SY5Y cells, 25,000 – 50,000 cells/cm^2, resulted in greater tightening over the higher 75,000 cells/cm^2 density used. This can be attributed to the possibility of overgrowth of the SH-SY5Y neurons at higher densities leading to possible decreases in viability and deleterious effects on the apical BBB cells. Additionally, less confluent neurons in the basolateral chamber would facilitate the observation of neurite outgrowth as there will be less cellular overlap. In addition to the neurons influencing barrier properties, results of our study demonstrate that the presence of the apical triculture has synergistic effects on the SH-SY5Y cells. The increase in neuronal viability and outgrowth when cocultured with the apical triculture suggests that the other cell types of the NVU are essential for optimal neuronal health by way of cellular cross-talk. It should be noted that the increase in viability and outgrowth that was observed for the neuronal cells in the NVU model can also be attributed to higher cell counts in these cultures compared the neurons cultured alone. Both systems were seeded at the same initial density with the same neuronal cultures and grown for the same length of time before analysis, therefore an increase in neuron proliferation over the course of culture in the NVU model further supports the possibility of the different cell types of the NVU positively influencing each other via synergistic cell-cell signaling.

The NVU was evaluated using paracellular markers in a range of sizes ([^{14}C]-sucrose < 4 kD FITC-dextran < 10 kD FITC-dextran < 40 kD FITC-dextran). The model performed as expected, showing a sequential reduction in permeability with increasing marker size suggesting that the model can prevent substantial paracellular permeation by a potential therapeutic compound—forcing the molecule to permeate through a transcellular route. Additionally R123 was used in the presence and absence of elacridar to determine the functional efflux of P-gp—an

essential validation characteristic of a BBB permeability screening tool. The NVU model showed a significant increase of R123 permeation when in the presence of P-gp inhibitor, which can be inferred to represent the relative function of P-gp in the *in vitro* model. Additionally, the presence of neurons in the NVU model further increases P-gp expression and/or function in comparison to the triculture alone (data reported in Chapter 3) as seen by the decrease in R123 permeation alone and in the presence of elacridar. This phenomenon could be a result of one or a combination of the following: increased localization of P-gp to the apical membrane of the BMECs; increased expression of the efflux transporter(s); and/or a higher function of P-gp in the BMECs or other NVU cells. This can plausibly be attributed to the inherent function of the BBB which is to protect the brain parenchyma. Thus, the presence of neurons increases the physiological relevancy of the basolateral chamber, therefore leading to increased function of efflux transporters. This is something that should be further explored based on the changes in mRNA and protein expression levels in the apical triculture in the presence and absence of the cultured neurons.

The utility of the NVU model for BBB permeability ranking was tested using a number of compounds that are known to be high or low BBB permeants. Caffeine is a psychoactive compound known for its ability to permeate and have an effect on the brain parenchyma and ranks as the most permeable compound to cross the NVU model.[31] Carbamazepine, an anticonvulsant shown to have limited P-gp interaction, is a positive BBB permeant showing adequate permeation across the NVU model.[32] The permeability of melatonin was evaluated as a positive permeant based on its relative production in the pineal gland located outside the BBB and associated neural effects.[33,34] The differentiation for positive and negative permeants was placed between the permeation of R123 in the presence and absence of elacridar as R123 alone should not positively permeate into the brain parenchyma. Although R123 is a P-gp substrate its BBB permeability in

the NVU model is greater than that of other substrates tested, which suggests that P-gp substrates have different affinities and efflux capacity, and different efflux substrates can infer varying degrees of functionality of the transporter. Concentration dependent analysis could be done to determine which substrates might be best suited for the assessment of efflux transporter function in *in vitro* models. Clozapine is a psychoactive molecule which has been shown to be a possible P-gp substrate, however it is highly metabolically active with its metabolites readily crossing the BBB.[32,35,36] This suggests that further analysis of the permeation samples should be done to determine the extent of permeation of the clozapine metabolites as the HPLC analytical technique used here may not be adequate for separation. Digoxin is a P-gp substrate that is actively effluxed from the BBB and its lack of permeation across the NVU model corresponds with expected outcomes from this molecule in BBB screening tools.[37] Prazosin is a substrate for the other predominantly expressed efflux transporter in the BBB, Breast Cancer Resistance Protein (BCRP)—the lack of permeation of this molecule across the NVU model suggests that there is functional expression of BCRP.[38] Lastly, the permeation of cyclosporin A in the NVU was the lowest observed as it is a broad spectrum inhibitor for a number of efflux transporters.[39] Further investigation of the effects of CsA on efflux transporter substrate permeability (*e.g.* prazosin, digoxin, etc.) would be useful to evaluate the degree to which efflux can be inhibited in the model for the predominant transporters P-gp and BCRP. Due to the lack of substrate specificity of BBB efflux transporters it is difficult to determine relative expression levels of BCRP in comparison to P-gp based on permeation rates alone. In the results obtained from this study, lapatinib could not be detected in the receiver chamber over 3 hours of BBB permeation in the NVU model (data not shown) suggesting that it does not cross the BBB, and is supported by *in vivo* findings

demonstrating the role efflux transporters play on limiting penetration of lapatinib into the brain parenchyma.[40,41]

Data that was presented in Chapter 3 for the optimized direct contact triculture was used to compare the changes in permeation of marker compounds in the NVU model. Of the compounds that overlap between the libraries used, the observed rates of permeation for BBB positive compounds caffeine and carbamazepine are not significant between the two models. These markers passively diffuse across the barrier via a transcellular pathway with some reported transporter contribution and limited efflux potential.[31,32,42] Of greater interest is the significant differences in permeation rates of effluxed or readily metabolized compounds in each *in vitro* model. As stated previously, R123 permeation with and without inhibitor is significantly decreased in the NVU model which may imply that the presence of the SH-SY5Y neuronal cells are modulating overall P-gp function to some degree. A significant difference is not observed for the P-gp substrate digoxin, however the permeation rate of BCRP substrate prazosin is significantly low in the NVU model compared to the optimized triculture alone. We postulate, based on the observed permeation rates in each model, that the presence of the neuronal cells in the basolateral chamber is facilitating synergistic signally between the neurons and the BBB triculture resulting in modulation of either efflux transporter function or overall expression. Additionally, the significantly higher permeation rate of metabolically active clozapine across the NVU model may imply a similar possibility for drug metabolizing enzymes. Ultimately, comparing the NVU model with the optimized triculture alone reveals significant differences in observed permeation of compounds with transporter contributions. This suggests that although we do not observe significant changes in paracellular tightness in the presence of the cultured neuronal cells there may be modulation of transporters that would warrant further investigation.

Initial assessment of BBB permeability linked neuroactivity was performed after a 3 hour permeation period to determine how the permeation barrier of the apical triculture would impact neuroactivity of the SH-SY5Y cells in comparison to reported effects in direct neuronal experiments. Of the six markers chosen, caffeine and prazosin have limited reports on neuroactivity, cyclosporin A and digoxin are reported to inhibit neuroactivity, and clozapine and carbamazepine have been observed to induce neuroactivity, which are all based on direct neuronal incubation of these compounds.[24,26,35,43] Compared to the control neuronal cells, caffeine accumulation resulted in a significant increase in neuroactivity but non-significant changes in outgrowth, which is expected based on its psychoactive and neuroprotective attributes.[31] Although carbamazepine and clozapine have been reported to induce neuroactivity as observed by increases in neurite outgrowth, the same was not seen in the NVU model.[35,43] In the NVU model, digoxin was the only marker which showed significant neuroactivity in both neuronal viability and outgrowth by the observed increases in both. This is in opposition of what has been reported from direct neuron evaluation and its potential for causing systemic toxicity.[24,44] Cyclosporin A 3 hour incubation in the NVU model resulted in the highest and most significant observed increase in neuronal viability relative to the other compounds tested. Cyclosporin A is an immunosuppressive compound which has been shown to increase the viability of neuronal precursor cells (NPCs), supporting the higher viability of the SH-SY5Y neurons in the NVU model.[45] Of interest here is the lack of correlation of neuroactivity to flux measurements or total accumulation in the neuronal chamber. With the exception of digoxin being the highest accumulated compound having significant increases in both viability and outgrowth, the neuronal response to cyclosporin A is the highest despite having the lowest flux of all compounds tested. In order to ensure that the neuroactivity responses were due to accumulation and not disruption of the triculture the relative

viability of the triculture cells was assessed using via MTT assay, but revealed no significant changes in viability in comparison to the control suggesting that the barrier cells were not disrupted throughout the course of screening.

In this work the SH-SY5Y neuroblastoma cell line was used as the neuronal cell source despite the limitations associated with its use in neuroactivity models.[28,29] The cells used in this work were in their undifferentiated stated based on reports on their sensitivity to neurotoxins and potential for use in neurotoxicity screening. Based on the results of this work we postulate that there may be modulation of the state of the SH-SY5Y cells in response to the synergistic signaling and that the state of the neuronal cells should be looked at in future invesitgations.

Ultimately, we have demonstrated that the presence of a BBB model in neuroactivity screening is essential for adequately mimicking the path of a compound *in vivo*. The BBB triculture presents not only as a permeation but also as a metabolic barrier of entry into the brain parenchyma or neuronal chamber of the *in vitro* model. *In vivo* the NVU responds to neuronal demands based on synergistic signaling from the neurons through direct contacts with astrocytes via neuronal secretion of a number of soluble factors.[15,20,46] This in turn modulates vascular diameter by pericyte action to protect the parenchyma.[15] We have demonstrated, in the optimized NVU model, that there is synergistic signaling occurring through all cell types by soluble factor secretion.

4.6 Conclusion

Presently, there is a lack of therapeutic agents aimed at mitigating neurological disorders such as neurodegenerative and neurodevelopmental diseases and mental illness.[47] This is due in large part to the high attrition rates in later stage clinical trials and the high costs associated with developing this class of compounds.[48,49] High attrition rates are often attributed to a lack of successful delivery

methods due to the restrictive BBB, a lack of efficacy when moving to *in vivo* studies and clinical trials, and neurotoxic side effects of drugs that permeate in excess into the brain parenchyma.[50] In an effort to provide a low-cost solution to the current need of the field, we have developed a physiologically relevant cell-based model of the NVU that incorporates BBB permeation and linked neuroactivity into a single screening tool. Additionally, we have demonstrated that the incorporation of all four cell types of the NVU leads to increased phenotypic expression of the BBB as well as cellular viability of the neuronal cells. The utility of the model serves to mimic the *in vivo* situation a therapeutic agent may encounter when attempting to cross the BBB into the brain parenchyma. By implementing this screening tool in pharmaceutical development of neurotherapeutic agents, as well as other classes of drugs, there is potential to decrease the resources needed for ranking hit and lead candidate compounds through the evaluation of BBB permeability linked neuroactivity using a single *in vitro* screening tool.

4.7 References

1. Pardridge WM. The Blood-Brain Barrier: Bottleneck in Brain Drug Development. *NeuroRx* 2005;**2**:3–14.
2. Pardridge WM. Why is the global CNS pharmaceutical market so under-penetrated? *Drug Discov Today* 2002;**7**:5–7. https://doi.org/10.1016/S1359-6446(01)02082-7.
3. Bicker J, Alves G, Fortuna A, Falcão A. Blood–brain barrier models and their relevance for a successful development of CNS drug delivery systems: A review. *Eur J Pharm Biopharm* 2014;**87**:409–32. https://doi.org/10.1016/j.ejpb.2014.03.012.
4. Helms HC, Abbott NJ, Burek M, Cecchelli R, Couraud P-O, Deli MA, *et al.* In vitro models of the blood-brain barrier: An overview of commonly used brain endothelial cell culture

models and guidelines for their use. *J Cereb Blood Flow Metab Off J Int Soc Cereb Blood Flow Metab* 2016;**36**:862–90. https://doi.org/10.1177/0271678X16630991.

5. Helms HC, Waagepetersen HS, Nielsen CU, Brodin B. Paracellular Tightness and Claudin-5 Expression is Increased in the BCEC/Astrocyte Blood–Brain Barrier Model by Increasing Media Buffer Capacity During Growth. *AAPS J* 2010;**12**:759–70. https://doi.org/10.1208/s12248-010-9237-6.
6. Kulczar C, Lubin KE, Lefebvre S, Miller DW, Knipp GT. Development of a direct contact astrocyte-human cerebral microvessel endothelial cells blood-brain barrier coculture model. *J Pharm Pharmacol* 2017;**69**:1684–96. https://doi.org/10.1111/jphp.12803.
7. Al Ahmad A, Taboada CB, Gassmann M, Ogunshola OO. Astrocytes and pericytes differentially modulate blood-brain barrier characteristics during development and hypoxic insult. *J Cereb Blood Flow Metab Off J Int Soc Cereb Blood Flow Metab* 2011;**31**:693–705. https://doi.org/10.1038/jcbfm.2010.148.
8. Canfield SG, Stebbins MJ, Morales BS, Asai SW, Vatine GD, Svendsen CN, *et al.* An isogenic blood-brain barrier model comprising brain endothelial cells, astrocytes, and neurons derived from human induced pluripotent stem cells. *J Neurochem* 2017;**140**:874–88. https://doi.org/10.1111/jnc.13923.
9. Xue Q, Liu Y, Qi H, Ma Q, Xu L, Chen W, *et al.* A Novel Brain Neurovascular Unit Model with Neurons, Astrocytes and Microvascular Endothelial Cells of Rat. *Int J Biol Sci* 2013;**9**:174–89. https://doi.org/10.7150/ijbs.5115.
10. Abbott NJ, Patabendige AAK, Dolman DEM, Yusof SR, Begley DJ. Structure and function of the blood-brain barrier. *Neurobiol Dis* 2010;**37**:13–25. https://doi.org/10.1016/j.nbd.2009.07.030.

11. Abbott NJ, Rönnbäck L, Hansson E. Astrocyte-endothelial interactions at the blood-brain barrier. *Nat Rev Neurosci* 2006;**7**:41–53. https://doi.org/10.1038/nrn1824.

12. Bouchaud C, Le Bert M, Dupouey P. Are close contacts between astrocytes and endothelial cells a prerequisite condition of a blood-brain barrier? The rat subfornical organ as an example. *Biol Cell* 1989;**67**:159–65.

13. Daneman R, Zhou L, Kebede AA, Barres BA. Pericytes are required for blood-brain barrier integrity during embryogenesis. *Nature* 2010;**468**:562–6. https://doi.org/10.1038/nature09513.

14. Dohgu S, Takata F, Yamauchi A, Nakagawa S, Egawa T, Naito M, *et al.* Brain pericytes contribute to the induction and up-regulation of blood-brain barrier functions through transforming growth factor-beta production. *Brain Res* 2005;**1038**:208–15. https://doi.org/10.1016/j.brainres.2005.01.027.

15. Hamilton NB, Attwell D, Hall CN. Pericyte-mediated regulation of capillary diameter: a component of neurovascular coupling in health and disease. *Front Neuroenergetics* 2010;**2**:. https://doi.org/10.3389/fnene.2010.00005.

16. Hall CN, Reynell C, Gesslein B, Hamilton NB, Mishra A, Sutherland BA, *et al.* Capillary pericytes regulate cerebral blood flow in health and disease. *Nature* 2014;**508**:55–60. https://doi.org/10.1038/nature13165.

17. Halassa MM, Fellin T, Takano H, Dong J-H, Haydon PG. Synaptic islands defined by the territory of a single astrocyte. *J Neurosci Off J Soc Neurosci* 2007;**27**:6473–7. https://doi.org/10.1523/JNEUROSCI.1419-07.2007.

18. Bushong EA, Martone ME, Jones YZ, Ellisman MH. Protoplasmic astrocytes in CA1 stratum radiatum occupy separate anatomical domains. *J Neurosci Off J Soc Neurosci* 2002;**22**:183–92.

19. Banerjee S, Bhat MA. Neuron-Glial Interactions in Blood-Brain Barrier Formation. *Annu Rev Neurosci* 2007;**30**:235–58. https://doi.org/10.1146/annurev.neuro.30.051606.094345.

20. McConnell HL, Kersch CN, Woltjer RL, Neuwelt EA. The Translational Significance of the Neurovascular Unit. *J Biol Chem* 2017;**292**:762–70. https://doi.org/10.1074/jbc.R116.760215.

21. Attwell D, Buchan AM, Charpak S, Lauritzen M, Macvicar BA, Newman EA. Glial and neuronal control of brain blood flow. *Nature* 2010;**468**:232–43. https://doi.org/10.1038/nature09613.

22. Bal-Price AK, Hogberg HT, Buzanska L, Coecke S. Relevance of in vitro neurotoxicity testing for regulatory requirements: Challenges to be considered. *Neurotoxicol Teratol* 2010;**32**:36–41. https://doi.org/10.1016/j.ntt.2008.12.003.

23. Radio NM, Mundy WR. Developmental neurotoxicity testing in vitro: Models for assessing chemical effects on neurite outgrowth. *NeuroToxicology* 2008;**29**:361–76. https://doi.org/10.1016/j.neuro.2008.02.011.

24. Sherman SP, Bang AG. High-throughput screen for compounds that modulate neurite growth of human induced pluripotent stem cell-derived neurons. *Dis Model Mech* 2018;**11**:. https://doi.org/10.1242/dmm.031906.

25. Anderl JL, Redpath S, Ball AJ. A Neuronal and Astrocyte Co-Culture Assay for High Content Analysis of Neurotoxicity. *J Vis Exp JoVE* 2009. https://doi.org/10.3791/1173.

26. Hallier-Vanuxeem D, Prieto P, Culot M, Diallo H, Landry C, Tähti H, *et al.* New strategy for alerting central nervous system toxicity: Integration of blood–brain barrier toxicity and permeability in neurotoxicity assessment. *Toxicol In Vitro* 2009;**23**:447–53. https://doi.org/10.1016/j.tiv.2008.12.011.

27. Toimela T, Mäenpää H, Mannerström M, Tähti H. Development of an in vitro blood–brain barrier model—cytotoxicity of mercury and aluminum. *Toxicol Appl Pharmacol* 2004;**195**:73–82. https://doi.org/10.1016/j.taap.2003.11.002.

28. Kovalevich J, Langford D. Considerations for the Use of SH-SY5Y Neuroblastoma Cells in Neurobiology. In: Amini S, White MK, editors. *Neuronal Cell Cult.*, vol. 1078. Totowa, NJ: Humana Press; 2013. p. 9–21.

29. Shipley MM, Mangold CA, Szpara ML. Differentiation of the SH-SY5Y Human Neuroblastoma Cell Line. *J Vis Exp JoVE* 2016. https://doi.org/10.3791/53193.

30. Savettieri G, Di Liegro I, Catania C, Licata L, Pitarresi GL, D'Agostino S, *et al.* Neurons and ECM regulate occludin localization in brain endothelial cells. *Neuroreport* 2000;**11**:1081–4.

31. Chen X, Ghribi O, Geiger JD. Caffeine protects against disruptions of the blood-brain barrier in animal models of Alzheimer's and Parkinson's disease. *J Alzheimers Dis JAD* 2010;**20**:S127–41. https://doi.org/10.3233/JAD-2010-1376.

32. Maines LW, Antonetti DA, Wolpert EB, Smith CD. Evaluation of the role of P-glycoprotein in the uptake of paroxetine, clozapine, phenytoin and carbamazapine by bovine retinal endothelial cells. *Neuropharmacology* 2005;**49**:610–7. https://doi.org/10.1016/j.neuropharm.2005.04.028.

33. Masters A, Pandi-Perumal SR, Seixas A, Girardin J-L, McFarlane SI. Melatonin, the Hormone of Darkness: From Sleep Promotion to Ebola Treatment. *Brain Disord Ther* 2014;**4**:. https://doi.org/10.4172/2168-975X.1000151.

34. Liu Y, Zhang Z, Lv Q, Chen X, Deng W, Shi K, *et al.* Effects and mechanisms of melatonin on the proliferation and neural differentiation of PC12 cells. *Biochem Biophys Res Commun* 2016;**478**:540–5. https://doi.org/10.1016/j.bbrc.2016.07.093.

35. Lu X-H, Dwyer DS. Second-generation antipsychotic drugs, olanzapine, quetiapine, and clozapine enhance neurite outgrowth in PC12 cells via PI3K/AKT, ERK, and pertussis toxin-sensitive pathways. *J Mol Neurosci MN* 2005;**27**:43–64.

36. Hellman K, Aadal Nielsen P, Ek F, Olsson R. An ex Vivo Model for Evaluating Blood–Brain Barrier Permeability, Efflux, and Drug Metabolism. *ACS Chem Neurosci* 2016;**7**:668–80. https://doi.org/10.1021/acschemneuro.6b00024.

37. Helms HC, Hersom M, Kuhlmann LB, Badolo L, Nielsen CU, Brodin B. An Electrically Tight In Vitro Blood–Brain Barrier Model Displays Net Brain-to-Blood Efflux of Substrates for the ABC Transporters, P-gp, Bcrp and Mrp-1. *AAPS J* 2014;**16**:1046–55. https://doi.org/10.1208/s12248-014-9628-1.

38. Mao Q, Unadkat JD. Role of the Breast Cancer Resistance Protein (BCRP/ABCG2) in Drug Transport—an Update. *AAPS J* 2014;**17**:65–82. https://doi.org/10.1208/s12248-014-9668-6.

39. Qadir M, O'Loughlin KL, Fricke SM, Williamson NA, Greco WR, Minderman H, *et al.* Cyclosporin A is a broad-spectrum multidrug resistance modulator. *Clin Cancer Res Off J Am Assoc Cancer Res* 2005;**11**:2320–6. https://doi.org/10.1158/1078-0432.CCR-04-1725.

40. Polli JW, Olson KL, Chism JP, John-Williams LS, Yeager RL, Woodard SM, *et al.* An Unexpected Synergist Role of P-Glycoprotein and Breast Cancer Resistance Protein on the Central Nervous System Penetration of the Tyrosine Kinase Inhibitor Lapatinib (N-{3-Chloro-4-[(3-fluorobenzyl)oxy]phenyl}-6-[5-({[2-(methylsulfonyl)ethyl]amino}methyl)-2-furyl]-4-quinazolinamine; GW572016). *Drug Metab Dispos* 2009;**37**:439–42. https://doi.org/10.1124/dmd.108.024646.

41. Polli JW, Humphreys JE, Harmon KA, Castellino S, O'Mara MJ, Olson KL, *et al.* The Role of Efflux and Uptake Transporters in N- -6-[5-(methyl)-2-furyl]-4-quinazolinamine (GW572016, Lapatinib) Disposition and Drug Interactions. *Drug Metab Dispos* 2008;**36**:695–701. https://doi.org/10.1124/dmd.107.018374.

42. Sun J, Xie L, Liu X. Transport of carbamazepine and drug interactions at blood-brain barrier. *Acta Pharmacol Sin* 2006;**27**:249–53. https://doi.org/10.1111/j.1745-7254.2006.00246.x.

43. Schultz L, Zurich M-G, Culot M, da Costa A, Landry C, Bellwon P, *et al.* Evaluation of drug-induced neurotoxicity based on metabolomics, proteomics and electrical activity measurements in complementary CNS in vitro models. *Toxicol In Vitro* 2015;**30**:138–65. https://doi.org/10.1016/j.tiv.2015.05.016.

44. Bauman JL, Didomenico RJ, Galanter WL. Mechanisms, manifestations, and management of digoxin toxicity in the modern era. *Am J Cardiovasc Drugs Drugs Devices Interv* 2006;**6**:77–86. https://doi.org/10.2165/00129784-200606020-00002.

45. Hunt J, Cheng A, Hoyles A, Jervis E, Morshead CM. Cyclosporin A Has Direct Effects on Adult Neural Precursor Cells. *J Neurosci* 2010;**30**:2888–96. https://doi.org/10.1523/JNEUROSCI.5991-09.2010.

46. Iadecola C. The Neurovascular Unit Coming of Age: A Journey through Neurovascular Coupling in Health and Disease. *Neuron* 2017;**96**:17–42. https://doi.org/10.1016/j.neuron.2017.07.030.

47. Miller G. Is pharma running out of brainy ideas? *Science* 2010;**329**:502–4. https://doi.org/10.1126/science.329.5991.502.

48. Kesselheim AS, Hwang TJ, Franklin JM. Two decades of new drug development for central nervous system disorders. *Nat Rev Drug Discov* 2015;**14**:815–6. https://doi.org/10.1038/nrd4793.

49. Choi DW, Armitage R, Brady LS, Coetzee T, Fisher W, Hyman S, *et al.* Medicines for the mind: policy-based 'pull' incentives for creating breakthrough CNS drugs. *Neuron* 2014;**84**:554–63. https://doi.org/10.1016/j.neuron.2014.10.027.

50. Gribkoff VK, Kaczmarek LK. The Need for New Approaches in CNS Drug Discovery: Why Drugs Have Failed, and What Can Be Done to Improve Outcomes. *Neuropharmacology* 2017;**120**:11–9. https://doi.org/10.1016/j.neuropharm.2016.03.021.

CONCLUDING REMARKS

There is an ever growing need for the development of neurotherapeutic compounds in order to mitigate the growing prevalence of neurodegenerative and neurodevelopmental diseases and mental illness. Currently there is a significant amount of attrition in later stages of development and clinical trials for these therapeutic agents due to the restrictiveness of the blood brain barrier and encompassing neurovascular unit. Additionally, permeation and associated neuroactive outcomes of a given compound are traditionally evaluated in separate assays or screens. The goal of this thesis is to aid in mitigation efforts through the development and optimization of physiologically relevant cell based *in vitro* models that are more semblant of the NVU and can be utilized for hit and lead candidate screening for both permeability and neuroactivity assessment.

Chapter 2 presents the preliminary work performed to screen for alternative endothelial cell lines that could further improve on our previously established direct contact BBB models. We concluded that the use of an alternative immortalized cell line, HBEC-5i, would be best suited for our future development, optimization, and validation efforts despite the trends of the field moving towards cell sources derived from pluripotent stem cells. This work laid the foundation for the future development efforts as it aided in the selection factors that would have the greatest impact on the model performance as well as helped to find informed ranges for these factors that were to be tested.

The work presented in Chapter 3 establishes the novel use of a design of experiments based optimization for the development of cell based systems. Traditionally this approach is used for non-biologically based process optimization, however we have demonstrated that the implementation of a DOE in cell based systems can significantly reduce the amount of time and resources required for development and validation of these models. We posit that this approach

can significantly impact the pharmaceutical industry and the field of permeation barrier research to aid in the development of more physiologically relevant screening tools.

Chapter 4 of this thesis presents the most novel improvement and enhancement, to our knowledge, of a BBB model that incorporates all cell types of the NVU. The four cell types, endothelium, pericytes, astrocytes, and neurons, are known to be synergistically active in the modulation of the barrier properties in order to maintain the neuronal environment. Most *in vitro* models do not incorporate all cells types of the NVU due to the difficulty associated with the culturing or overlooking the impact the cells have on the barrier properties, however we have developed and performed early validation of an *in vitro* cell based screening tool that incorporates all four cell types of the NVU in a physiologically relevant configuration that can be implemented in screening of hit and lead compounds. We have shown that the presence of the neurons in the basolateral chamber underneath the apical direct contact triculture results in synergistic modulation of both the permeation barrier of the BBB cells as well as the neuronal health and viability. Herein, we have presented the utility of including multiple cell types of the NVU in screening tools for potential therapeutic agents, and established that permeation and neuroactivity should be assessed in concert rather than approached separately.

The work performed in this thesis has presented great opportunity for improvement of translation of brain permeating compounds to the market, however there is still room for improvement of the model and areas that can be investigated to gain a better understanding of the NVU physiology from a molecular level and how that can be mimicked *in vitro*. A future direction that is suggested is the investigation of other naïve neuronal cell lines. The work presented here utilized the SH-SY5Y neuroblastoma cell line that may not be best suited for continued screening due to its limitations. We propose that this model can be further improved using primary or stem

cell derived neuronal sources that may be more responsive to therapeutic agents for neuroactivity screening. Additionally, we have proposed that there is synergistic modulation of the neuronal cells by the apical BBB as observed by increases in viability and outgrowth as well as modulation of transporter expression or function in the apical triculture. The findings here suggest that inclusion of neurons in any BBB screening tool could have a great impact on how potential therapeutic agents are chosen or classified, therefore it is suggested that the modulation of transporter function and expression be investigated on a molecular level in future work. Lastly, we have established that using a DOE is a useful optimization tool for improvement and validation of *in vitro* cell based screening models. The goal of this work has been to continually improve on the physiological relevancy of the model, however, stem cell derived cell sources and primary cells are typically cost and resource prohibitive for early optimization. With this work we have established that a DOE based optimization approach is amenable to cell based systems, ultimately aiding in the implementation of *in vivo* relevant cell sources that were previously viewed as cost prohibitive.